

ON THE INFLUENCE OF WEB OUT-OF-PLUMBNESS ON HORIZONTALLY CURVED
STEEL I-GIRDER BRIDGE SERVICEABILITY DURING CONSTRUCTION

by

Thomas D. Howell

B.S., United States Military Academy, 1999

Submitted to the Graduate Faculty of

School of Engineering in partial fulfillment

of the requirements for the degree of

Master of Science

University of Pittsburgh

2006

UNIVERSITY OF PITTSBURGH
SCHOOL OF ENGINEERING

This thesis was presented

by

Thomas D. Howell

It was defended on

March 14th, 2006

and approved by

Dr. J.S. Lin, Associate Professor, Civil and Environmental Engineering

Dr. K.A Harries, Assistant Professor, Civil and Environmental Engineering

Thesis Advisor: Dr. C.J. Earls, Associate Professor, Civil and Environmental Engineering

ON THE INFLUENCE OF WEB OUT-OF-PLUMBNESS ON HORIZONTALLY CURVED STEEL I-GIRDER BRIDGE SERVICEABILITY DURING CONSTRUCTION

Thomas D. Howell, MS

University of Pittsburgh, 2006

The effects on horizontally-curved steel I-girder bridge serviceability of various degrees of web out-of-plumbness are discussed in the present work within the context of performance during construction. Specifically, the consequences in terms of girder flange tip stresses, vertical and lateral deflections, and cross frame demands are discussed for various regions of a subject bridge when subjected to up to 5 degrees of out-of-plumbness. The effective mitigation of detrimental effects of out-of-plumbness is discussed in the context of current erection practices. This research does not aim to increase the capacity of horizontally curved bridges, but to report on the effects of typically-encountered degrees of web-tilt on construction-critical aspects of bridge erection. The research work discussed herein is primarily analytical in nature. Detailed nonlinear finite element models are created using the commercially available software system ADINA.

TABLE OF CONTENTS

ACKNOWLEDGEMENTS	x
1.0 INTRODUCTION	1
1.1 HORIZONTALLY CURVED BRIDGE BACKGROUND	4
1.2 LITERATURE REVIEW	4
1.3 OBJECTIVE AND SCOPE OF WORK	17
1.4 THESIS ORGANIZATION	18
2.0 CURVED I-GIRDER BEHAVIOR	20
2.1 REACTIONS	20
2.2 FLEXURAL MOMENT	22
2.3 TORSIONAL MOMENT	22
2.4 LATERAL FLANGE BENDING	23
3.0 MODEL OVERVIEW	25
3.1 SUBJECT BRIDGE	25
3.2 IDEALIZED CROSS SECTION DIMENSIONS	27
3.3 FINITE ELEMENT MODEL	28
3.3.1 Bridge girder modeling	28
3.3.2 Girder stiffeners and connection plates	30
3.3.3 Cross frame modeling	31
3.3.4 Artificially induced out-of-plumbness	32

3.3.5	Constraints	35
3.3.6	Boundary conditions	36
3.3.7	Loading	39
4.0	RESULTS PRESENTATION	41
4.1	GIRDER FLANGE STRESSES	41
4.2	VERTICAL AND LATERAL DEFLECTIONS	48
4.3	CROSS FRAME FORCES	54
5.0	RESULTS DISCUSSION.....	62
5.1	GIRDER FLANGE TIP STRESSES	62
5.2	VERTICAL AND LATERAL DISPLACEMENTS	68
5.3	CROSS FRAME FORCES	70
6.0	CONCLUSIONS.....	72
	APPENDIX A.....	74
	RESULTS TABLES AND GRAPHS.....	74
	BIBLIOGRAPHY	106

LIST OF TABLES

Table 1.1 Changes in Stresses Due to Structure Rotation- 4 Girder Span (Lobo, 2002).....	13
Table 1.2 Bridge 207 Dead Load Camber Table (Domalik, 2005)	15
Table 1.3 CB1 Girder Ultimate Load and Bottom Flange Tip Stress Summary (Chavel, 2004). .	17
Table 3.1 Web Thickness Simplification Procedure for Girder #6	27

LIST OF FIGURES

Figure 1.1 Erection of Two Curved Girders with Cross Frames Installed (Gillespie, 1968)	2
Figure 1.2 Subject Bridge Plan and Corresponding Finite Element Models (Linzell, 1999).....	7
Figure 1.3 MN Bridge # 27998 Framing Plan (Galambos et al., 2000)	8
Figure 1.4 Typical Mid-Span Deflection and Rotation of a Curved Span (Yadlosky, 2001).....	9
Figure 1.5 Ford City Veteran’s Bridge Superstructure (Chavel, 2001).....	11
Figure 1.6 ABAQUS Finite Element Model of the Ford City Veteran’s Bridge (Chavel, 2001)	12
Figure 1.7 Bridge 207 Framing Plan (Domalik, 2005).....	14
Figure 1.8 CB1 Beam Plan View (Chavel, 2004).....	16
Figure 2.1 Statically Determinate Single Curved Girder (Nakai, 1988).....	21
Figure 2.2 Non-Uniform Torsion of an I-Girder Subject to Longitudinal Moment	23
Figure 2.3 Manifestation of Compressive and Tensile Regions in Support Vicinity	24
Figure 3.1 Framing Plan for Subject Bridge (Chelyan Bridge)	25
Figure 3.2 Typical K-type Cross Frame Used in Subject Bridge and Finite Element Model	26
Figure 3.3 Girder Web and Flange Mesh Construction.....	29
Figure 3.4 Cross frame Brace Plate and Web Stiffener Mesh Construction	31
Figure 3.5 Plan View of Model With Cross frame Locations	32
Figure 3.6 Original and Out-of-plumb Position of Typical Girder Cross-section.....	33
Figure 3.7 Superposition of Existing and Additional Lateral Displacement.....	34
Figure 3.8 Five-Degree Out-of-Plumb Mesh.....	35

Figure 3.9 Constraint Equation Relationship Along Edges (ADINA, 2003)	36
Figure 3.10 Establishment of the Local Coordinate Systems for Support Locations	37
Figure 3.11 ADINA Input of Skewed Coordinate System Vectors (ADINA, 2003)	38
Figure 3.12 Local Coordinate System Establishment.....	39
Figure 4.1 Flange Tip Stress Locations, Pier 3 Location (typical for other locations).....	42
Figure 4.2 Critical Locations Under Consideration (plan view).....	42
Figure 4.3 Maximum Bottom Flange Tip Stresses, 0.5L Main Span	43
Figure 4.4 Maximum Top Flange Tip Stresses, 0.5L Main Span.....	44
Figure 4.5 Maximum Bottom Flange Tip Stresses, Pier 3.....	45
Figure 4.6 Maximum Top Flange Tip Stresses, Pier 3	46
Figure 4.7 Maximum Bottom Flange Tip Stresses, 0.4L End Span	47
Figure 4.8 Maximum Top Flange Tip Stresses, 0.4L End Span.....	47
Figure 4.9 Maximum Top Flange Vertical Deflection, 0.5L Center Span	49
Figure 4.10 Maximum Bottom Flange Vertical Deflections, 0.5L Center Span	50
Figure 4.11 Maximum Top Flange Vertical Deflections, 0.4L End Span.....	51
Figure 4.12 Maximum Bottom Flange Vertical Deflections, 0.4L End Span	51
Figure 4.13 Top Flange Lateral Deflection, 0.5L Main Span.....	52
Figure 4.14 Bottom Flange Lateral Deflection, 0.5L Center Span.....	53
Figure 4.15 Top Flange Lateral Deflection, 0.4L End Span.....	53
Figure 4.16 Bottom Flange Lateral Deflection, 0.4L End Span	54
Figure 4.17 Top Chord Cross Frame Demands, Girders 6-7 at 0.5L Center Span.....	55
Figure 4.18 Bottom Chord Cross Frame Demands, Girders 6-7 at 0.5L Center Span	56
Figure 4.19 Bottom Chord Cross Frame Demands, Girders 8-9 at 0.5L Center Span	57

Figure 4.20 Bottom Chord Cross Frame Demands, Girders 10-11 at 0.5L Center Span	58
Figure 4.21 Top Chord Cross Frame Demands, Girders 6-7 at Pier 3.....	59
Figure 4.22 Top Chord Cross Frame Demands, Girder 8-9 at Pier 3	59
Figure 4.23 Top Chord Cross Frame Demands, Girders 10-11 at Pier 3.....	60
Figure 4.24 Bottom Chord Cross Frame Demands, Girders 6-7 at Pier 3	61
Figure 5.1 Relationship Between Cross Frame Forces and Girder Curvature.....	63
Figure 5.2 Effective Stresses Band Plot of Girders 6 and 7, 0.5L Center Span	64
Figure 5.3 Effective Stresses Band Plot of Girders 6 and 7, 0.4L End Span.....	65
Figure 5.4 Lateral Flange Bending Regions at Pier 3	66
Figure 5.5 Effective Stresses Band Plot of Girders 6-8 at Pier 3	67
Figure 5.6 Z-Displacement Band Plot of Model.....	69
Figure 5.7 Displacement Magnitude Band Plot, 0.5L Center Span.....	70

ACKNOWLEDGEMENTS

I would especially like to thank my advisor, Dr. C.J. Earls for his constant support and guidance throughout my undergraduate and graduate career. I would also like to give a special thanks to Dr. K.A. Harries, Dr. J.S. Lin, and Dr. M.A.M. Torkamani for their mentorship in my graduate work. Special gratitude is extended to my colleagues in the Department of Civil and Environmental Engineering for the invaluable support and assistance provided throughout the project.

1.0 INTRODUCTION

The congested environment of contemporary large urban highway interchanges has spawned a number of unique design approaches to solve the myriad of problems associated with handling increasing traffic volume within increasingly-confined spaces. Notable among these innovations is the advent of the elevated, horizontally-curved bridge structure. Increasingly common site considerations are highlighting the desirability of specifying a horizontally curved structure over a straight structure of similar span.

While the advent of the horizontally-curved bridge heralds a new and powerful method to manage increasingly complex traffic patterns, their employment brings rise to challenging issues concerning design, fabrication, and erection. A horizontally curved I-girder of any radius, placed on two supports (uplift unrestrained), cannot remain stable under gravity loading due to the fact that a horizontally curved girder's center of gravity is not coplanar with the web. This inherent instability occurs since the distance between a chord line drawn between the bearings of a simply supported girder and the center of gravity of the girder represents the eccentricity at which these gravity loads possess with respect to the support condition; thereby inducing torsion about an axis coinciding with the same chord line. Once gravity is "turned on," (physically effected by the removal of cranes, shoring, or both) the girder will tend to deflect and rotate out of plane in the absence of torsional restraint at one or both ends. This rigid body translation and rotation may be problematic if proper account of it has not been taken.

Oftentimes during construction of these types of bridges, it is incumbent on the steel erector, and their engineers, to devise and employ erection strategies that combat these instabilities in the

incomplete superstructure; as it is incrementally erected. These methods include the application of temporary support towers at critical points along the span, the use of cables and wood blocking to torsionally restrain the lighter bridge superstructure members against rotation, and the simultaneous erection of a stable girder pair subassembly with lateral bracing installed as shown in figure 1.1. The latter option is preferred; however, depending on the size of the superstructure members, a very large capacity crane may be required. This method can still be inadequate in the case of skewed supports or small radii of curvature due to the requirement to assemble more than two girders for the bridge superstructure to attain a stable configuration (Chavel, 2001.)



Figure 1.1 Erection of Two Curved Girders with Cross Frames Installed (Gillespie, 1968)

Complicating the job of the erector are several detailing practices that may be employed by the engineer of record in an effort to curtail significant girder deformations and rotations in the completed bridge. These significant deformations and rotations in the finished steel superstructure are accounted for and corrected through the use of various detailing practices. The engineer of record may instruct the steel detailer to create detailing dimensions that counteract the tendency of a curved structure to deflect and rotate downward in order for the girder webs to be plumb at different loading conditions. In some cases, these detailing practices intentionally lead to demonstrated component misalignments. To close these component misfits and achieve closure on the structure, the contractor is expected to force the bridge together using mechanical means such as jacks and high-capacity cranes. These methods can induce significant, and un-designed for, stresses in the girders and lateral bracing. In more extreme cases, this practice can lead to localized yielding at certain points prior to onset even of the deck load. This approach may arise out of concern from the bridge owner regarding a perceived loss of bridge capacity due to the girder webs being out-of-plumb. This is understandable since there currently exists no guidance in the dominant specifications in use around the world with regard to acceptable degrees of girder web out-of-plumbness. What initially seems an advantageous fix to a potential problem can ironically lead to even more significant capacity issues and accelerate the formation of collapse mechanisms for the return of mitigating a potentially insignificant concern. Effects on curved bridge performance caused by the web out-of-plumb condition warrant further investigation to determine their severity and application to current erection practices.

1.1 HORIZONTALLY CURVED BRIDGE BACKGROUND

The contemporary surface transportation industry encounters an increasing use of horizontally curved bridge structures for many reasons. The application of these structures is becoming more common as highway infrastructure is continually rebuilt atop existing structures in order to handle increasing traffic volumes or new interchange geometries within the context of urban settings. Horizontally curved bridges have the ability to change direction within each span, and thus are ideal structures for applications such as highway interchanges, or to connect existing roadways where abutments cannot be relocated for physical or economic reasons. Additionally, specification of the curved structure, while generating more superstructure costs in terms of materials and engineering, actually reduces the structure's cost through the elimination of interior supports, significant deck overhangs, and expensive right-of-way acquisitions. However, these attractive features come with some costs.

Curved steel I-girder bridge erection oftentimes proves to be a challenge in that each girder tends to rotate due to its self-weight; or any other load applied perpendicular to the plane of curvature. Varied erection strategies attempt to correct for and, in some cases, actively counteract the girders' tendency to deflect and rotate out of plumb. One of the goals of the current research effort is to contribute to the profession's understanding regarding the need for such efforts aimed at mitigating girder web out-of-plumbness.

1.2 LITERATURE REVIEW

The use of horizontally curved steel I-girder bridges is relatively new to the U.S. surface transportation system. The subject of curved beam behavior as it relates to bridge structures has been the focus of innumerable research papers beginning in the 1960's. Accounting for this

somewhat sudden interest in curved girder behavior, in 1961 there were not more than a half-dozen bridges in service that employed horizontally curved steel girders. The U.S. Steel Corporation reported in 1965 there had only been inquiries for 1500 tons of steel for use in curved bridge systems cumulatively. By the end of 1966; however, inquiries totaled more than 1600 tons for that year alone (Thatcher, 1967.) Subsequent years saw a marked increase in curved bridge system employment throughout the United States and the world.

The state-of-the-art related to the design of horizontally curved I-girder bridges has evolved appreciably since the inception of research work in this area in the late 1960's. At first, curved steel I-girder bridge systems were treated as straight spans subjected to an amplification factor to account for curved girder behavior in some sense. Subsequent analysis methods refined the agreement between theoretical predictions and experimental observations through the use of grillage analyses and U.S. Steel's "V-Load Method" (Grubb, 1984.)

In 1999, a benchmark study by Daniel Linzell at the Georgia Institute of Technology sought to quantify the behavior of curved steel systems during erection by instrumenting a full-scale bridge superstructure and producing companion finite element models to replicate the instrumented behavior. This work aimed to predict behavioral trends during erection when the girders were more apt to act individually rather than part of a full 3-dimensional structure and confirm the veracity of predictive studies from 3-dimensional finite element modeling techniques (Linzell, 1999.)

The three-girder erection studies by Linzell served to record the behavior of a full-scale curved bridge system at different stages of erection, validate detailed finite element methods used to model curved structures, and provide guidance on the relative conservativeness of the V-Load method as reported by AISC.

Linzell conducted experimental tests on the three girder full-scale structure shown in figure 1.2. The girders' spans and radii of curvature ranged from approximately 86 ft to 94 ft and 191 ft to 209 ft, respectively. The resulting radius of curvature to un-braced length (R/L) ratio equals 13.33 for each girder, placing them on the extreme end of current practical R/L ratios which span values from 13.33 to 20. Results of the shoring removal and effects of cross frames were analyzed to draw conclusions as to the effects on the structure at different stages of construction. It was found that by placing the shoring in regions of positive bending, deflections could be controlled to produce only elastic deformations. Subsequent replication of these construction effects was performed using the finite element analysis program ABAQUS in order to validate Linzell's modeling techniques using the model shown in figure 1.2. Subsequent analysis of the experimental and finite element results was compared to the V-load method of analysis. This comparison showed that the V-Load method gave conservative results for the exterior girders' mid-span moments and cross frame forces but gave non-conservative estimates of the mid-span moment for the interior girder.

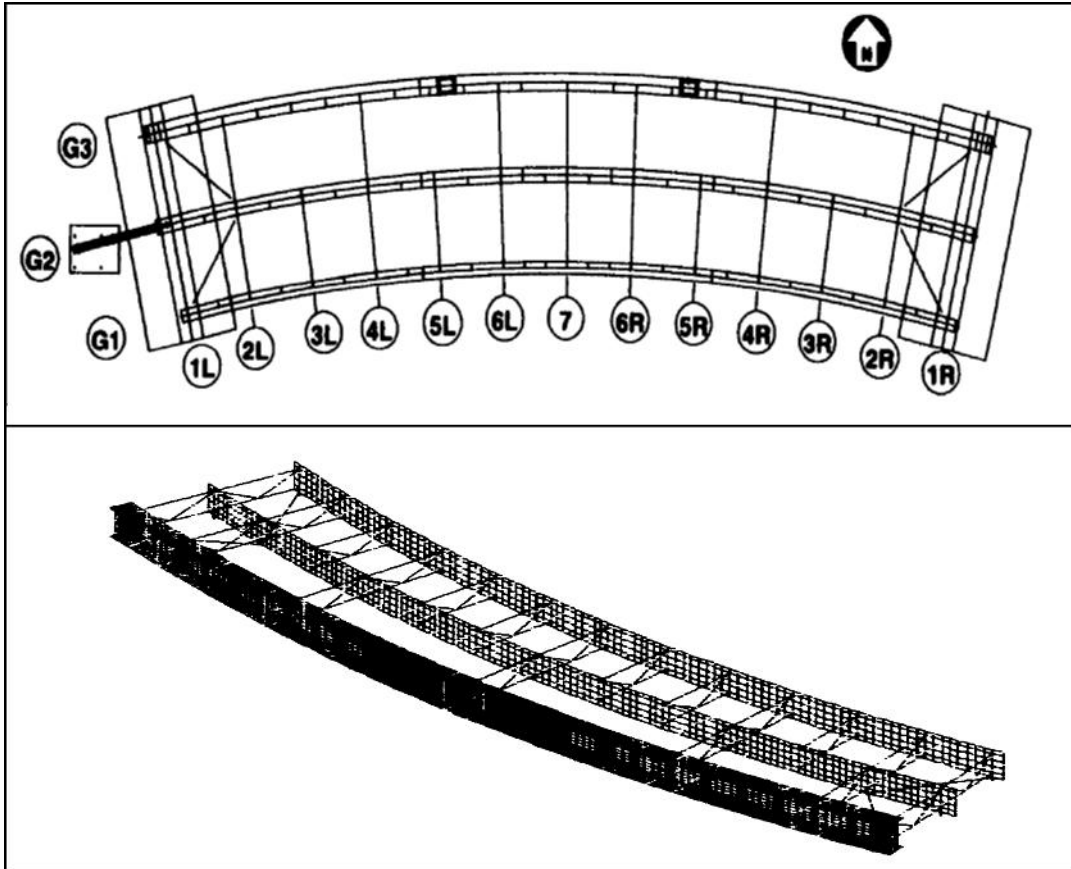


Figure 1.2 Subject Bridge Plan and Corresponding Finite Element Models (Linzell, 1999)

Following Linzell’s field monitoring of curved girder bridge systems at different stages of erection, a significant portion of construction-related curved-bridge research obtaining experimental results was conducted at the University of Minnesota in the late 1990’s. Experimental results showed that curved girders are particularly prone to deflection and out-of-plane rotation during construction due to their curvature. Using sixty vibrating wire strain gauges on a two-span, four-girder bridge (shown in figure 1.3) during its erection, the project sought to acquire several states of stress experienced by the structure prior to being stabilized by a hardened concrete deck (Galambos, et al., 1996.)

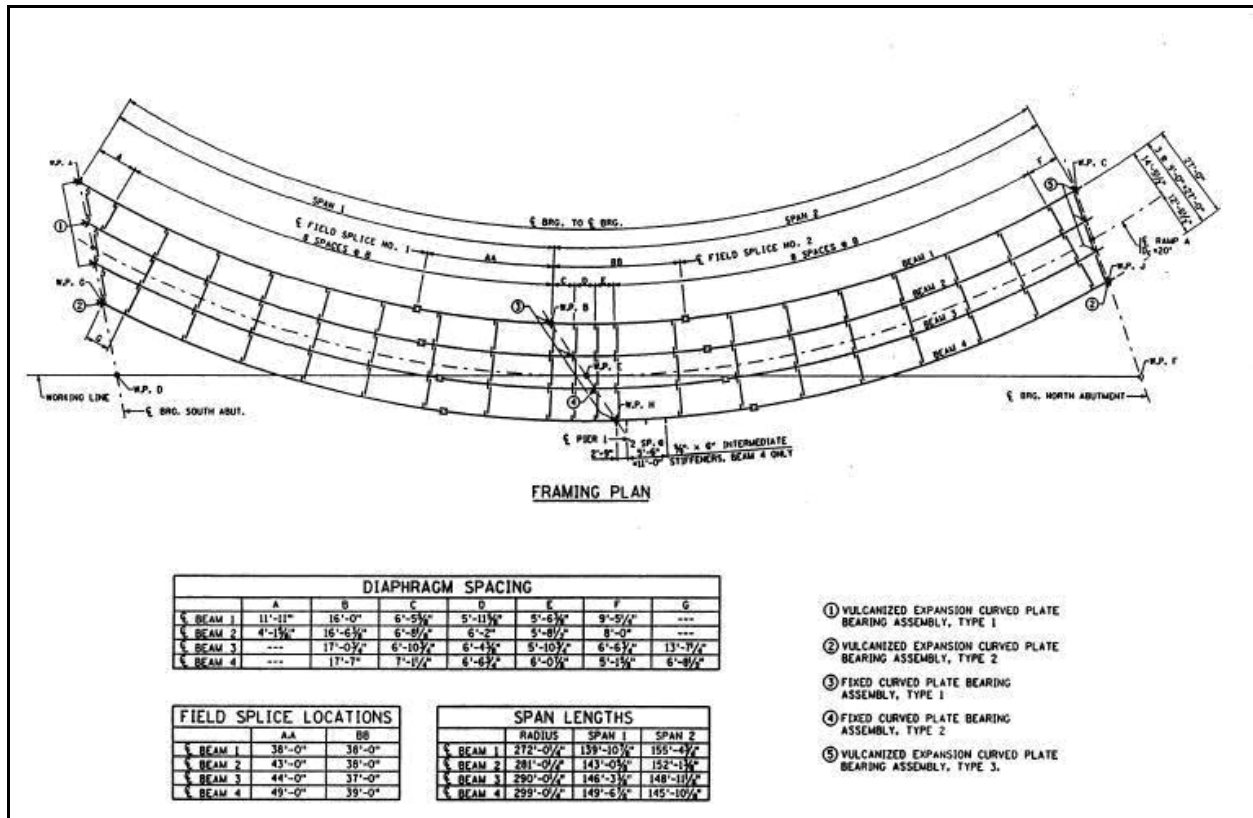


Figure 1.3 MN Bridge # 27998 Framing Plan (Galambos et al., 2000)

These resulting states of stress were subsequently compared with computational predictions from a stiffness-based 2-dimensional grillage model (Galambos et al., 2000.) Results from this study confirmed Linzell's findings in that it showed that if deflections were a primary design concern, then adequate shoring provided at the option of the erector could easily constrain maximum stresses well beneath yield (Linzell, 1999.) Additionally, the differences between the field measured results and the computed values for stresses at various points during construction were surmised to be due to variations in the restraint of warping effects, coupled with non-captured weak axis bending of the girders. As a means for approximately accounting for these important differences in predicted versus observed behavior, the Minnesota study recommended that a 20-30 psf live load allowance be imposed on the structure so as to account for this

behavior. Finally, the project illustrated the important point that as the concrete deck hardened, the stresses in the cross frames relaxed, highlighting the importance of considering the hardened deck in distributing forces between girder lines; thus permitting load sharing (Galambos et al., 2000.)

Succeeding efforts focused on the construction and erection problems associated with curved bridge behavior. Within the area of construction considerations was the prediction and mitigation in the field of the web out-of-plumb condition. The mitigation of out-of-plumbness can be achieved through manipulation of the cross frame geometry to induce torsional stresses in the form of couples applied to the girders' flanges. In 2001, Yadlosky and Fuller highlighted the severity of this problem in industry. They published a summary of studies that illustrated the inapplicability of straight girder detailing practice to curved girder structures. Figure 1.4 illustrates the deflected and rotated shape for a typical four-girder curved bridge.

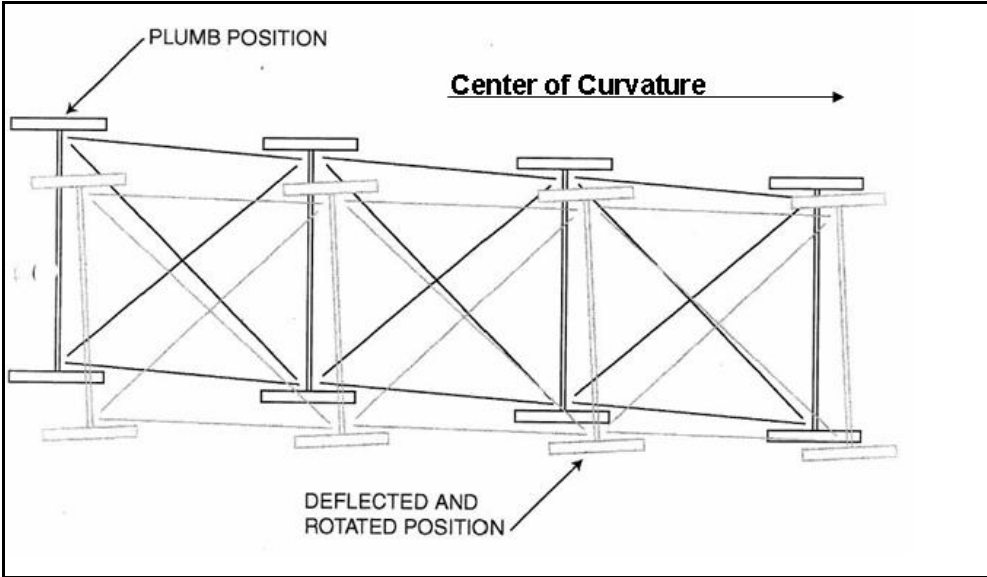


Figure 1.4 Typical Mid-Span Deflection and Rotation of a Curved Span (Yadlosky, 2001)

Since the curved I-girder has a greater designed torsional stiffness to resist the twisting moment, closer cross frame spacing, and support conditions, a common detailing practice is to detail the girders to be web-plumb at one condition and the cross frames to be web-plumb at another, this procedure is termed inconsistent detailing. In this manner, the bridge girder is subjected to a torsion applied as a couple (due to intentional member misfits) at the flanges to return it to a plumb condition. For example, on a curved girder bridge, the girders will typically be detailed to be web-plumb at the onset of total permanent dead load. However, the cross frames must be detailed for steel dead load in order to close the superstructure prior to initiating the pour sequence. Interestingly, the cross frames are instead detailed to be web-plumb in the permanent dead load condition, sometimes requiring significant applied forces to close the steel superstructure. By specification of this detailing approach, the engineer of record aims to make the structure web-plumb at the full dead load condition, possibly at the expense of inducing significant locked-in stresses during erection.

Work at the University of Pittsburgh in 2001 evaluated the problems encountered during the erection of the Ford City Veteran's Bridge in Ford City, Pennsylvania. In this bridge, the primary source of construction difficulties was the inconsistent detailing of the girders and cross frames. Using the case study, finite element modeling techniques were applied to investigate the demonstrated erection problems to promote awareness in the area of curved girder erection (Chavel, 2001.)

The Ford City Veteran's bridge has 322 ft ends spans and a 417 ft center span. The North end span is curved to a radius of approximately 510 ft measured at the roadway centerline. The report focused on the strategy of inconsistent detailing of the cross frames in order to control vertical and lateral deflections in the curved span. In the case of the Ford City Bridge, the

girders were detailed to be web-plumb at the no-load condition and the cross frames detailed to be web-plumb at the steel dead load condition. Work by Chavel and Earls showed that this inconsistent detailing failed to produce a web-plumb condition at steel dead load and produced significant fit-up problems during erection. Figure 1.5 shows the completed Ford City Veteran's Bridge steel superstructure.



Figure 1.5 Ford City Veteran's Bridge Superstructure (Chavel, 2001)

Subsequent finite element models were constructed using the finite element program ABAQUS to predict the component misalignments that occurred in the field during erection of the structure. Subsequent analysis of the structure using the model shown in figure 1.6 predicted component misalignments of 1.25 in at some cross frame locations. Interviews with the erector confirmed that during erection of the curved span, component misalignments on the order of 1.5 in were observed, necessitating the employment of high-capacity cranes and jacks to close these gaps after repeated attempts to achieve closure using more traditional approaches failed. Predictably, the same component misalignments occurred during subsequent erection of the fascia girders.

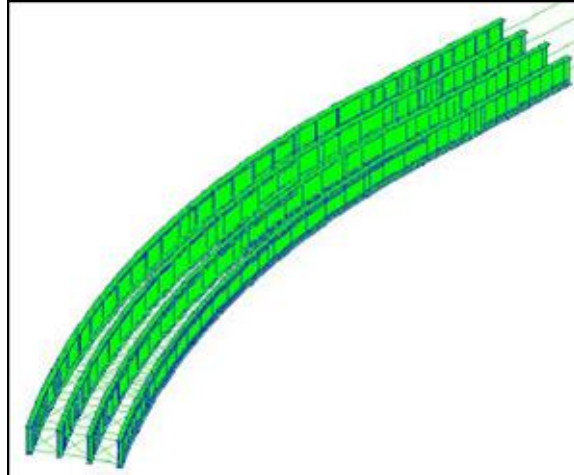


Figure 1.6 ABAQUS Finite Element Model of the Ford City Veteran's Bridge (Chavel, 2001)

The case study and subsequent replication of the erection misalignments encountered during construction of the Ford City Veteran's Bridge served to validate the finite element modeling techniques and highlight the consequences of inconsistent detailing with regards to erection difficulties. The pursuit of web-plumbness at steel dead load through inconsistent detailing was shown to produce significant difficulties and expense in terms of construction (Chavel, 2001.)

While this earlier research focused on the state of understanding regarding the behavior of curved steel I-girder bridges systems during construction, work was performed in the area of section imperfections. In the Fall of 2002, the Pennsylvania State University conducted a parametric study quantifying the effects of various geometric imperfections applied to horizontally curved girders. The models used were especially useful in that non-composite action was utilized, depicting behavior representative of the bare steel bridge system during construction. The study considered the effects of several different cross-sectional imperfections: flange rotations with respect to the web; web rotation while keeping flanges parallel; and rotation of the completed superstructure cross-section. The latter case was employed as a means of applying structural loads at an other-than-perpendicular direction (Lobo, 2002.)

The study found that a direct positive relationship existed between top flange stresses in the girders and the magnitude of imperfection applied. Table 1.1 illustrates results for a typical four-girder span for various curvature radii to span length (R/L) ratios:

Table 1.1 Changes in Stresses Due to Structure Rotation- 4 Girder Span (Lobo, 2002)

Location Along Span		Flange Stresses ^a (N/mm ²)																	
		R / L = 13.33						R / L = 16.67						R / L = 20.00					
		Stresses ^a			Change in Stresses ^d			Stresses			Change in Stresses			Stresses			Change in Stresses		
		Inner	Center	Outer	Inner	Center	Outer	Inner	Center	Outer	Inner	Center	Outer	Inner	Center	Outer	Inner	Center	Outer
1 in 500	0.25 t _{web} ^b	-162	-146	-141	12.3	2.3	8.8	-148	-144	-136	0.0	0.0	0.0	-149	-146	-140	0.0	0.0	0.0
	0.50 t _{web}	-219	-199	-190	6.3	1.1	5.6	-207	-196	-188	0.0	0.0	0.0	-205	-198	-193	0.0	0.0	0.0
1 in 100	0.25 t _{web}	-164	-146	-140	13.6	2.6	8.1	-152	-138	-135	4.2	-5.3	-0.5	-145	-133	-131	-4.1	-13.1	-8.9
	0.50 t _{web}	-221	-199	-189	8.6	1.5	4.0	-205	-188	-182	-1.5	-8.8	-6.4	-194	-179	-176	-11.2	-19.0	-16.9
-1 in 500	0.25 t _{web}	-162	-146	-141	11.7	2.2	9.1	-150	-138	-136	2.0	-5.8	0.6	-142	-132	-133	-6.5	-13.6	-7.7
	0.50 t _{web}	-218	-198	-191	5.2	1.0	6.5	-202	-187	-184	-5.1	-9.3	-3.8	-190	-179	-179	-15.0	-19.5	-14.2
-1 in 100	0.25 t _{web}	-148	-148	-150	-1.9	4.6	18.3	-149	-138	-137	0.7	-5.9	1.6	-141	-132	-134	-7.8	-13.7	-6.7
	0.50 t _{web}	-204	-201	-200	-9.0	4.0	15.1	-199	-187	-186	-7.3	-9.4	-1.8	-188	-179	-181	-17.2	-19.5	-12.2

Lobo showed that for a curved structure with a radius to length ratio of 16.67, after application of a 1/100 imperfection, the average change in quarter point top flange stresses at the web centerline was only 5.3 MPa. Considering the stress in the “perfect” structure was 132.7 Mpa, this represents an increase of only 3.9%. Interestingly, this result was obtained from a structure with a relatively tight radius of curvature, showing that even relatively large web rotational imperfections applied to curved structures did not appreciably increase flange tip stresses (Lobo, 2002.)

A more recent study (Domalik, 2005) reported on results of importance of construction problems from the standpoint of arriving at an efficient deck pour sequence. Specifically at issue

in this work was the effect of asymmetrical span lengths on the overall, system-wide, bridge response during construction and in service. Domalik and Linzell performed field monitoring activities on the S.R. 0220 Bridge 207, (framing plan shown in Figure 1.7) a horizontally curved 2 span structure with span lengths of 214'-6" and 266'-3". Using vibrating wire strain gauges and tilt-meters, strains and rotations were obtained for critical sections of the structure during all phases of steel erection; all the way through the hardening of the concrete deck.

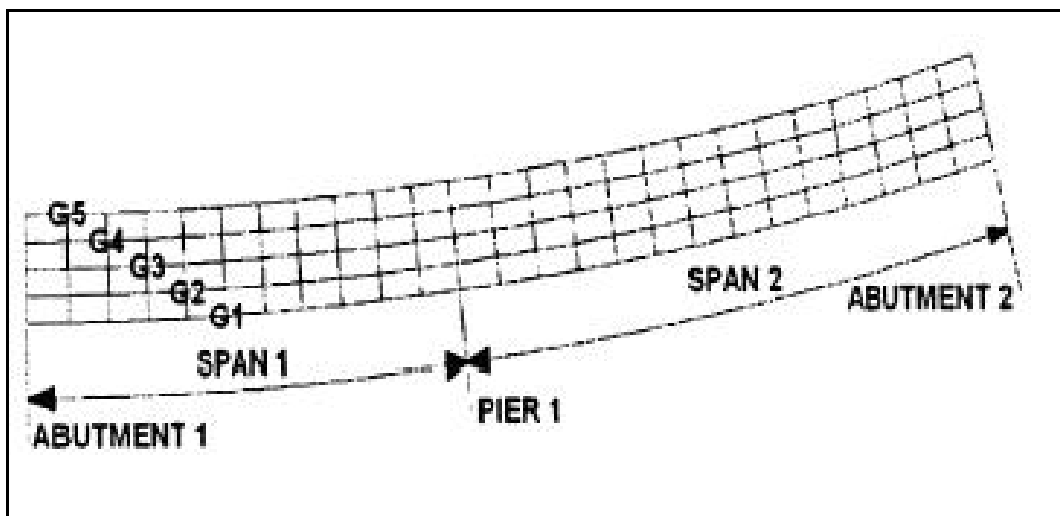


Figure 1.7 Bridge 207 Framing Plan (Domalik, 2005)

Results from the study showed that the structure's behavior under the action of self-weight was initially counter-intuitive in the shorter span as an artifact of the unequal span lengths. The steel dead load camber table is provided in table 1.2 to illustrate this atypical behavior. Since the supports are arranged radially (i.e., no skew) each girder had a slightly different span length due to its unique radius of curvature over a consistent subtended angle. Span 2 exhibited "normal behavior": a direct positive relationship between deflection, span length, and distance from the supports. Span 1, however, exhibits the opposite relationship with regard to these same

variables: within this shorter span, the longest girder has the least (in this case an upward) deflection and the shortest girder has the largest deflection. The field study concluded that this effect was due to a global torsion being applied to the structure. The heavier, longer spans comprised by the outer girders of the longer Span 1 induced deflections in the shorter spans against the influence of their own dead weight.

Table 1.2 Bridge 207 Dead Load Camber Table (Domalik, 2005)

GIRDER	GIRDER LENGTH	SPAN 1 = 214' - 6" (65.38m) measured along G3								
		1.10	1.20	1.30	1.40	1.50	1.60	1.70	1.80	1.90
G5	475' - 5" (144.91m)	0.27" 7mm	0.46" 12 mm	0.55" 14 mm	0.52" 13 mm	0.38" 10 mm	0.18" 5 mm	-0.02" 1 mm	-0.15" -4 mm	-0.15" -4 mm
G4	478' - 1" (145.72m)	0.20" 5mm	0.33" 8mm	0.35" 9 mm	0.28" 7 mm	0.12" 3 mm	-0.08" -2 mm	-0.25" -6 mm	-0.32" -8 mm	-0.24" -8 mm
G3	480' - 9" (146.53m)	0.13" 3 mm	0.19" 5 mm	0.15" 4 mm	0.03" 1 mm	-0.15" -4 mm	-0.35" -9 mm	-0.48" -12 mm	-0.49" -12 mm	-0.34" -9 mm
G2	483' - 5" (147.35m)	0.05" 1 mm	0.04" 1 mm	-0.05" -1 mm	-0.22" -6 mm	-0.43" -11 mm	-0.62" -16 mm	-0.72" -18 mm	-0.66" -17 mm	-0.42" -11 mm
G1	486' - 1" (148.16m)	-0.02" -1 mm	-0.10" -3 mm	-0.26" -7 mm	-0.47" -12 mm	-0.71" -18 mm	-0.91" -23 mm	-0.96" -24 mm	-0.84" -21 mm	-0.51" -13 mm
GIRDER	GIRDER LENGTH	SPAN 2 = 266' - 3" (81.15m) measured along G3								
		2.10	2.20	2.30	2.40	2.50	2.60	2.70	2.80	2.90
G5	475' - 5" (144.91m)	0.49" 12 mm	1.19" 30 mm	1.95" 50 mm	2.54" 65 mm	2.89" 73 mm	2.93" 74 mm	2.62" 67 mm	2.00" 51 mm	1.11" 28 mm
G4	478' - 1" (145.72m)	0.62" 16 mm	1.46" 37 mm	2.34" 59 mm	3.01" 76 mm	3.39" 86 mm	3.41" 87 mm	3.05" 77 mm	2.32" 59 mm	1.28" 33 mm
G3	480' - 9" (146.53m)	0.76" 19 mm	1.73" 44 mm	2.73" 69 mm	3.47" 88 mm	3.88" 99 mm	3.89" 98 mm	3.47" 88 mm	2.63" 67 mm	1.45" 37 mm
G2	483' - 5" (147.35m)	0.90" 23 mm	2.01" 51 mm	3.12" 79 mm	3.93" 100 mm	4.37" 111 mm	4.36" 111 mm	3.88" 99 mm	2.94" 75 mm	1.62" 41 mm
G1	486' - 1" (148.16m)	1.03" 26 mm	2.29" 58 mm	3.52" 89 mm	4.40" 112 mm	4.67" 124 mm	4.85" 123 mm	4.30" 109 mm	3.26" 83 mm	1.80" 46 mm

Similar trends were illustrated with respect to girder reactions, moments, and locations for inflection points (thereby having implications on field splice locations and deck pour limits.) The study highlighted that geometric effects due to the partially completed curved structure's true deflected shape deserve special attention. Special consideration must be given to the fact

that unusual geometries may produce typical results in tangent structural analysis, but very atypical results may occur in curved structures of similar span (Domalik, 2005.)

Following the research aimed at the effectiveness of different procedures at combating the web out-of-plumb issue, studies were conducted in 2004 at the University of Pittsburgh in order to investigate the effects of girder out-of-plumbness on ultimate capacity for single curved girders (Chavel, 2004.) In modeling this behavior, Chavel utilized a non-linear finite element model of the “CB1” beam, Figure 1.8, from Shanmugam’s 1995 study, one of 10 such curved beams used for this study.

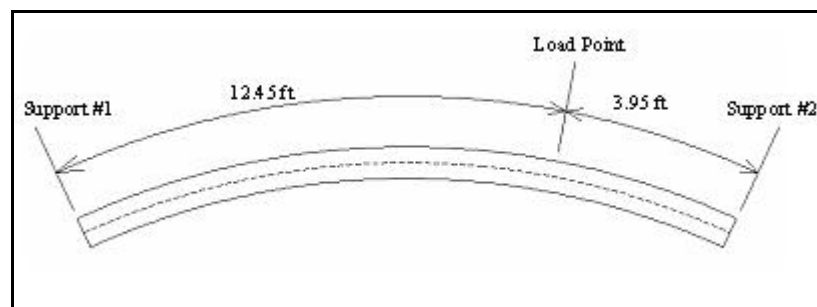


Figure 1.8 CB1 Beam Plan View (Chavel, 2004)

Chavel applied lateral restraints at each of the girder ends and at the 20 kip load point to address the inherent instability of the single curved girder. By manipulating the mesh geometry, different degrees of web out-of-plumbness were applied to the section and the resulting influence on the beam’s capacity analyzed. By varying the degrees of out-of-plumbness from 0 to 5 degrees (in 1-degree increments), the study showed that imperfect web alignment produced quantifiable effects in the areas of flange tip stresses and ultimate load; however, these changes were relatively minor for typically-encountered out-of-plumb conditions of zero to two degrees. Table 1.3 summarizes the studies’ findings.

Table 1.3 CB1 Girder Ultimate Load and Bottom Flange Tip Stress Summary (Chavel, 2004)

Web Out-of-Plane Rotation (deg)	Ultimate Load (kip)	% Reduction from 0-deg case	Tensile Bottom Flange Longitudinal Stress (ksi)	% Increase from 0-deg case
0.0	41.27	n/a	9.86	n/a
1.0	41.08	0.46%	10.03	1.7%
2.0	40.84	1.05%	10.16	3.0%
3.0	40.60	1.62%	10.29	4.4%
4.0	40.33	2.28%	10.44	5.9%
5.0	40.07	2.91%	10.61	7.6%

While Chavel's 2004 study quantified the effects of out-of-plumbness on single curved beams, it is clear from this research progression that studies are required to investigate the effects on serviceability of certain degrees of web out-of-plumbness in complete curved bridge girder superstructures during construction. The required effort to counteract deflections and out-of-plane rotations is demonstrated to create and aggravate component misalignments, requiring expensive and potentially dangerous field methods to achieve structure closure. If certain degrees of web-tilt can be shown to produce controllable, minor serviceability degradation, these expensive closure methods may be avoided and satisfactory structural performance achieved in an economical, realistic fashion. This study serves to consider this void in the current area of research, recognizing the considerable potential of this area yet to be researched.

1.3 OBJECTIVE AND SCOPE OF WORK

The objective of the present study is to investigate the effects of girder web out-of-plumbness on the response of a horizontally curved girder superstructure subject to construction loads such as steel self-weight and concrete deck loading prior to the onset of composite action. In this study, efforts are made to quantify the effects of girder web out-of-plumbness on a structure of typical

geometry (number of girder lines and radii of curvature.) The current research work aims to quantify the effects the out-of-plumb condition has on the serviceability of curved steel I-girder bridges during construction. The monitoring of locked-in stresses in the structure, as compared with those initially predicted, is considered. Case studies are reviewed for structures recently constructed to illustrate these problems and the solutions previously applied.

Computational studies are conducted on a bare steel bridge superstructure model with proportions that are consistent with those used in existing practice. Recognizing that the dominant detailing practices used to control girder web out-of-plumbness may lead to difficulties during construction, the current research uses nonlinear finite element analysis techniques to investigate what detrimental effects accompany girder web out-of-plumbness in the completed superstructure.

Results from the study are used to make recommendations concerning the validity of standard detailing practices for structures of similar spans, number of girders, radii of curvature, and skew. The implications of these new recommendations are discussed as they pertain to erection sequencing.

1.4 THESIS ORGANIZATION

Chapter 2 provides relevant theory dealing with the behavior of curved girder systems. A review of the geometric implications of curvature and manifestation of twisting moments is presented. Chapter 3 details the geometry of the subject bridge used in the study and some relevant background information related to the commercial finite element software system used in the conduct of this research: ADINA. The geometry of the subject steel superstructure, details regarding the elements used, and the construction of the finite element model are also presented in this chapter. The background, methods, inputs, and products of ADINA are also discussed.

The results of the present study for several degrees of out-of-plumbness are presented in Chapter 4; this includes graphs and figures depicting the behavior of the modeled girders and resulting influence on girder flange tip stresses, deflections, and cross frame forces. Chapter 5 provides a discussion on the results presented in Chapter 4. Conclusions based on these results and discussions are made in Chapter 6 of the presented work; with recommendations for future research in this vein.

2.0 CURVED I-GIRDER BEHAVIOR

The analysis of curved girder systems differs greatly from that of straight girders. Any structural analysis must take into account the unique response that results from the horizontal curve. Any loads introduced that are perpendicular (or have perpendicular components) will serve to produce not only the shear and flexural moment normally seen in straight girder analysis, but also a torsional moment about the girder's longitudinal axis. It is this inherent torsional moment that tends to produce out-of-plane rotations and is the source of torsional stresses that can be visualized as arising form of lateral flange bending. In order to familiarize the reader with curved girder behavior, a brief overview of curved beam analysis fundamentals is presented.

2.1 REACTIONS

Consider the simply-supported single-girder system subjected to the arbitrary point load P shown in figure 2.1; assume torsional restraint at the end denoted B.

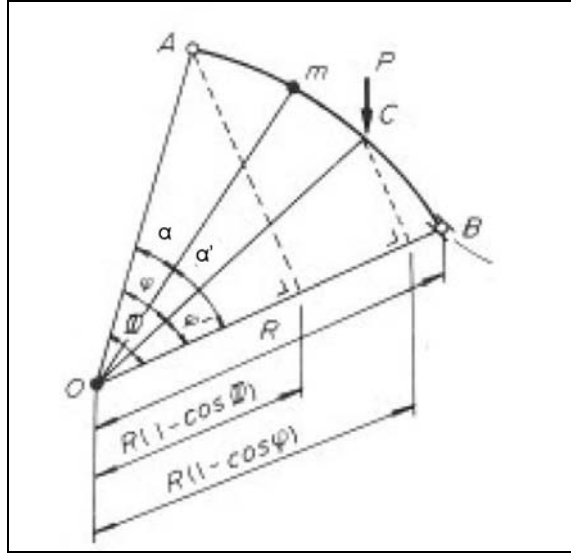


Figure 2.1 Statically Determinate Single Curved Girder (Nakai, 1988)

In much the same manner as straight girder analysis the reactions at ends A and B of the idealized girder can be obtained by satisfying the equilibrium equation requiring:

$$\sum M_{OB} = 0 \quad (2-1)$$

Using the central angle Φ and assigning the angular coordinate φ' to denote the position of the point load P, we find that the moment arms for the reaction at pt A and the load at point P to be:

$$\begin{aligned} r_A &= R * \sin(\Phi) \\ r_P &= R * \sin(\varphi') \end{aligned} \quad (2-2)$$

Summation of moments about axis OB yields the following expressions for the reactions at A and B:

$$\sum M_{OB} = 0 = R_A * R * \sin(\Phi) - P * R * \sin(\varphi') \quad (2-3)$$

$$R_A = P * \left[\frac{\sin(\varphi')}{\sin(\Phi)} \right] \quad (2-4)$$

$$R_B = P * \left[1 - \frac{\sin(\phi')}{\sin(\Phi)} \right] \quad (2-5)$$

2.2 FLEXURAL MOMENT

The internal bending moment for the beam is obtained in a similar manner as for a straight girder, by employing simple trigonometric relations to account for the geometric changes due to curvature. The bending moment at an arbitrary point “m” with a position denoted by α is given by the following expressions:

For the interval $0 \leq \alpha \leq \phi$:

$$M_m = R_A * R \sin(\alpha) = P * \left[\frac{\sin(\phi')}{\sin(\Phi)} \right] * R \sin(\alpha) \quad (2-6)$$

For the interval $\phi \leq \alpha \leq \Phi$:

$$M_m = R_A * R \sin(\alpha) - PR * \sin(\alpha - \phi) = PR * \left[\frac{\sin(\phi')}{\sin(\Phi)} \right] \sin(\alpha) - \sin(\alpha - \phi) \quad (2-7)$$

2.3 TORSIONAL MOMENT

The eccentricity of the load with respect to a chord line drawn between the supports produces a torsional moment in the girder. The eccentricity of the applied load to the chord line drawn between the supports is thus of critical importance. This moment arm determines the torsional moment that must be resisted in order to ensure structural stability. Indeed, as the eccentricity of the load with respect to the chord line decreases as each support is approached, the torsional moment becomes zero.

Using trigonometry to find this relationship, it can be shown that the torsional moment at the arbitrary location m is represented for the interval $0 \leq \alpha \leq \phi$ by:

$$T_o = R_A * (R - R \cos \alpha) \quad (2-8)$$

Substitution of (2-4) into (2-8) yields the expression for the torsional moment for the interval $0 \leq \alpha \leq \varphi$:

$$T_o = PR * \frac{\sin(\varphi')}{\sin(\Phi)} * (1 - \cos(\alpha)) \quad (2-9)$$

Using an analogous procedure to find the torsional moment for the interval $\varphi \leq \alpha \leq \Phi$:

$$T_o = R_A * R[(1 - \cos(\alpha))] - PR[1 - \cos(\alpha - \varphi)] \quad (2-10)$$

By substitution of (2-4) into (2-10) and simplifying:

$$T_o = \frac{PR(\sin(\varphi'))}{\sin(\Phi)} [1 - \cos(\alpha)] - PR[1 - \cos(\alpha - \varphi)] \quad (2-11)$$

2.4 LATERAL FLANGE BENDING

Since the member cross sections of a horizontally curved I-girder bridge are non-circular, they may experience warping stresses when twisted (Boresi, 2003.) Figure 2.2 depicts how the non-uniform torsion manifests itself in an I-shaped cross-section as a notional flange bending effect.

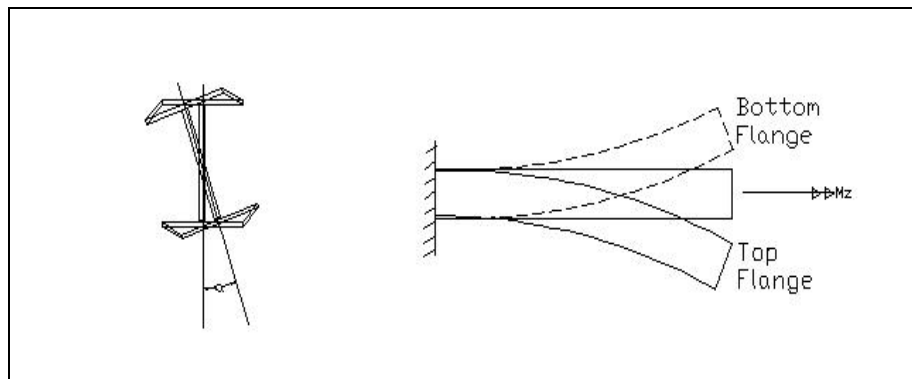


Figure 2.2 Non-Uniform Torsion of an I-Girder Subject to Longitudinal Moment

The effect of lateral flange bending is extremely important at support locations as it can influence flange stresses in these negative bending regions of continuous structures. It is pointed out that the influence of the flange bending stresses (occurring normal to the cross-section) is additive to the in-plane flexural normal stresses as shown in figure 2.3.

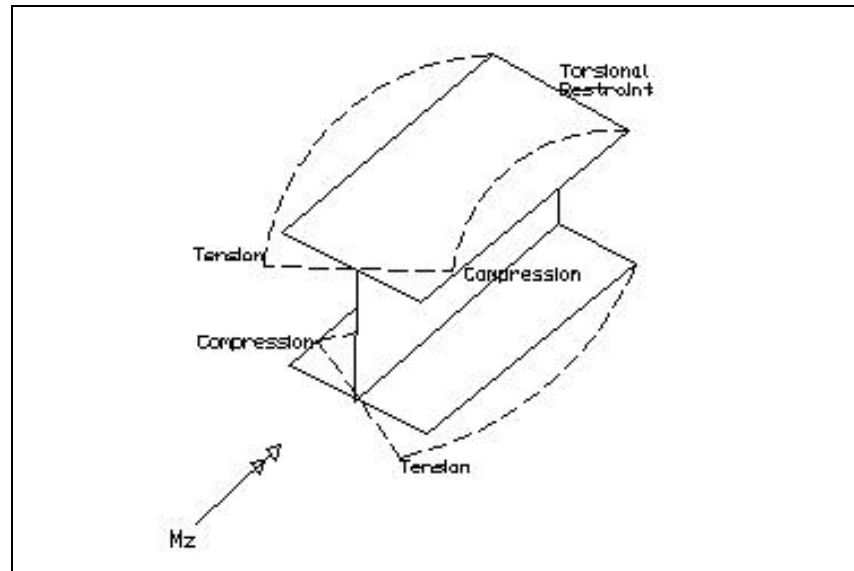


Figure 2.3 Manifestation of Compressive and Tensile Regions in Support Vicinity

With this overview, it is obvious that the behavior of a horizontally curved I-girder is very different from its straight counterpart. In addition to the shear and flexural moments found in straight girders, the curved beam experiences a torsion about its longitudinal axis due to the varying eccentricity of the beam geometry measured from the chord line connecting the supports. This varying torsional moment (resulting from the varying eccentricity of the the beam centerline from the support chord line) causes warping of the non-symmetric cross-section and considerable lateral flange bending in the support regions.

3.0 MODEL OVERVIEW

3.1 SUBJECT BRIDGE

The bridge chosen for this study was the Chelyan Bridge in the town of Chelyan, West Virginia. Spanning the Kanawha River, the completed structure has seven spans in total; with a three-span curved approach bridge (i.e. spans 4-6). Spans 4-6 of this bridge are comprised of six concentric girder lines of horizontally curved steel girders continuous over three spans and supporting a reinforced concrete deck with a constant radius of 509 ft measured along the roadway centerline. The structure's pier caps are radial with the horizontal curve; thus no skew exists at the supports. The radii of curvature for the girders vary from 484 feet to 535 feet at the outer girder. Figure 3.1 shows a plan view for this section.

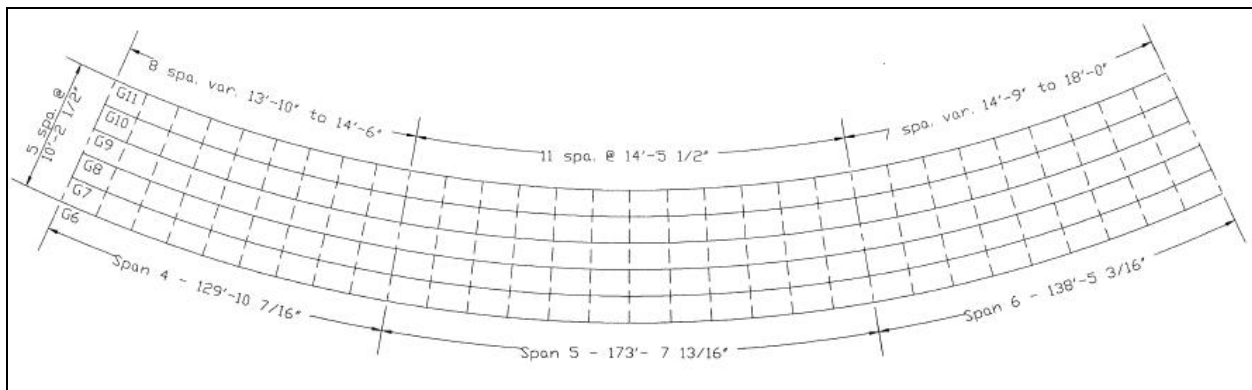


Figure 3.1 Framing Plan for Subject Bridge (Chelyan Bridge)

The six girders have a constant web depth of 72 in, with a web thickness that varies from 3/8 in to 5/8 in at high-shear locations. The top and bottom flanges are of variable thickness; achieved by splicing plates of varying thickness but maintain a constant width of 16 inches. Each girder has 47 web stiffeners and 31 individual cross frame connection plates to facilitate attachment of the K-type cross frames. The web stiffeners are located on the side of the web corresponding with the outside of the radius of curvature for the innermost three girders and on the inside for the outermost trio. This switch in web side for the stiffener installation is done primarily for aesthetic reasons. The cross frame connector plates are positioned on the interior faces of the exterior girders (with respect to the roadway centerline), and each side of interior girder webs at each of the radial cross frame locations. Each girder pair is connected through the use of 27 K-type cross frames and four Channel diaphragms located above the piers. Cross frames are arranged radially from the center of curvature at approximately equal intervals of 14.5 ft; measured along the curved bridge longitudinal axis. Figure 3.2 shows a typical K-type cross frame set of the type used in this structure.

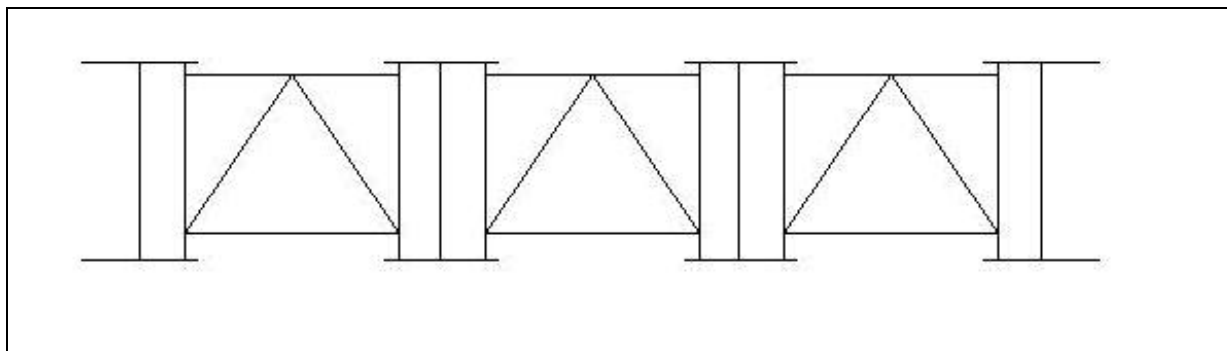


Figure 3.2 Typical K-type Cross Frame Used in Subject Bridge and Finite Element Model

3.2 IDEALIZED CROSS SECTION DIMENSIONS

It was decided to idealize the dimensional variations somewhat in order to mitigate the already considerable computational effort associated with a detailed three-dimensional finite element analysis for this relatively sizeable structure. In pursuit of this objective to simplify the modeled geometry, a weighted average was obtained based on plate width and thickness, as a function of their length; as measured along the longitudinal axis. This value for each span dimension was then applied throughout the web or flange for that entire span in order to obtain a prismatic member before the application of stiffeners and cross frame connection plates. An example of this simplification procedure, for one girder, is shown in Table 3.1.

Table 3.1 Web Thickness Simplification Procedure for Girder #6

Girder #6					
Total Length, span 4	1637.25	in			
Web thickness (in):	Web Width	Length at thickness (in)	% total length	Weighted Web Thickness (in)	Weighted Web Width (in)
0.5	72	1157.25	71%	0.3534	50.8914
0.5625	72	348	21%	0.1196	15.3037
0.5625	72	132	8%	0.0454	5.8049
			100%	0.5183	72.0000
Total Length, Span 5	2188.1875	in			
Web thickness (in):	Web Width	Length at thickness (in)	% total length	Weighted Web Thickness (in)	Weighted Web Width (in)
0.5625	72	132	6%	0.0339	4.3433
0.5625	72	348	16%	0.0895	11.4506
0.5	72	1228.1875	56%	0.2806	40.4122
0.5625	72	336	15%	0.0864	11.0557
0.5625	72	144	7%	0.0370	4.7382
			100%	0.5274	72.0000
Total Length, Span 6	1723.1875	in			
Web thickness (in):	Web Width	Length at thickness (in)	% total length	Weighted Web Thickness (in)	Weighted Web Width (in)
0.5625	72	144	8%	0.0470	6.0168
0.5625	72	348	20%	0.1136	14.5405
0.5	72	1231.1875	71%	0.3572	51.4427
			100%	0.5178	72.0000
				0.521	

The exterior curved girder (the girder with the largest radius of curvature) consists of heavier sections than the others. This is no surprise; as the demonstrated behavior of curved bridges is such that the exterior girders play a proportionately larger role in resisting the internal bending moments. The geometry, location, and thickness of the web stiffeners, bearing stiffeners, and cross frame connection plates remain unchanged.

3.3 FINITE ELEMENT MODEL

3.3.1 Bridge girder modeling

The bare steel girders of the Chelyan Bridge are modeled in ADINA using shell finite elements placed at the mid-planes of the constituent cross-sectional plate components. The shell elements employed in these models are the four node MITC-4 nonlinear finite elements. ADINA automatically assigns five degrees of freedom to each node of the MITC-4; unless the loading or mesh compatibility require 6 degrees of freedom. Elimination of the “drilling” rotational degree of freedom, about the axis normal to the shell surface, helps to maintain efficiency with regard to computational expense. However, whenever element intersections require, such as web-flange junctions, plate locations, or cross frame connection regions, all six degrees of freedom are utilized. Sizing of the web elements was achieved with a mean aspect ratio of 2 by partitioning the web into approximately 2 inch long by 4 inch deep elements and carrying this mesh density throughout the web for each girder line. Flanges were modeled with a minimum of eight elements across the flange width in order to ensure satisfactory resolution to properly model the occurrence of local buckling at ultimate capacity (the models are to be used as part of later research). A ratio of near unity was maintained throughout the flange mesh. The web stiffeners

and cross frame connector plates were modeled with two lines of shell elements and have a mean aspect ratio of 1.5 to ensure mesh compatibility with the web at attachment locations. Figure 3.3 shows a representative portion of the steel I-girder finite element mesh with cross frames omitted for clarity.

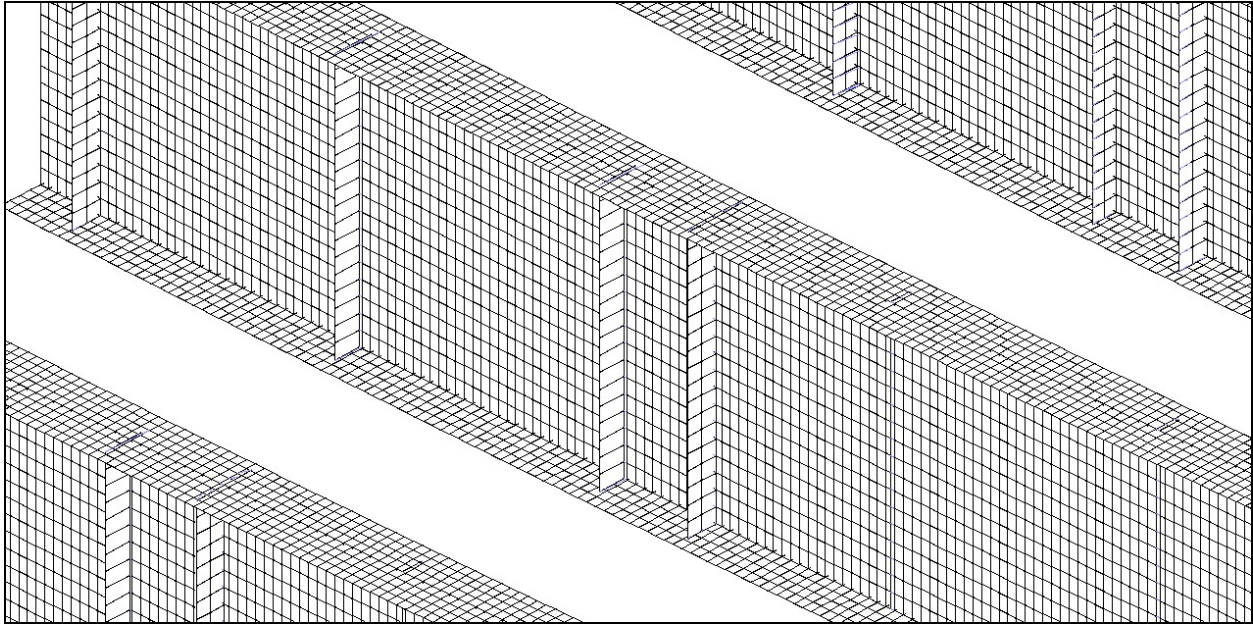


Figure 3.3 Girder Web and Flange Mesh Construction

Since the connector plates were generated as separate mesh entities, multi-point constraints were used at plate-to-member intersection locations in order to provide nodal connectivity throughout the model where these disparate mesh components must connect. Within the context of multi-point constraints, degrees of freedom at one node are coupled to the same degrees of freedom at another in a master-slave type relationship. In fact, within the assembled system of equations, the slave degrees of freedom no longer exist and only the master's degrees of freedom remain. As a result, application of multi-point constraints reduce the total number of system degrees of freedom. For this model, the web served as the master surface for each girder line

because all plate elements are connected to it at their respective locations. In applying shell elements to model this bridge, the centerline of each cross-sectional plate component is used to define the shell reference surface; a uniform shell thickness is then applied to the element group. In order to achieve this mesh density, each girder model required approximately 100,000 elements. This refinement was necessary to enable follow-research aimed at understanding the ultimate strength of these types of bridge systems. With such a context, the interaction or geometric and material nonlinearity requires very high mesh densities.

3.3.2 Girder stiffeners and connection plates

Each girder line in the structure contains 47 transverse web stiffeners placed at constant spacing for various intervals measured along the girder's longitudinal axis. Since the unit is a three-span continuous structure, the tension flange region alternates between the top and bottom along each girder's length. In practice, transverse stiffeners are welded on both sides and are routinely cut short of the tension flange; this creates a class C fatigue detail (AASHTO, 2005.) The actual structure details $\frac{1}{4}$ in gaps between the unattached edges of each transverse stiffener and tension flange, whether top or bottom. Since the purpose of this study is to quantify elastic response under varying degrees of web out-of-plumbness, and subject to monotonic construction loading, this fatigue detail is omitted and stiffeners are connected to both flanges in the same manner as the connector plates at diaphragm locations. The structure contains no longitudinal stiffeners. Figure 3.4 depicts a typical connection region for a cross frame connection plate and web stiffener to the girder.

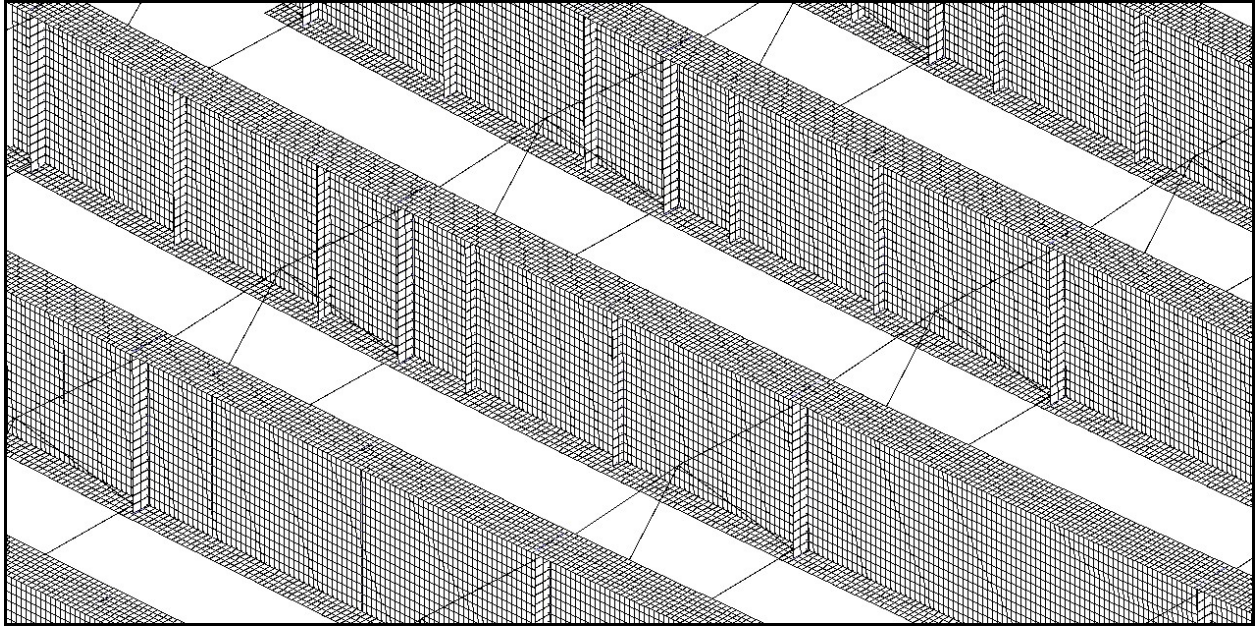


Figure 3.4 Cross frame Brace Plate and Web Stiffener Mesh Construction

The girders function as a single cross-section by transmitting their torsion and shear among the other girders within the cross-section by way of the cross frames. Attachment of each K-type cross frame to the girders is effected through the modeling of cross frame connection plates. Each girder carries 31 such attachment locations on either one or both sides of the web depending on whether the girder is located on the fascia.

3.3.3 Cross frame modeling

Linear beam elements were chosen to model the cross frame members. At bearing locations, channel-type diaphragms existed in the actual structure; however, K braces were utilized in this model for these four bracing locations as they provided adequate moment transfer between girder lines for the objectives of this study in addition to eliminating unnecessary complexity. Cross frame forces are transferred into the girders via the previously described connection plates. Figure 3.5 shows the cross frame arrangement and connection regions for the global structure.

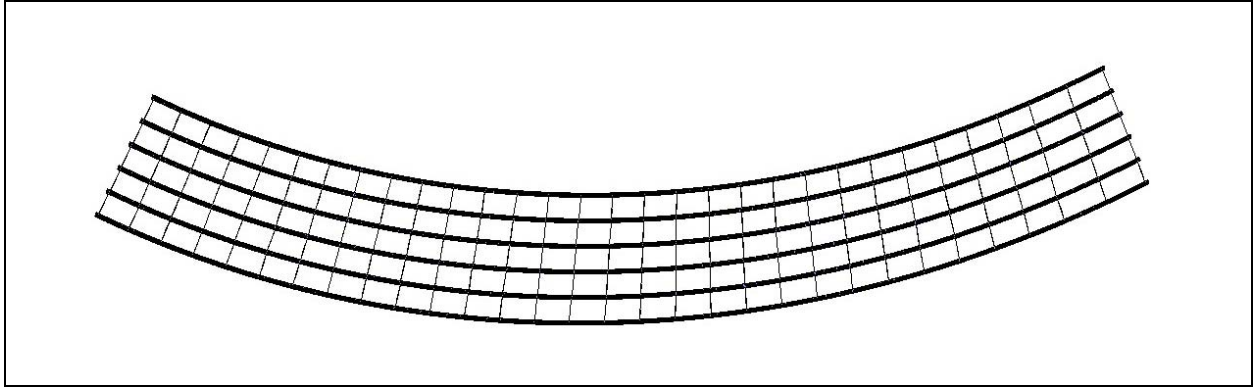


Figure 3.5 Plan View of Model With Cross frame Locations

3.3.4 Artificially induced out-of-plumbness

In applying the various degrees of out-of-plumbness to the completed plumb mesh, several alternatives were considered. In order to accurately represent field conditions, each girder deflects and rotates about the bottom web-flange intersection (work point). Vertical camber is neglected.

Girder web tilting (out-of-plumbness) is introduced within a give girders cross-section by rotating the cross-section about the bottom flange-web unction in a fashion consistent with what is schematically in figure 3.6.

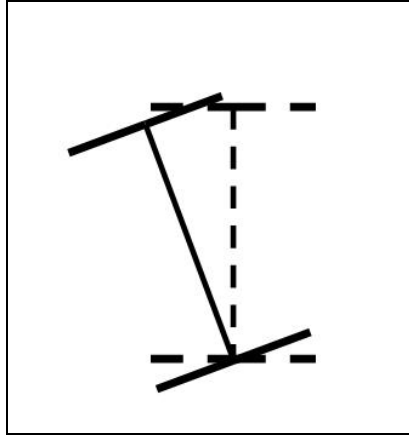


Figure 3.6 Original and Out-of-plumb Position of Typical Girder Cross-section

Since the girders receive considerable torsional restraint from the channel diaphragms over the pier lines, the girders are returned to a plumb position at the piers. Considering these ordinates, a sine function is fit to the top web-flange intersection such that the function has a period of twice the span length measured along the girder's centerline.

$$y(x, \delta) = \delta \sin\left(\frac{\pi x}{L}\right); \delta = f(h) \quad (3.1)$$

Where: δ : Maximum lateral displacement; occurring at mid-span

L: Span length

x: Longitudinal position from pier

y(x): incremental lateral displacement imperfection imposed at an arbitrary position "x"

h: vertical distance from bottom web-flange intersection

This function's values represent the additional lateral deflection, measured from the bridge's center of curvature axis, imposed to achieve the desired degree of web out-of-plumbness at the

mid-span point. Superposition of the lateral deflection induced by web out-of-plumbness, and the original positions from the plumb model, yields the new top web-flange intersection for the girder line. To facilitate this process, extensive use is made of a cylindrical coordinate system. Figure 3.7 depicts the superposition of the original and new top web-flange intersection procedure to determine the new cross-section's position.

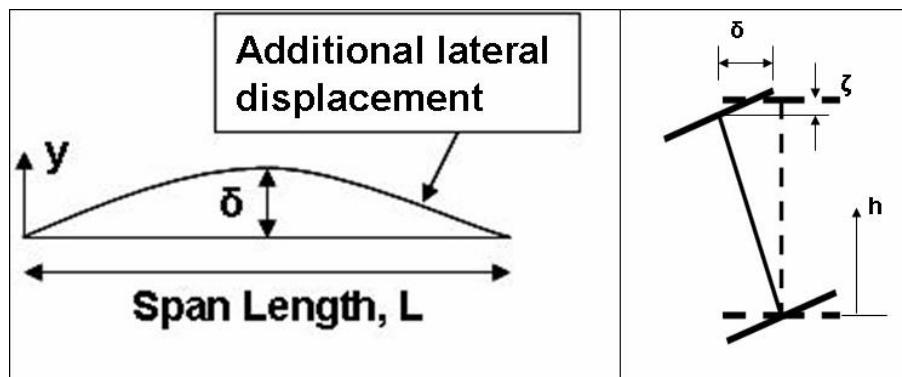


Figure 3.7 Superposition of Existing and Additional Lateral Displacement

From this new top web-flange intersection, certain assumptions about cross section compatibility are preserved. The cross section is assumed to retain its original shape, thus the top and bottom flanges remain perpendicular to the web throughout each span. Due to the web tilt, the top web-flange intersection is located within the global reference frame vertical axis by multiplying the cross-sectional depth by the cosine of the web out-of-plumbness angle. Corresponding values are computed to preserve the positions of web stiffeners, cross frame brace plates, and cross frames with respect to the girder cross section. Since the bottom flanges are maintained as parallel to the plane of curvature at support locations, no alteration to the boundary conditions local reference frame is necessary.

In this manner, new node clouds are computed to update the initial positions of each of the nodes while element and section connectivity are preserved in full. The completed finite element mesh of the outer three girders is shown below for the 5-degree rotated case in figure 3.8 (note the cross-sectional twist that accommodates the change from 0-degree web out-of-plumbness at the girder supports to the maximum 5-degree web out-of-plumbness occurring at mid-span of the girders.)

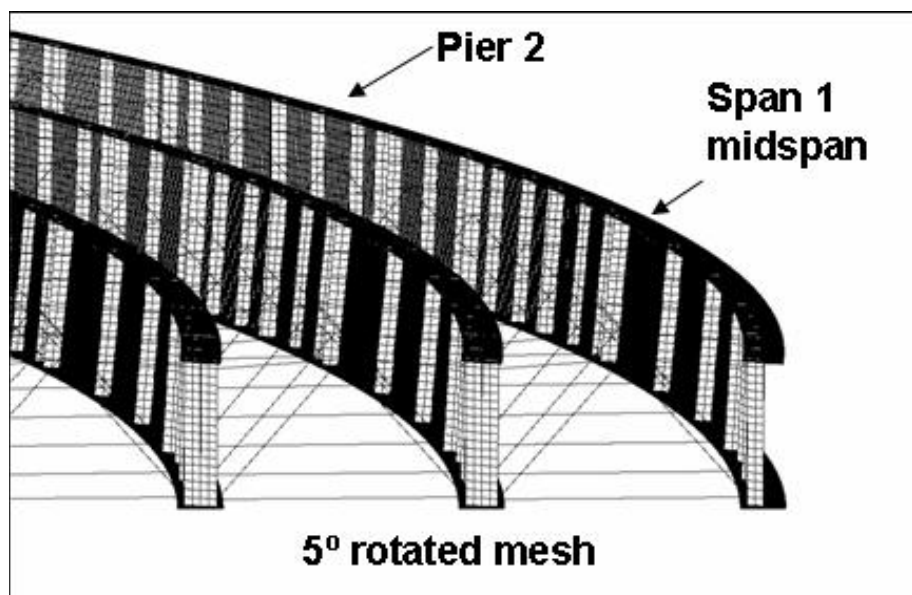


Figure 3.8 Five-Degree Out-of-Plumb Mesh

3.3.5 Constraints

Constraint equations in ADINA (the same principle as multi-point constraints in ABAQUS) specify a dependent degree of freedom (slave) as a linear combination of independent (master) degrees of freedom (ADINA, 2003.) For this model, the girder web top and bottom edges are master node sets to the top and bottom flange centerlines, respectively. Web stiffeners and cross

frame brace plates are slaved to the webs, and appropriate flange locations, while the cross frame beam elements nodal terminuses are slaves to the appropriate locations on the cross frame brace plates as shown in figure 3.9. Subsequent support conditions at pier locations fully constrain the model against rigid body motion.

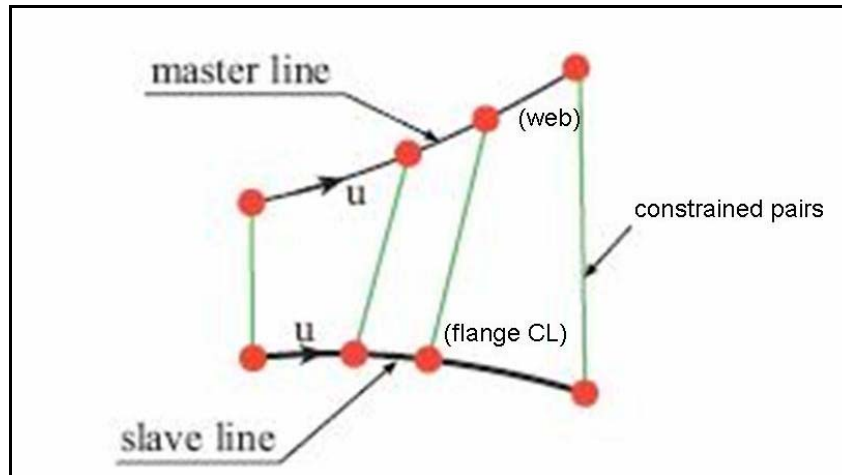


Figure 3.9 Constraint Equation Relationship Along Edges (ADINA, 2003)

Since it is that the nodes to be constrained are in effect mean to coincide, coefficients of unity are employed to ensure that the master and slave nodes share the same degrees of freedom. It is pointed out that the ADINA RIGIDLINK option is not used since the kinematics associated a rigid link of any off-set distance would not correctly model the condition being sought: nodal coincidence.

3.3.6 Boundary conditions

The actual boundary conditions in the subject bridge are composed of longitudinally and transversely guided rollers as well as non-directional bearing pads. In modeling the guided rollers, local skewed coordinate systems were applied to the node sets at the pier locations.

In establishing the skewed coordinate system, a tangential local x-axis and radial local y-axis are desired such that application of the boundary conditions in these local directions accurately reproduces the effects of the guided bearings. Coordinate system rotation about the z-axis is unnecessary as the axis perpendicular to the plane of curvature is not affected by these new gravity resisting support alignments.

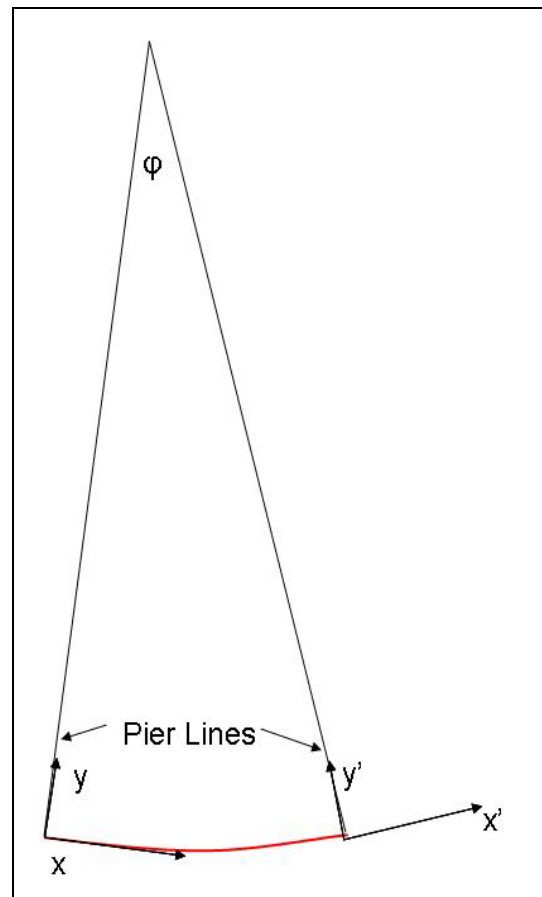


Figure 3.10 Establishment of the Local Coordinate Systems for Support Locations

Rotation of the local coordinate axes is established by applying standard trigonometric principles. The central angle formed between pier radials is the same as the angle between tangents of the same radial pier lines as shown in figure 3.10. By establishing the first pier

coincident with the global x-y coordinate system, successive transformed $x'-y'$ coordinate systems are established for each succeeding support region. ADINA requires input of transformed radials in terms of position vectors from the global system in the manner depicted in figure 3.11.

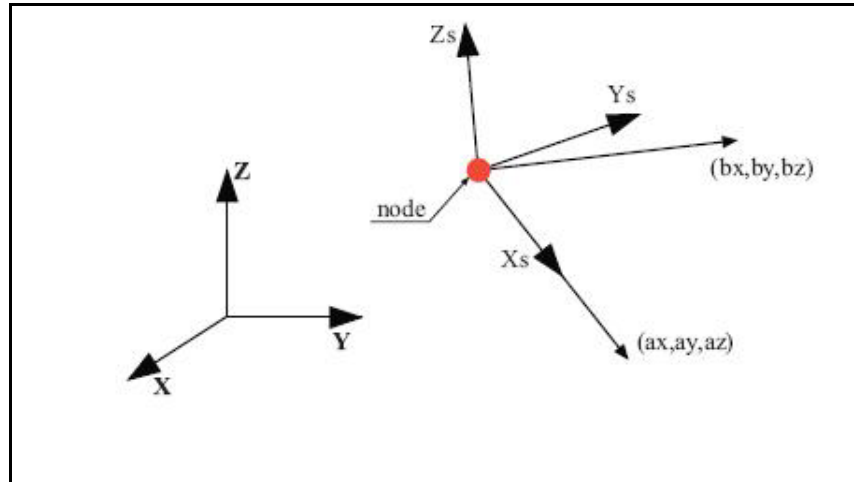


Figure 3.11 ADINA Input of Skewed Coordinate System Vectors (ADINA, 2003)

Since the global z-axis (the axis perpendicular to the plane of curvature) is constant for these transformations, the skewed axes position vectors are computed by utilizing the planar procedure illustrated in figure 3.12.

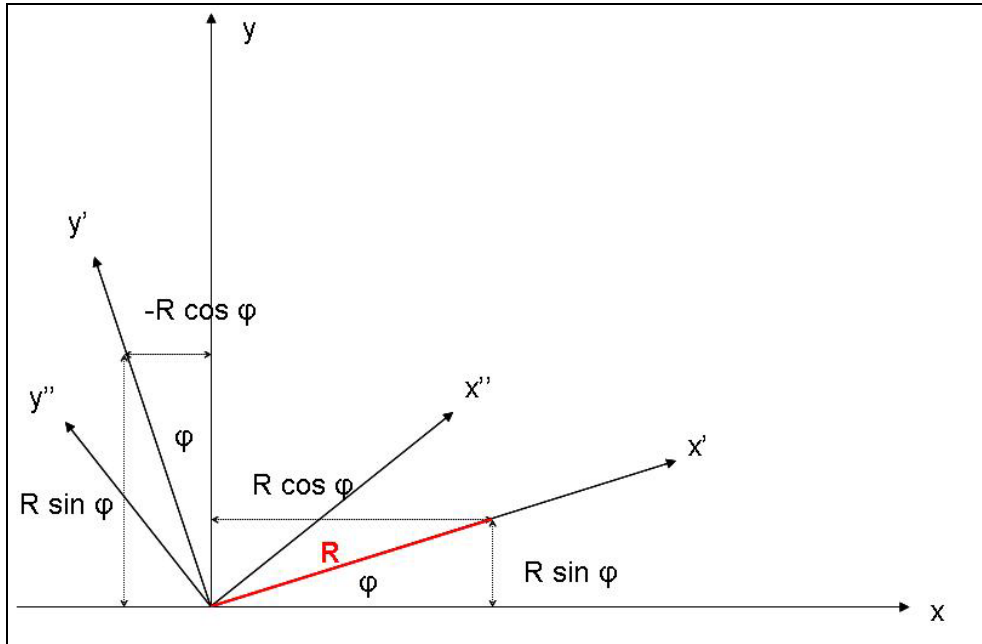


Figure 3.12 Local Coordinate System Establishment

Upon successful creation of these local coordinate systems, the appropriate boundary conditions are formed by variously applying translational and rotational fixity in each of the three transformed axes.

3.3.7 Loading

Each of the six girder finite element models is subjected to two discrete load cases to evaluate serviceability under construction loading. The first load case is steel self-weight. By specifying the material density of steel at 490 lb/ft^3 , a mass-proportional body force is applied to the

structure in order to model the influence of gravity induced self-weight. This load case reproduces the loading at the completion of steel erection. At this state, inferences can be made as to the effects of out-of-plumbness prior to the application of the concrete deck. The second load case is superposition of steel superstructure self-weight plus the weight of the wet concrete deck. Specifying the concrete deck thickness at 8.5 inches in accordance with the subject bridge's geometry, equivalent tributary-width-based line loads are applied to the girders' top web-flange intersections (so as to avoid local flange bending).

4.0 RESULTS PRESENTATION

4.1 GIRDER FLANGE STRESSES

The girder flange effective stresses (von Mises stresses) are monitored in three specific model regions in order to quantify the effects of web out-of-plumbness on the vertical and lateral bending moments. By investigating the flange tip stresses, conclusions can be made as to the effects of the varying distance of the flange tips from the neutral axis, as well as interaction effects between the vertical bending moment and the bi-moment. Since the maximum vertical bending moment is of primary interest, the locations to be evaluated are the midpoint of the center (longest) span, 0.4L of span 3 (longer of the two ends spans), and the negative moment generated at pier 3 between the two longer spans. At each location, investigations are made at the quarter points between cross frame locations for flange tip stresses at the top and bottom flange extremities as depicted in figures 4.1 and 4.2.

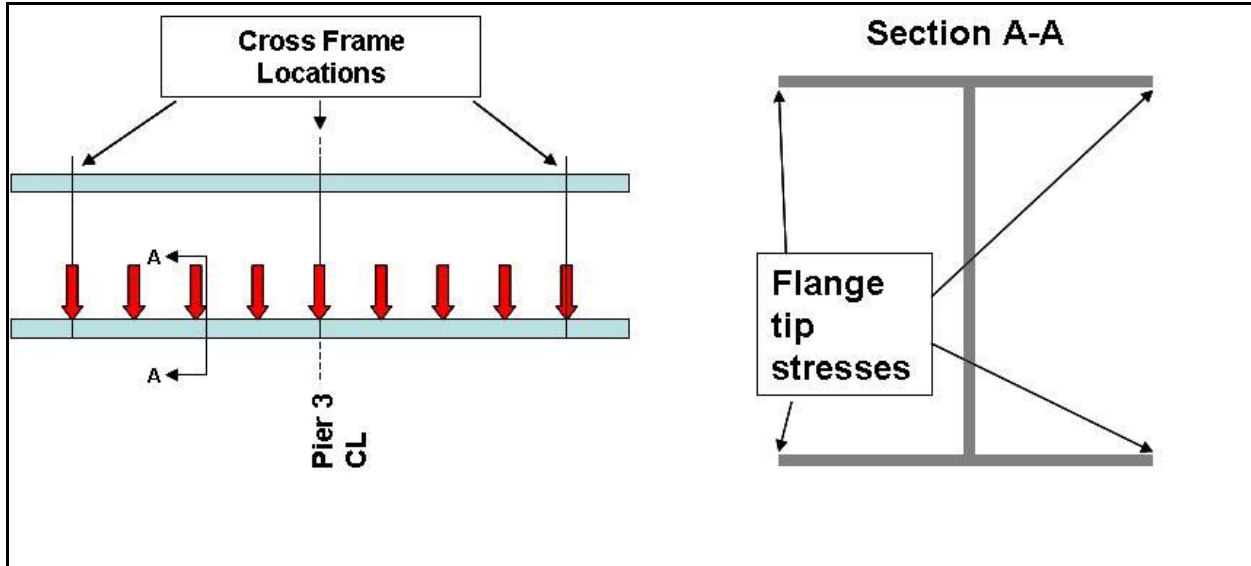


Figure 4.1 Flange Tip Stress Locations, Pier 3 Location (typical for other locations)

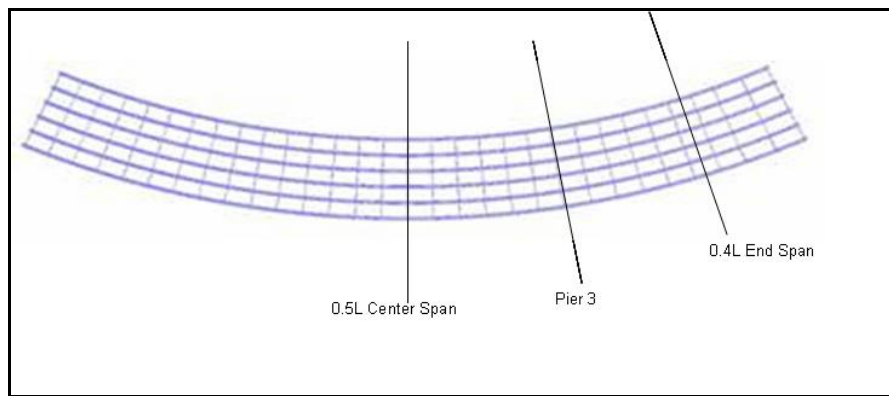


Figure 4.2 Critical Locations Under Consideration (plan view)

Investigation of the bottom flange tip stresses on the outside of the radius of curvature for the 0.5L section of the center span yielded a positive relationship between increasing angles of out-of-plumbness and maximum flange tip stresses. At the mid-span location for the plumb model, the bottom flange tip stress was 3.023 ksi. The bottom flange tip stresses at 2 and 5 degrees of web-out-of-plumbness were 3.360 ksi and 3.811 ksi, respectively. This change in web angle resulted in an 11% increase in flange tip stress at 2 degrees (a common out-of-plumbness in

practice) and a 26% increase at the 5 degree out-of-plumbness condition. Figure 4.3 shows only the result for the girder with the maximum radius of curvature, Girder 6. Subsequent girder lines exhibited similar behavior and can be viewed in the appendix.

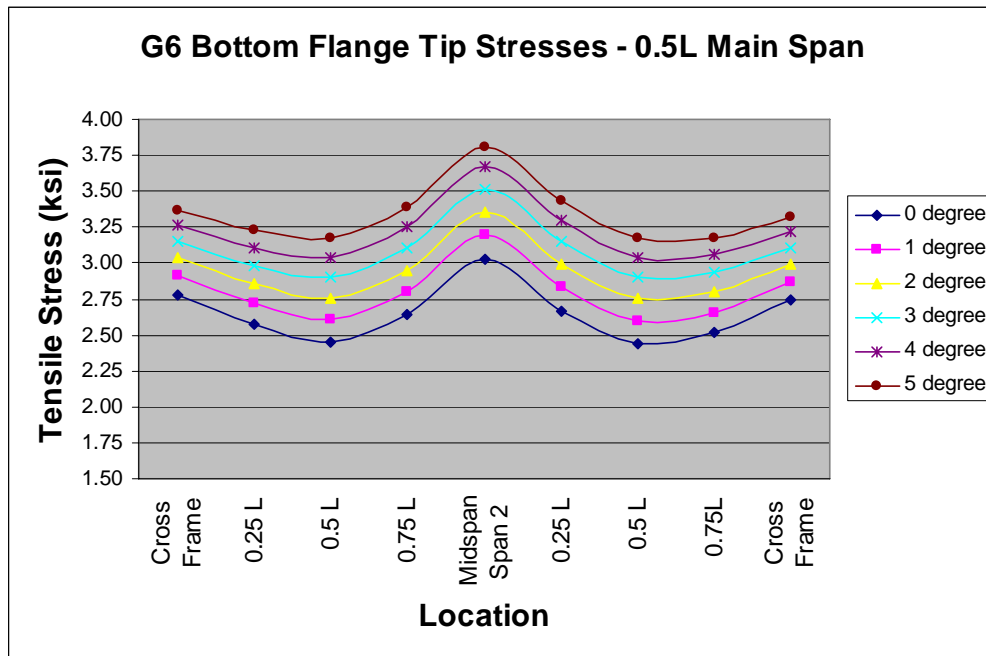


Figure 4.3 Maximum Bottom Flange Tip Stresses, 0.5L Main Span

Investigation of the top flange tip stresses on the outside of the radius of curvature yielded an inverse relationship between the flange tip compressive stress and increasing out-of-plumbness, that is, increasing out-of-plumbness yielded lower tip stresses. At the plumb condition, the midspan outside top flange tip compressive stress was 4.28 ksi. Inducing a web-tilt of 2 and 5 degrees produced flange tip stresses of 3.97 ksi and 3.41 ksi, representing drops of 7.2% and 20.5%, respectively. For succinctness, results are presented only for Girder 6 in figure 4.4 as they are representative of the other girders' behavior (see appendix for complete results for all girders.)

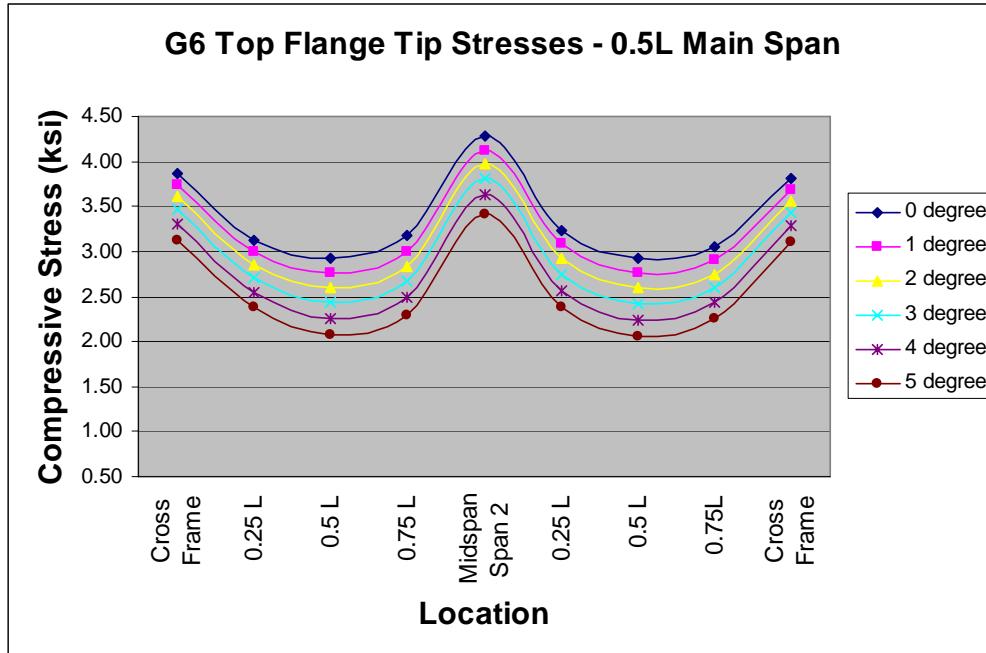


Figure 4.4 Maximum Top Flange Tip Stresses, 0.5L Main Span

In evaluating the effects of out-of-plumbness on vertical bending moment and bi-moment, the negative moment region located at Pier 3 was investigated. The top flange tip stresses on the outside of the radius of curvature tended to decrease as the degree of web out-of-plumbness increased. With 2 degrees of out-of-plumbness, the compressive stress at this location dropped from 4.47 ksi to 3.91 ksi, representing a drop of 12%. The results for girder 6 are presented in figure 4.5.

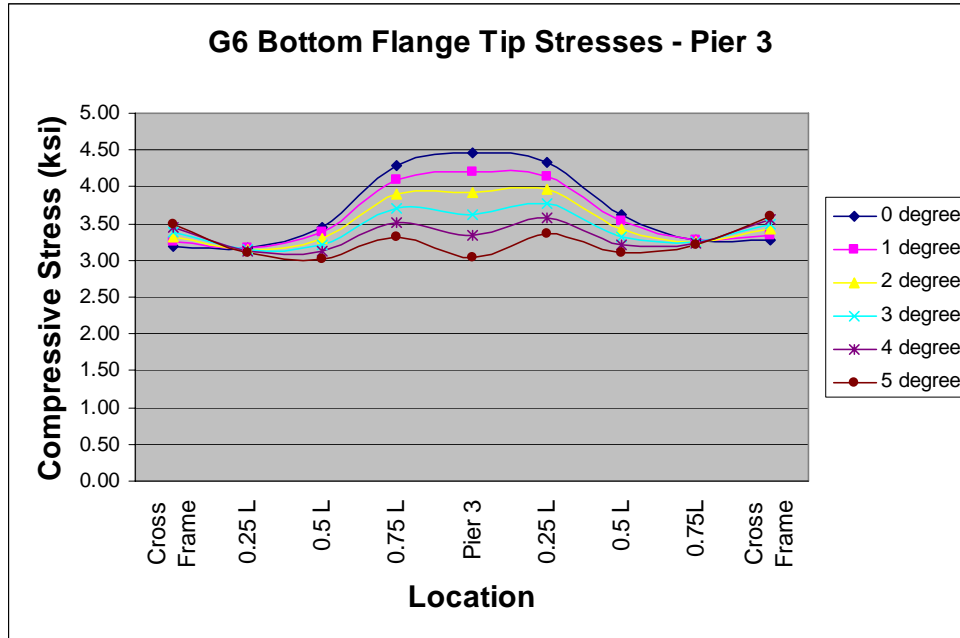


Figure 4.5 Maximum Bottom Flange Tip Stresses, Pier 3

Consideration of the tensile stresses in the top flange at the pier location formed the basis used to quantify the effects of web out-of-plumbness in the negative moment region. The outside top flange tip stress showed a positive relationship with increasing degrees of web out-of-plumbness. While the effects were not as pronounced as in the positive moment regions, there was still a 7% rise in maximum tensile stress for a 2 degree out-of-plumb rotation and an 18% rise for the 5 degree case. Figure 4.6 shows the relationship for girder 6 (typical).

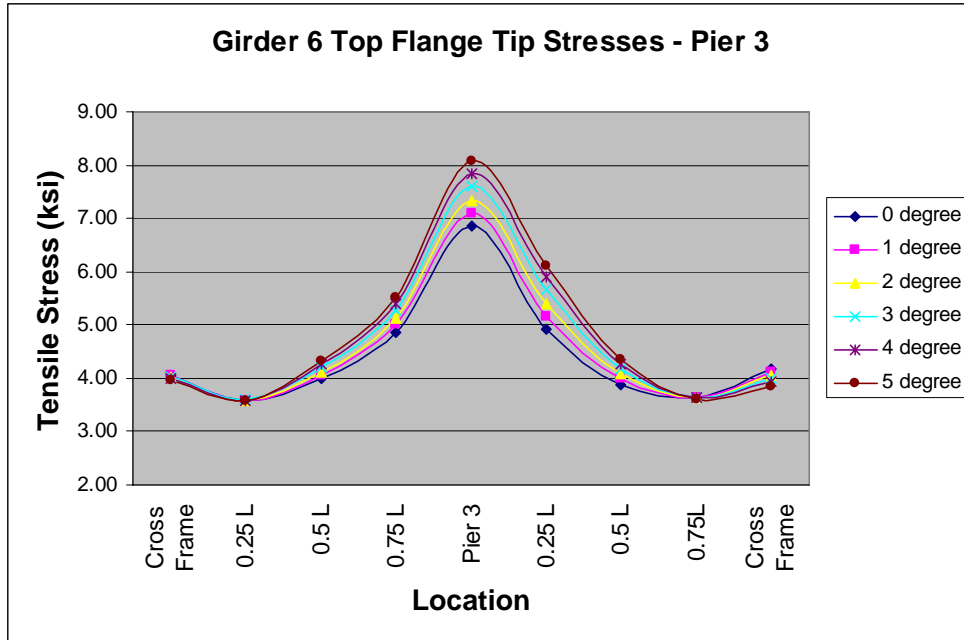


Figure 4.6 Maximum Top Flange Tip Stresses, Pier 3

The positive bending region of span 3 was investigated to determine the effects of out-of-plumbness on flange tip stresses in the longer end span. The outside bottom flange tip stress, and top flange tip stress, showed similar behavior to that of the mid-span cross-section at the same distance from the Pier (see 0.5L Span 2.) The plumb case produced maximum top and bottom stresses 2.72 ksi and 2.37 ksi, respectively. Inducing rotations of 2 and 5 degrees caused 11% and 27% increases in the bottom flange tensile stress. The same rotations caused 7% and 19% drops in the top flange compressive stresses. Behavior for girder 6 is illustrated in figures 4.7 and 4.8.

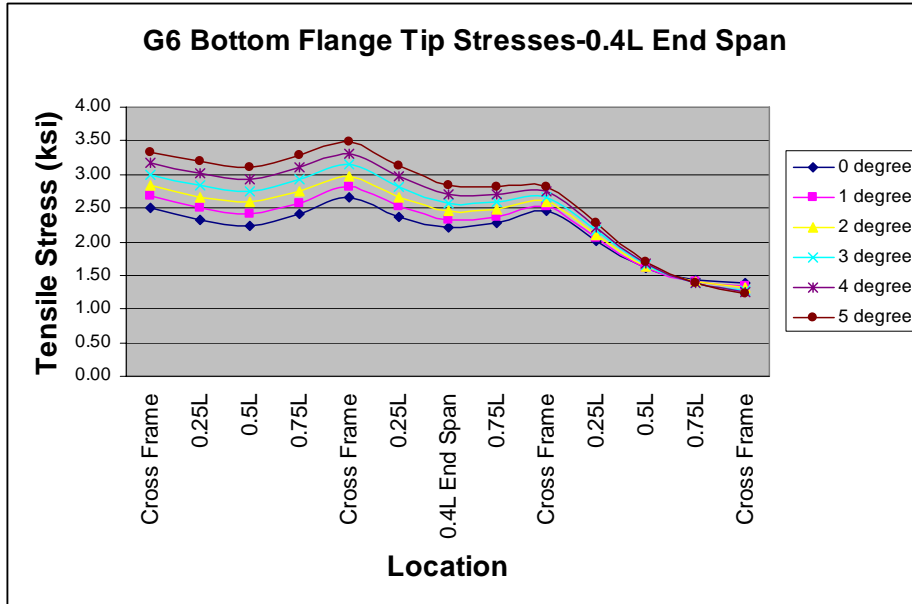


Figure 4.7 Maximum Bottom Flange Tip Stresses, 0.4L End Span

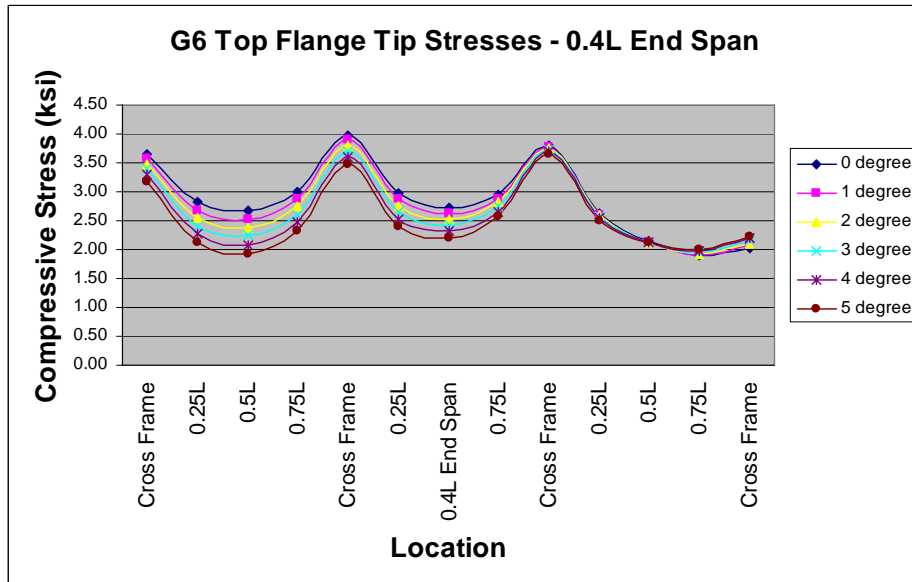


Figure 4.8 Maximum Top Flange Tip Stresses, 0.4L End Span

Thus, increasing web out-of-plumbness showed the tendency to increase the maximum tensile flange outside tip stresses in the positive moment regions and decrease the maximum

compressive flange outside tip stresses. At the pier locations, it is shown that web out-of-plumbness tended to increase top flange outside tip stresses and decrease bottom flange outside compressive tip stresses. Increasing degrees of web out-of-plumbness showed an approximately linear relationship to effects on the flange stresses in all cases.

4.2 VERTICAL AND LATERAL DEFLECTIONS

Vertical and lateral deflections are measured for the top and bottom web-flange intersections at the mid-span of the center span and at the 0.4L point of span 3, the longer of the two unequal length end spans. Investigation of the deflections indicated the effect of the out-of-plumb condition on maximum deflections.

The vertical deflections for the top and bottom web flange intersections were measured for each of the positive bending regions mentioned previously. The top web-flange intersection vertical deflections increased with increasing degrees of web out-of-plumbness. For girder 6 the web-plumb condition resulted in a vertical deflection of 0.989 inches at mid-span. Inducing a 5 degree out-of-plumb condition in the model resulted in a vertical deflection of 1.007 inches at the same location; an increase of 1.8% for this extreme case. This effect tended to be amplified slightly as the radius of curvature for the girders decreased. Figure 4.9 displays the effects of web out-of-plumbness on the top web-flange intersection vertical deflections.

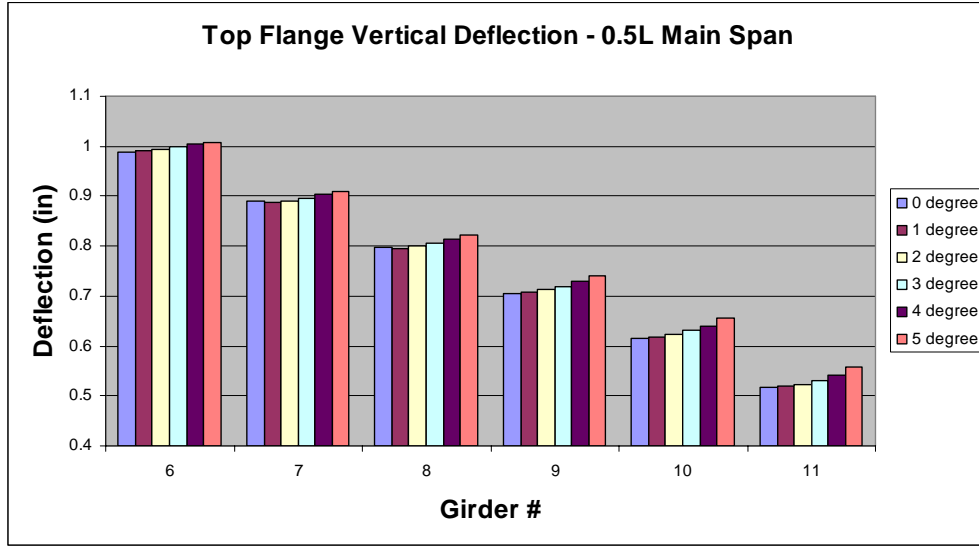


Figure 4.9 Maximum Top Flange Vertical Deflection, 0.5L Center Span

The bottom web-flange intersections' vertical deflections exhibited a tendency to decrease with the application of increasing degrees of out-of-plumbness. As web out-of-plumbness increased, bottom web-flange intersection vertical deflections tended to decrease slightly. At the web-plumb condition, girder 6 exhibited a vertical deflection of 0.06 inches; under steel dead-weight at the mid-span point of span 2. 5 degrees of web out-of-plumbness resulted in a vertical deflection of only 0.055 inches at the same point. This represents an 8% loss in deflection between the two extreme cases. Intermediate values of web out-of-plumbness exhibited proportionately similar behavior though the effect diminished as the radius of curvature (as well as span length) increased. Figure 4.10 shows the effect of out-of-plumbness on bottom web-flange intersection vertical deflections.

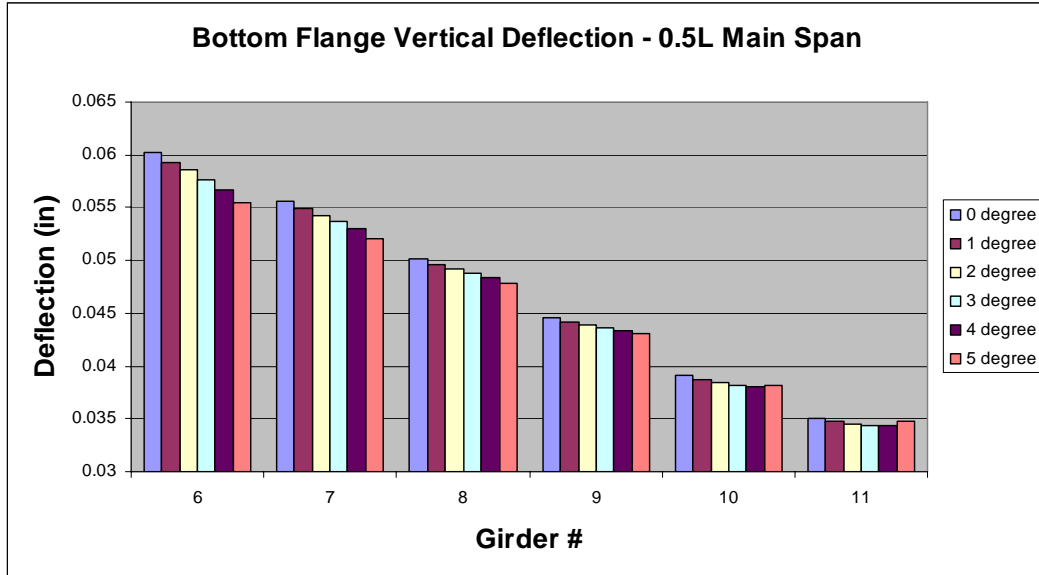


Figure 4.10 Maximum Bottom Flange Vertical Deflections, 0.5L Center Span

Evaluation of the 0.4L location of the end span showed behavior similar to that of the 0.5L center span region. Investigation of the positive moment region showed that top flange vertical deflection grew as the out-of-plumb condition worsened; while the opposite trend surfaced in terms of the bottom flange vertical deflection. Figures 4.11 and 4.12 show the effects of out-of-plumbness on vertical deflections at the 0.4L region of span 3.

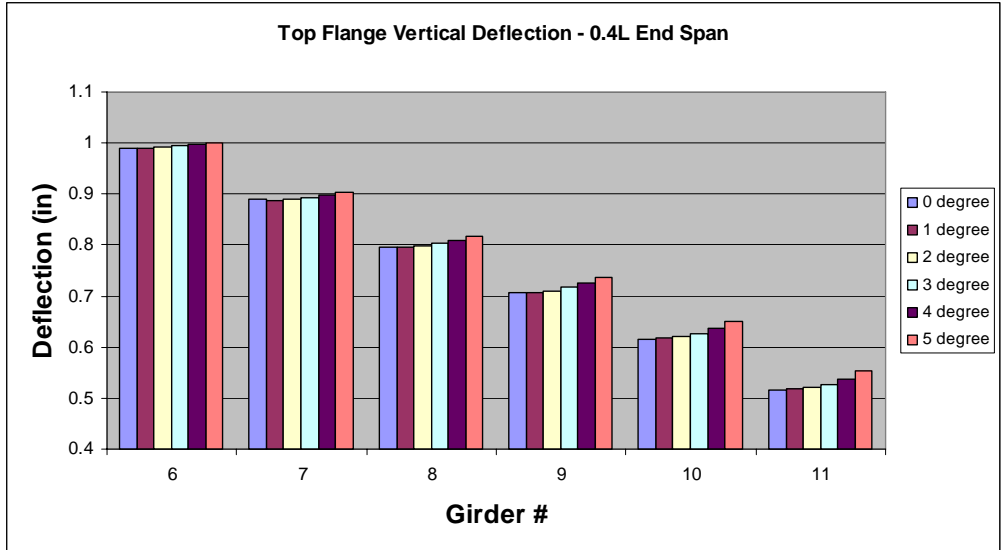


Figure 4.11 Maximum Top Flange Vertical Deflections, 0.4L End Span

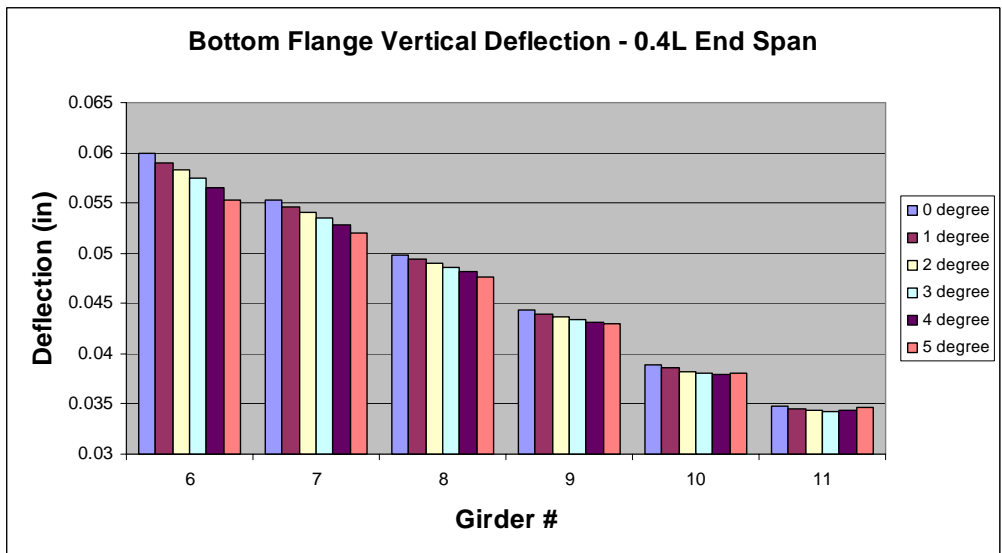


Figure 4.12 Maximum Bottom Flange Vertical Deflections, 0.4L End Span

Girder lateral deflections showed a different relationship in response with increasing degrees of web out-of-plumbness. For the top web-flange intersection of the main span, increasing degrees of out-of-plumbness produced sizable increases in top flange lateral deflections. The effects of the out-of-plumbness showed considerable consistency across each girder line,

regardless of the radius of curvature. This is expected as the girder lines are connected with closely spaced cross frames. Girder 6 showed a lateral deflection (measured on a radial from the center of and parallel to the plane of curvature) of 0.1 inches for the plumb condition and 0.35 inches for the 5-degree rotated case. This represented an increased lateral deflection of 250%. The following figure details the effects on the remainder of the structure.

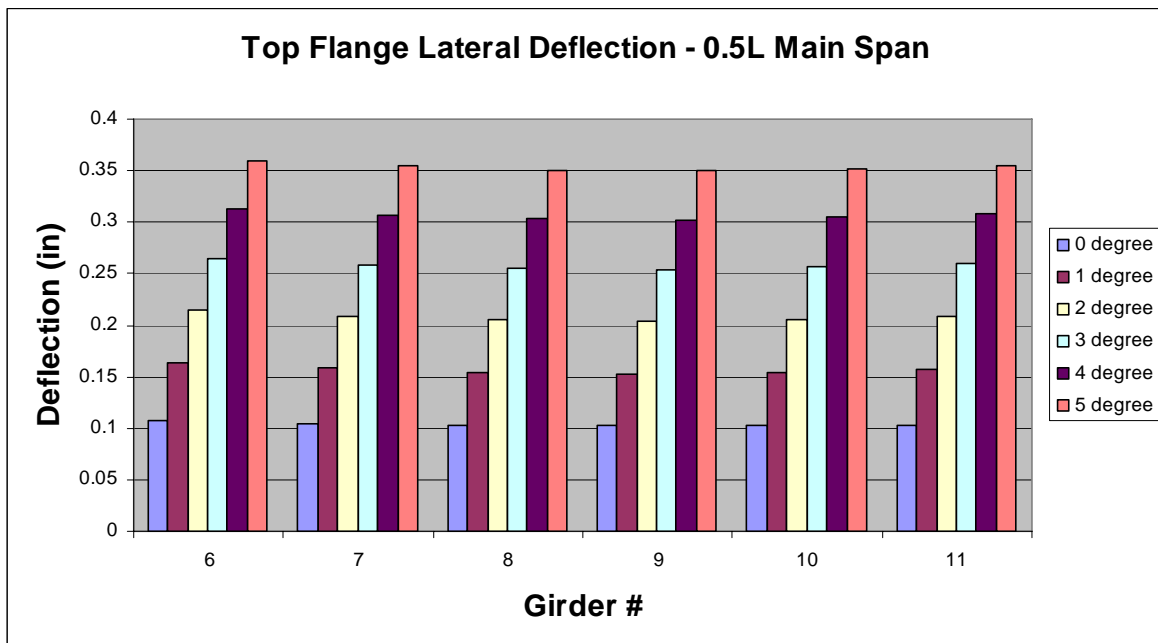


Figure 4.13 Top Flange Lateral Deflection, 0.5L Main Span

The bottom web-flange intersections' lateral deflections again showed a propensity to increase with increasing degrees of web out-of-plumbness. Girder 6 deflected 0.043 inches for the plumb case and 0.047 inches when the web was tilted 5 degrees, indicating a 9% increase; of note, however, is that the influence of the out-of-plumb condition tended to increase as the radius of curvature decreased. Girder 11 showed a plumb-condition bottom flange lateral deflection of 0.022 inches and the same deflection increased to 0.031 inches with a 5-degree rotated web,

represented a 43% increase. The remainder of the structure exhibited proportionately similar behavior with respect to the radii of curvature. Figure 4.14 displays this result.

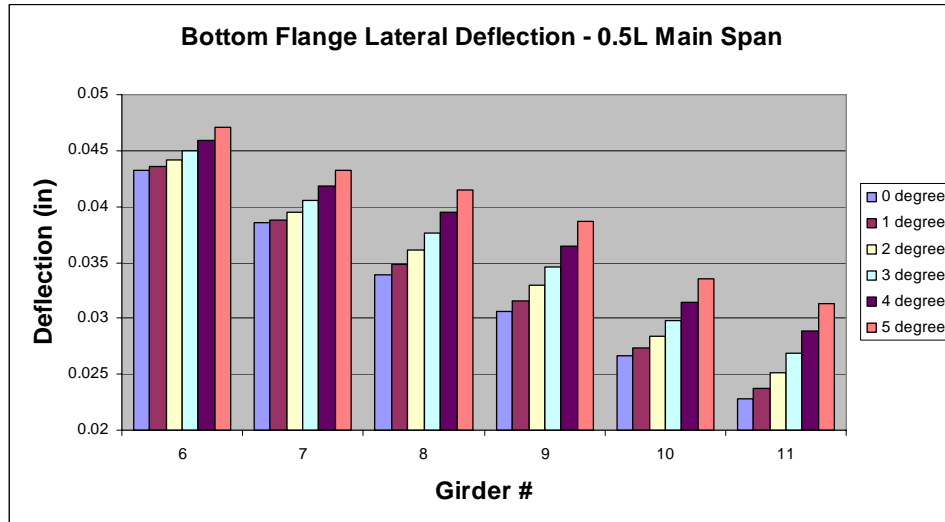


Figure 4.14 Bottom Flange Lateral Deflection, 0.5L Center Span

The 0.4L end span location again exhibited similar trends as the 0.5L center span positive moment region with respect to out-of-plumbness effects on lateral deflections. Figures 4.15 and 4.16 illustrate the results for this region.

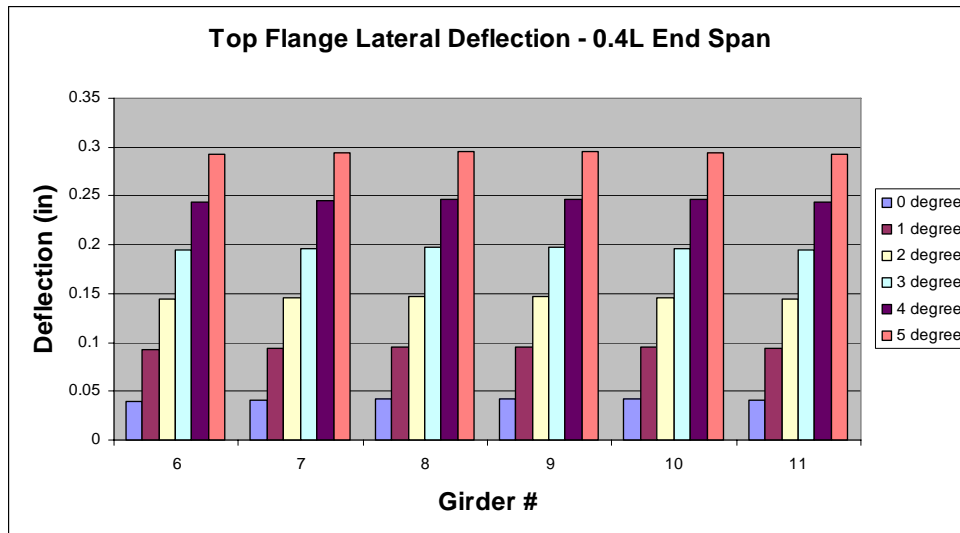


Figure 4.15 Top Flange Lateral Deflection, 0.4L End Span



Figure 4.16 Bottom Flange Lateral Deflection, 0.4L End Span

4.3 CROSS FRAME FORCES

Cross frame demands in a curved bridge structure are of particular importance since the cross frames act as the primary torsional brace for the girders to ensure compatibility in girder rotations across a given bridge cross-section. Additionally, the cross frames act as restraint points along the girder longitudinal axis, with respect to lateral flange bending; at specific locations the cross frame forces are indicators of the warping moment severity. This is flange lateral bending may be thought of as being analogous to the case where the flange is thought of as a continuous beam where the cross frames are conceived of as support locations (Chavel, 2005.)

The positive moment region cross frame demands are quantified in terms of the top and bottom chord cross frame forces at different degrees of web out-of-plumbness. The top chord (tensile) cross frame demands showed initially detrimental effects due to the out-of-plumb condition up to 3 degrees; and then some mitigation of these deleterious effects for additional web out-of-plumbness. At the mid-span point, the top chord showed a tensile load of 1.62 kips

while at 3 degrees 1.74 kips and at 5 degrees 1.66 kips. This represented a maximum increase of 7% subsequently diminishing to a net increase of 2.5% as the web out-of-plumbness increases to the 5-degree case. The bottom chord (compressive) forces showed considerable axial force mitigation in the positive moment region due to increasing degrees of out of plumbness. The plumb condition results in a compressive load of 1.45 kips; decreasing to 1.13 kips at the 5-degree case (representing a drop of 22%). Figures 4.17 and 4.18 display these trend in behavior for the cross frames connecting girders 6 and 7 (i.e. the outermost girder lines).

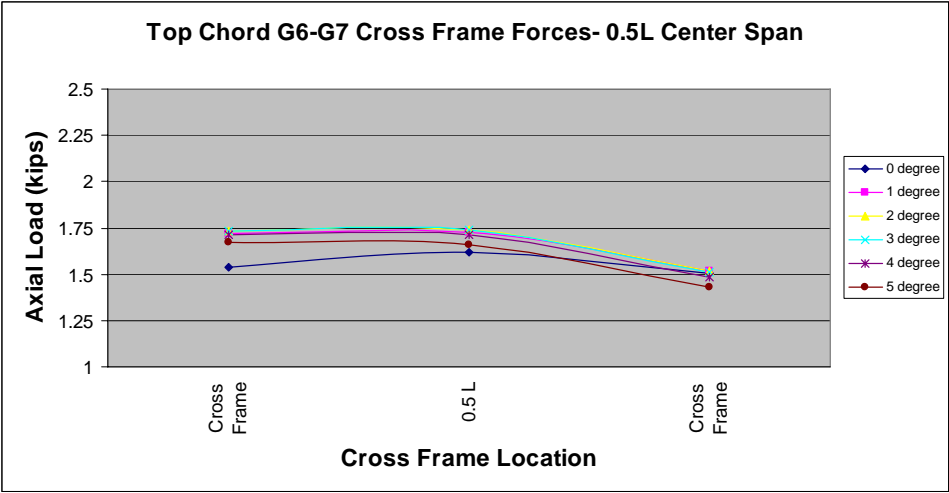


Figure 4.17 Top Chord Cross Frame Demands, Girders 6-7 at 0.5L Center Span

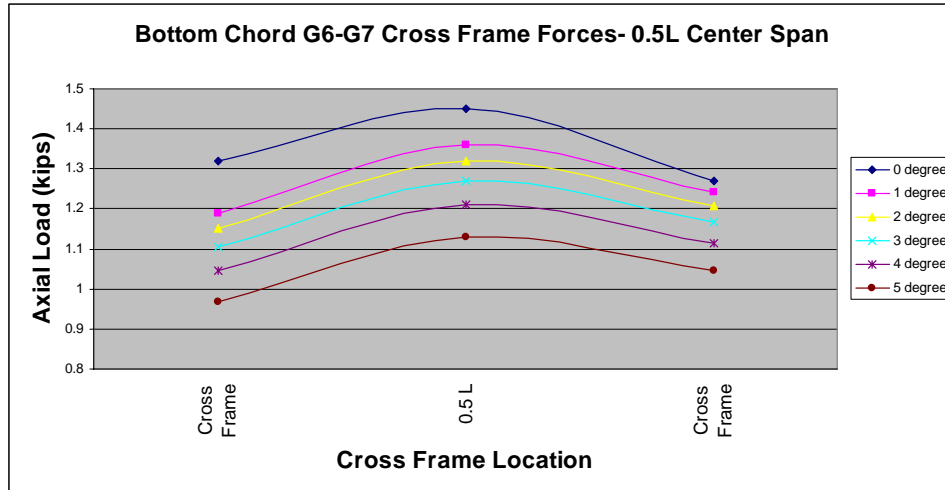


Figure 4.18 Bottom Chord Cross Frame Demands, Girders 6-7 at 0.5L Center Span

While the behavior for the top chords was relatively uniform among the girder lines, the bottom chord demands varied considerably as the radius of curvature (and thus structural location) varied. In the outermost cross frame set, it was shown that increasing degrees of web out-of-plumbness tended to decrease the compressive demands on the cross frame in the positive moment region. This was true also for the second outermost set of cross frames between girders 7 and 8. For girders 8 and 9, at the centerline set of cross frames, web out-of-plumbness of up to 2 degrees resulted in decreasing cross frame demands. However, further increases in web out-of-plumbness resulted in increasing demand on the bracing as depicted in figure 4.19.

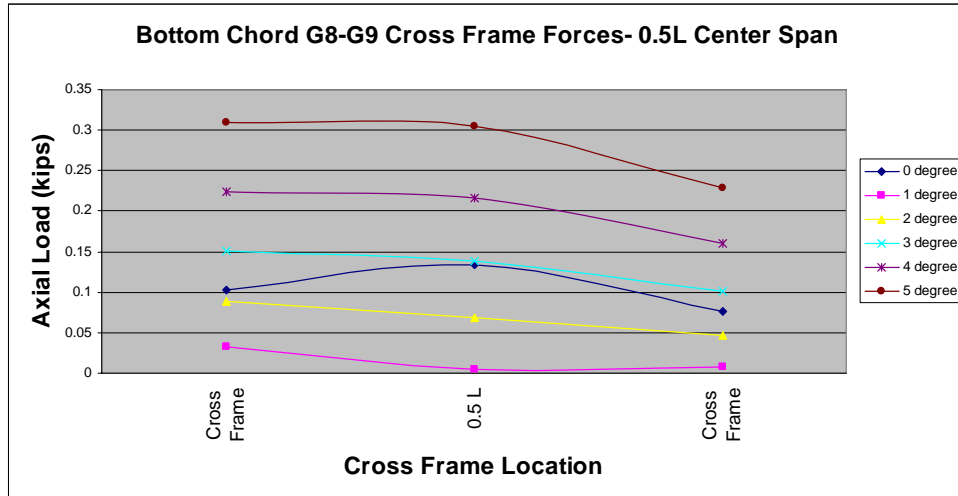


Figure 4.19 Bottom Chord Cross Frame Demands, Girders 8-9 at 0.5L Center Span

Decreases in the radius of curvature (i.e. as the girders are considered, in succession, approaching the center of curvature) resulted in the trend that bottom chord cross frame forces eventually reverses in that increasing degrees of out-of-plumbness increase demands in the bottom cross frame chords. Figure 4.20 shows this demand increase on the innermost cross frame set within the positive moment region.

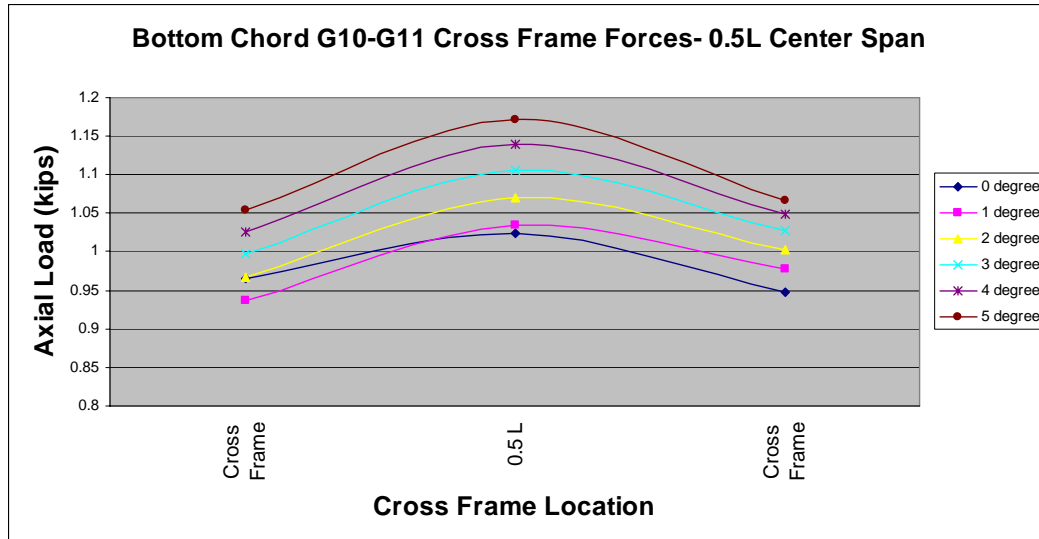


Figure 4.20 Bottom Chord Cross Frame Demands, Girders 10-11 at 0.5L Center Span

In quantifying the effects of out-of-plumbness, investigations are conducted in the negative bending moment regions in the vicinity of pier 3. Ensuing study of the negative moment region showed that for increasing degrees of out-of-plumbness, cross frame demands on the top chord tended to decrease on the order of 17% for 2 degrees of web-tilt and 45% for the 5-degree case. As the radius of curvature decreased, this trend in bracing force remained constant in its direction though the effect diminished.

Of particular note with respect to the top chord cross frame demands is that in the outermost cross frame set, between girders 6 and 7, at locations adjacent to the pier, internal forces of as much as 3 times that of the pier cross frame set were observed; however, as the radius of curvature decreases this relationship reverses and further degrees of web tilt produce less disparate results at the innermost cross frame set. Thus, the data indicates that the outermost (in terms of radius of curvature) bay top chords are relatively unaffected by the out-of-plumb condition at the pier location. The effects of out-of-plumbness intensifies for subsequent inside bays, though the relationship between the top chord demands over the pier and on adjacent top

chords reverses (ie: the pier location experiences higher cross frame demands than adjacent frames.) Figures 4.21-4.23 depict this behavior for the outer, middle, and inner cross frame bays at the pier location.

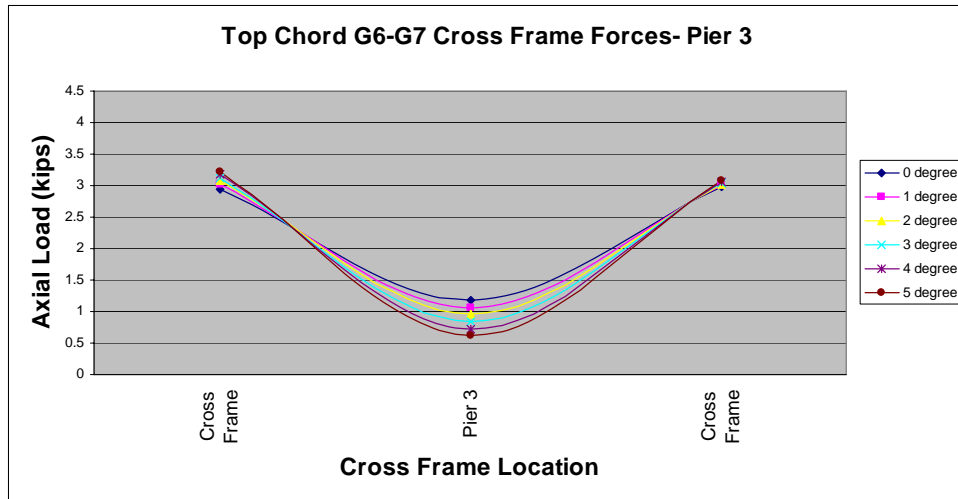


Figure 4.21 Top Chord Cross Frame Demands, Girders 6-7 at Pier 3

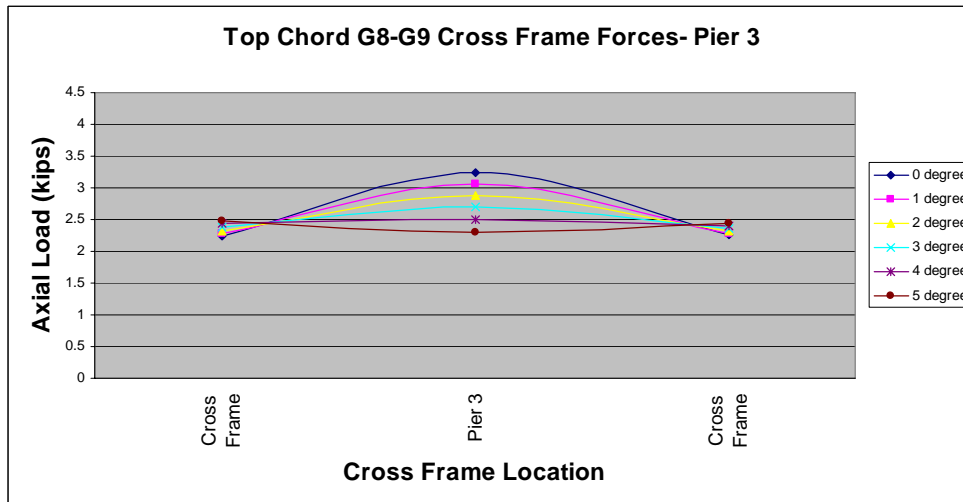


Figure 4.22 Top Chord Cross Frame Demands, Girder 8-9 at Pier 3

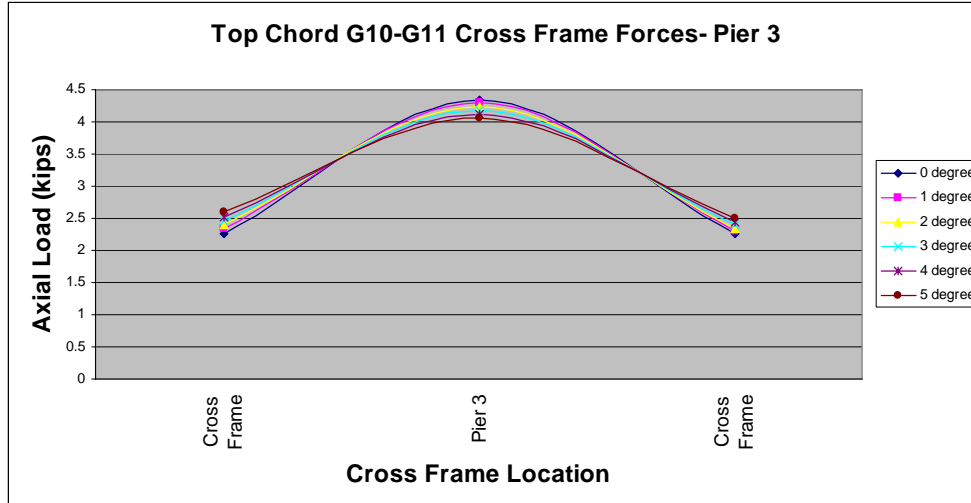


Figure 4.23 Top Chord Cross Frame Demands, Girders 10-11 at Pier 3

The bottom chord cross frame demands within the negative moment region generally lessened as a result of increasing degrees of web-tilt. For the outermost cross frame set, between girders 6 and 7, the web-plumb case showed a cross frame demand of 3.44 kips. Inducing a 5-degree web-tilt resulted in lowering of the force to 2.1 kips, a reduction corresponding to more than 30%. Application of the 2-degree web out-of-plumbness (a value representing common field conditions) resulted in a reduction in demand of 15%. There was little deviation in the bottom chord cross frame demands as the radius of curvature and structural location changed. Figure 4.24 shows the results for girder 6. The complete results for all cross frames can be found in the appendix.

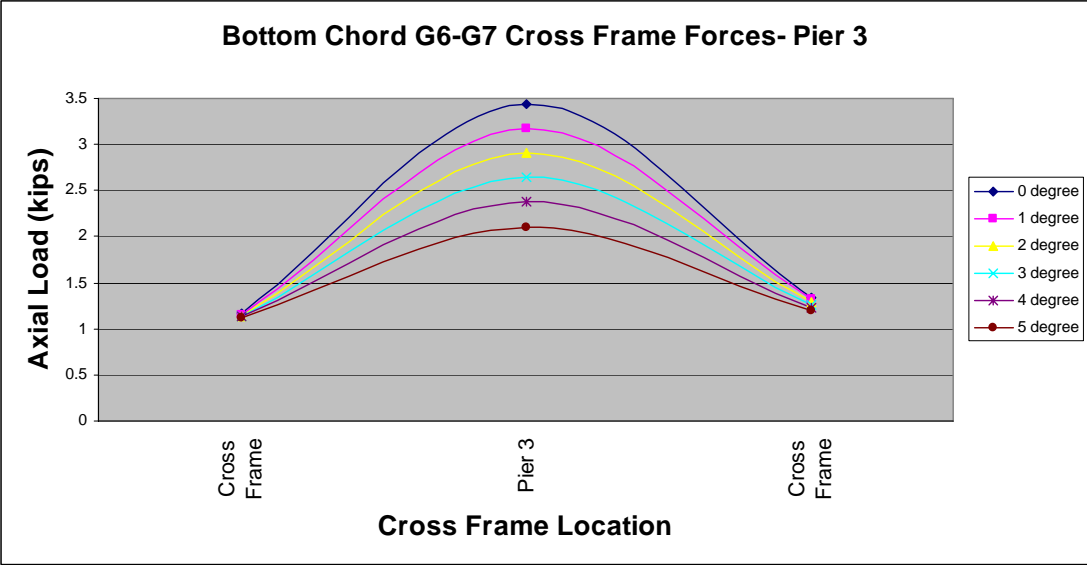


Figure 4.24 Bottom Chord Cross Frame Demands, Girders 6-7 at Pier 3

5.0 RESULTS DISCUSSION

5.1 GIRDER FLANGE TIP STRESSES

Prior to thorough study of the flange tip stresses, is it necessary to address the significant increase in longitudinal stress that theoretically occur coincident with cross frame locations. These longitudinal stresses arise out of restrained lateral flange bending due to non-uniform torsion. The warping restraint effect may be thought of notionally as resulting in the flanges being loaded with a so-called bi-moment. Under the action of the bi-moment, the flanges act as a continuous beam; with the cross frame locations serving as support points (in the sense of restraining translation occurring in the plane of bending). Because the single girder tends to rotate out of plane due to the eccentricity of the center of gravity from the chord line drawn directly between supports, a global torsion is induced about the girder's longitudinal axis as shown in the figure 5.1.

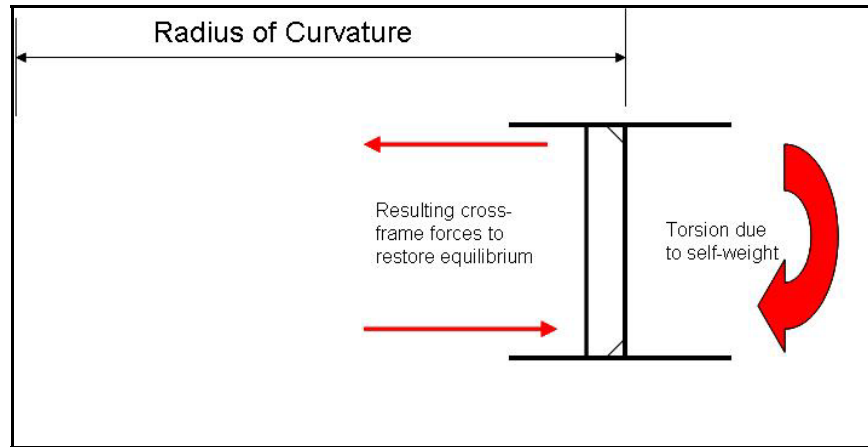


Figure 5.1 Relationship Between Cross Frame Forces and Girder Curvature

Resistance to this torsion is accomplished by a series of moments applied as couples at the top and bottom chord cross frame locations. In positive moment regions, where the bottom flange is in tension, the effect of the bottom chord compressive force is to induce a lateral twisting moment that manifests itself as tensile normal stress on the outside of the radius of curvature. Hence, the lateral flange bending moment will produce an increase in effective stress at the outside bottom flange edge at cross frame locations. This effect will reverse for the inside bottom flange edge since the tensile stress from the vertical bending moment and the compressive stress from the lateral flange bending moment will be subtractive at this location. It is important to note that this behavior is characteristic of horizontally curved I-girder structures regardless of any out-of-plumb condition, a plot of the effective stresses illustrating this behavior is shown in figure 5.2.

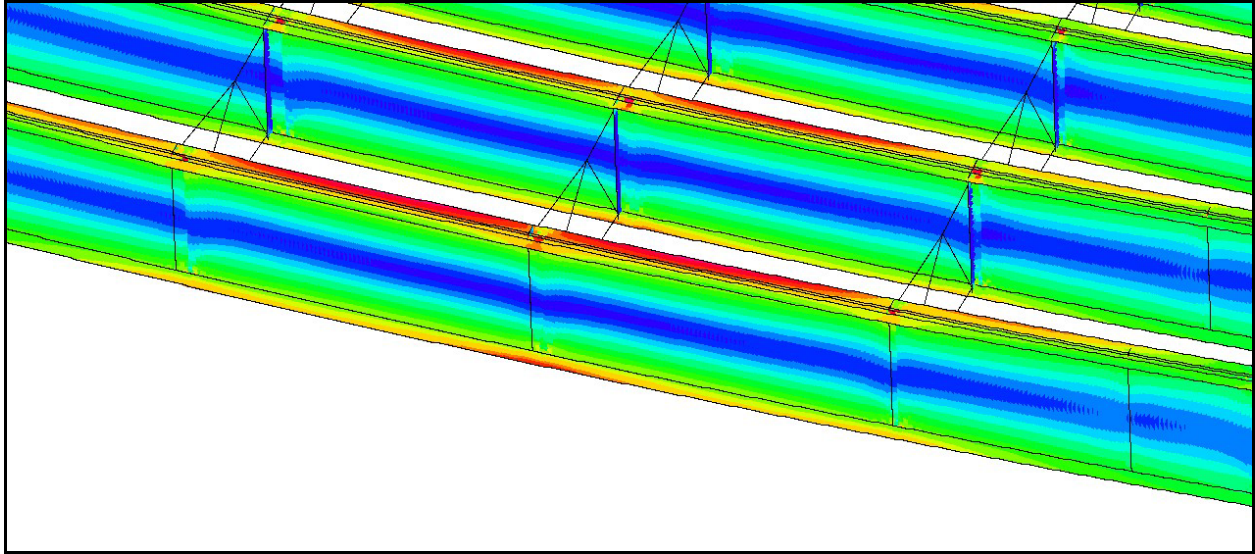


Figure 5.2 Effective Stresses Band Plot of Girders 6 and 7, 0.5L Center Span

Investigation of the girder outside bottom flange tip stresses within the positive moment regions showed that maximum tensile flange stresses rose with increasing degrees of the out-of-plumbness. This behavior was exhibited by each girder, regardless of the radius of curvature. Out of plane rotation of the girder cross section yields an increased distance from the neutral axis to the bottom outside flange tip, thus creating a larger elastic stress at this location in order to resist the same internal bending moment. Again, the effect of the cross frames' couple, resisting the twisting moment, is additive in all case for this location. On the inside top flange edge (closest to the center of curvature), lower tensile stresses are experienced with increasing out-of-plumbness due to the diminishing distance between the elastic neutral axis and the inside flange tip.

The top flange tip stresses showed expectedly similar behavior to the bottom flange tip stresses. Since the location of the results is the outside top flange tip (as measured with respect to the radius of curvature) out of plane rotation of the cross sections yields progressively smaller distances between the elastic neutral axis and the outside top flange tip. Thus, the stress at this

flange tip will decrease due to increasing degrees of web out-of-plumbness. Additional degrees of out-of-plumbness serve to decrease the outside top flange tip stress. The results support this prediction as well as the longitudinal stress increases at the cross frame locations. Due to equilibrium about the girders' longitudinal axes, the couple created from the top and bottom chords of the cross frame set must counteract the twisting moment. This drives the top chord into tension, pulling the top flange to the inside of the radius of curvature. Due to this lateral flange bending, the portion of the flange on the inside of the web will experience a tensile stress while the opposite flange edge will experience a compressive stress. Since this is a positive moment region, the outside top flange tip stresses due to vertical bending and lateral flange bending are additive and a stress riser is developed. On the inside flange edge stress depressions exist at the cross frame locations for analogous reasons. Figure 5.3 depicts the effective stress contours in the other investigated positive moment region, at 0.4L of the longer end span, showing similar behavior to mid-span of the center span. Complete results for each span can be found in the appendix.

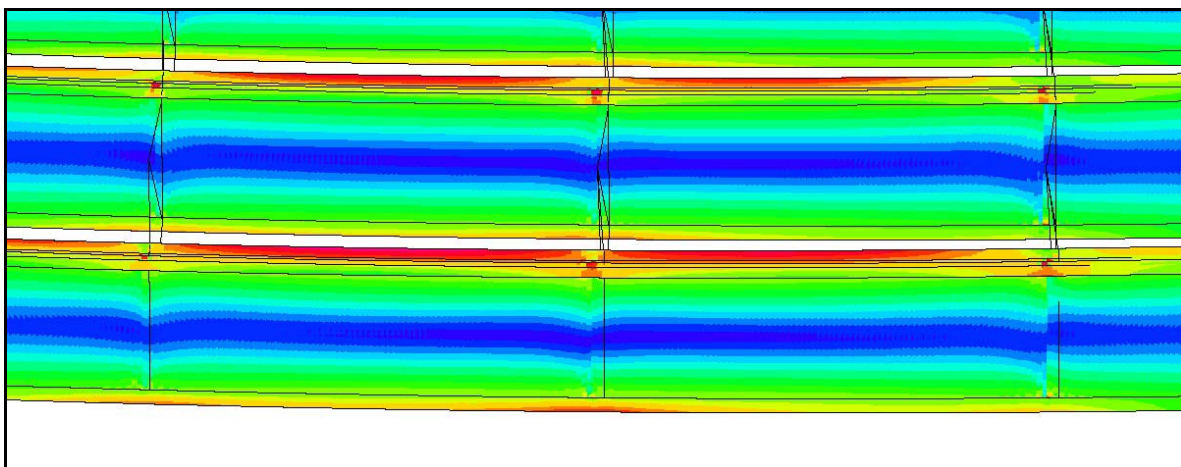


Figure 5.3 Effective Stresses Band Plot of Girders 6 and 7, 0.4L End Span

In regions of negative bending, a different condition exists. At the bottom flange outside edge for increasing degrees of out-of-plumbness, the bottom flange tip compressive longitudinal stress actually decreases suddenly at the support. This is due to the influence of significant lateral flange bending in the support region. As the vertical bending moment is resisted by inducing compressive stress throughout the bottom flange at the continuous support, the twisting moment induced to the outside of the radius of curvature is resisted by lateral flange bending as shown in the figure 5.4.

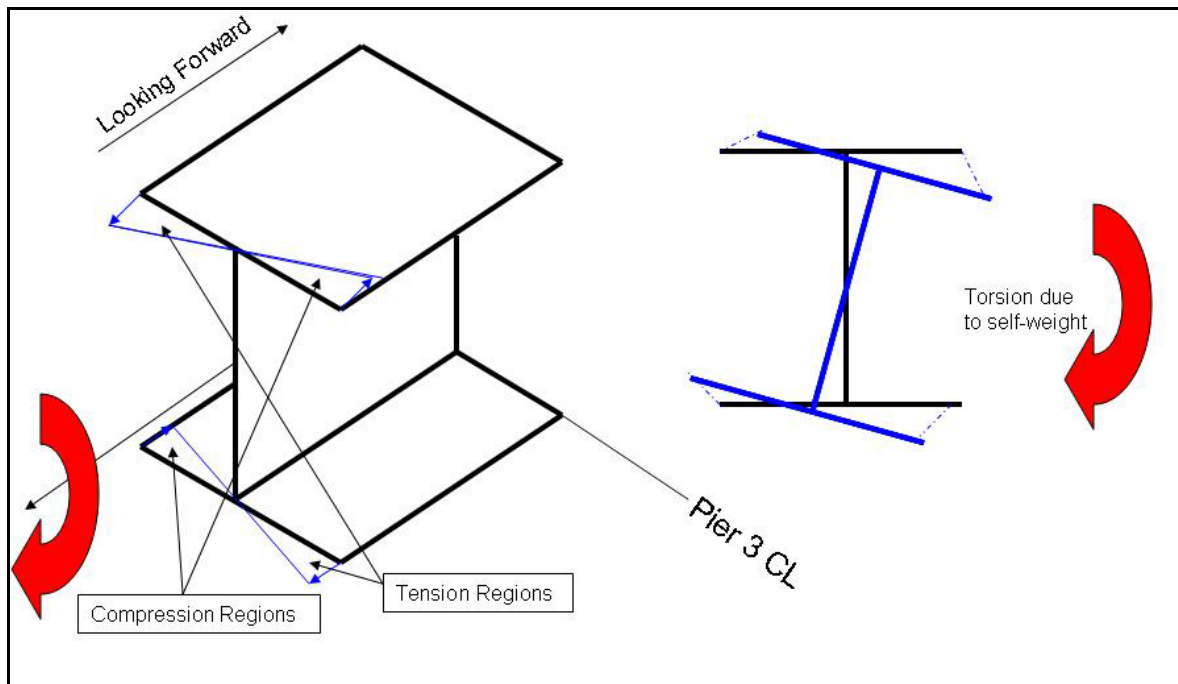


Figure 5.4 Lateral Flange Bending Regions at Pier 3

Thus, at the outside of the radius of curvature at support locations along the bottom flange, tensile longitudinal stress is produced due to the influence of lateral flange bending. This influence becomes apparent suddenly in the immediate vicinity of the support location. The bottom flange tip stress rises as expected, at each quarter point, until the quarter point

immediately adjacent to the support; as the restraint here becomes robust enough to produce significant lateral flange bending that then decreases compressive longitudinal stress produced by the vertical bending moment. In the top flange, tensile longitudinal stress is induced at the inside flange edge, and compressive stress is induced at the top flange tip on the outside of the radius of curvature. Since the intermediate support regions of this continuous structure experience negative bending moment, the expectation is that the outside bottom flange compressive tip stress will be reduced somewhat by the occurrence of lateral flange bending induced tensile longitudinal stress associated with this warping restraint. The same phenomenon does not manifest itself at the top flange outside tip stress; as this region experiences a milder superposition of tensile stress from the vertical bending moment and compressive stress from the lateral bending moment due to the lack of restraint in the form of rigid boundary conditions at the top flange. The continuous lateral bracing provided by the addition of a rigid concrete deck will change this behavior significantly. Figure 5.5 depicts the von Mises stresses in the vicinity of pier 3.

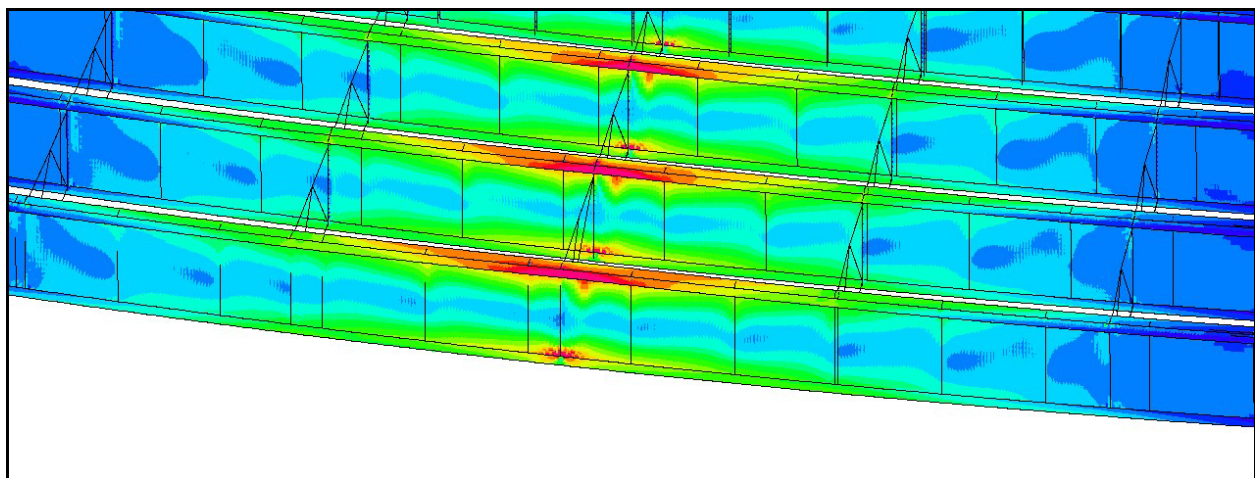


Figure 5.5 Effective Stresses Band Plot of Girders 6-8 at Pier 3

5.2 VERTICAL AND LATERAL DISPLACEMENTS

Investigation of the vertical and lateral displacements was most important in the positive moment regions due to the absence of restraint in these regions by boundary conditions. Vertical deflection (perpendicular to the plane of curvature) of the bottom web-flange intersections showed interesting behavior. It was found that for both positive moment regions studied, $0.5L$ center span and $0.4L$ end span, that the bottom web-flange intersection's vertical (perpendicular to the plane of curvature) deflection was relatively unchanged with increased degrees of induced web out-of-plumbness. This is due to the inherent torsional rigidity of the curved girder participating in the vertical bending restraint and creating a torsional fulcrum in the web. Since for the same applied load more of the bending moment is resisted from lateral flange bending for increased degrees of web-tilt, this bottom web-flange intersection vertical deflection remains relatively constant. The consequence is paid in lateral deflection as will be discussed in following sections. It is interesting to note that the sensitivity of the bottom flange vertical deflection decreases as the girder span decreases, due to reduced unsupported length, leading to increased flexural stiffness. Figure 5.6 confirms the maximum vertical displacements at these locations and decreasing vertical displacements with decreasing span length.

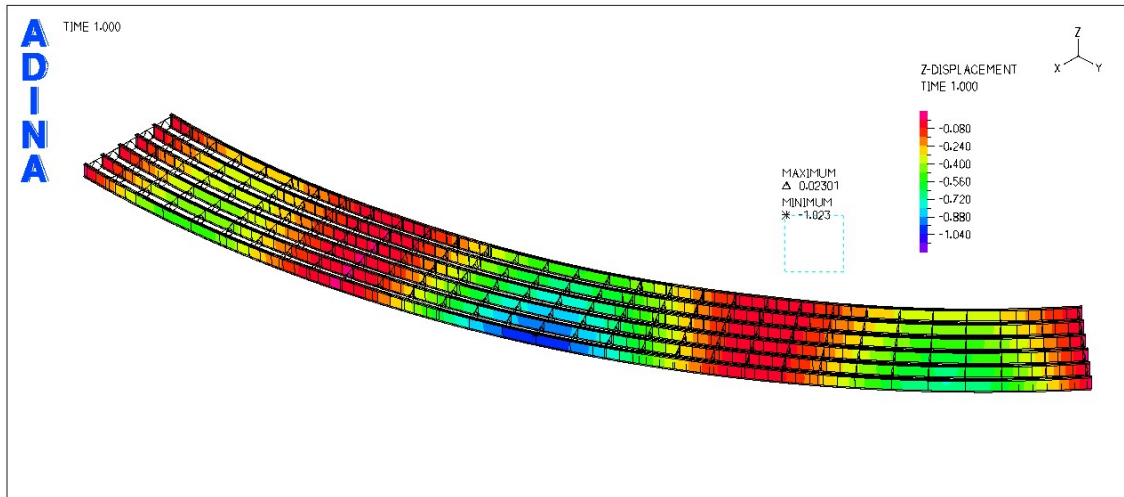


Figure 5.6 Z-Displacement Band Plot of Model

The vertical deflection of the top web-flange intersection grew as the degree of web out-of-plumbness increased. This is due to the fact that the significant lateral deflections of the top web-flange intersection have a vertical component as the cross section rotates out-of-plane about the center of curvature. For increasing degrees of web-tilt, this lateral deflection increases as more of the vertical bending moment is resisted by lateral flange bending, thus increasing the vertical deflection. As the girder radius of curvature decreases, the sensitivity to the out-of-plumb condition increases since a tighter radius girder will resist more vertical bending moment in lateral flange bending action than its “straighter” counterpart.

The lateral deflection of the bottom web-flange intersection showed a positive relationship to increasing degrees of web-tilt. As the web out-of-plumb condition becomes more severe, the girder will resist a lower proportion of the gravity loading in flexure and more in lateral bending. Again, girders with a shorter radius of curvature proved more susceptible to the amplification of bottom flange lateral deflections under increasing degrees of out-of-plumbness.

The lateral deflection of the top web-flange intersection experienced the most severe deflection under an out-of-plumb condition. The top web-flange intersection lateral deflections increased significantly as the out-of-plumb condition increased. All six girders displayed the same response for the out-of-plumbness, with regards to top flange lateral deflections. Figure 5.7 illustrates the regions of maximum total displacement, representing the vector sum of lateral and vertical displacements. Evaluation of the displacement contour plot confirms the greater lateral displacement of the top web-flange intersection than the bottom for a particular longitudinal position.

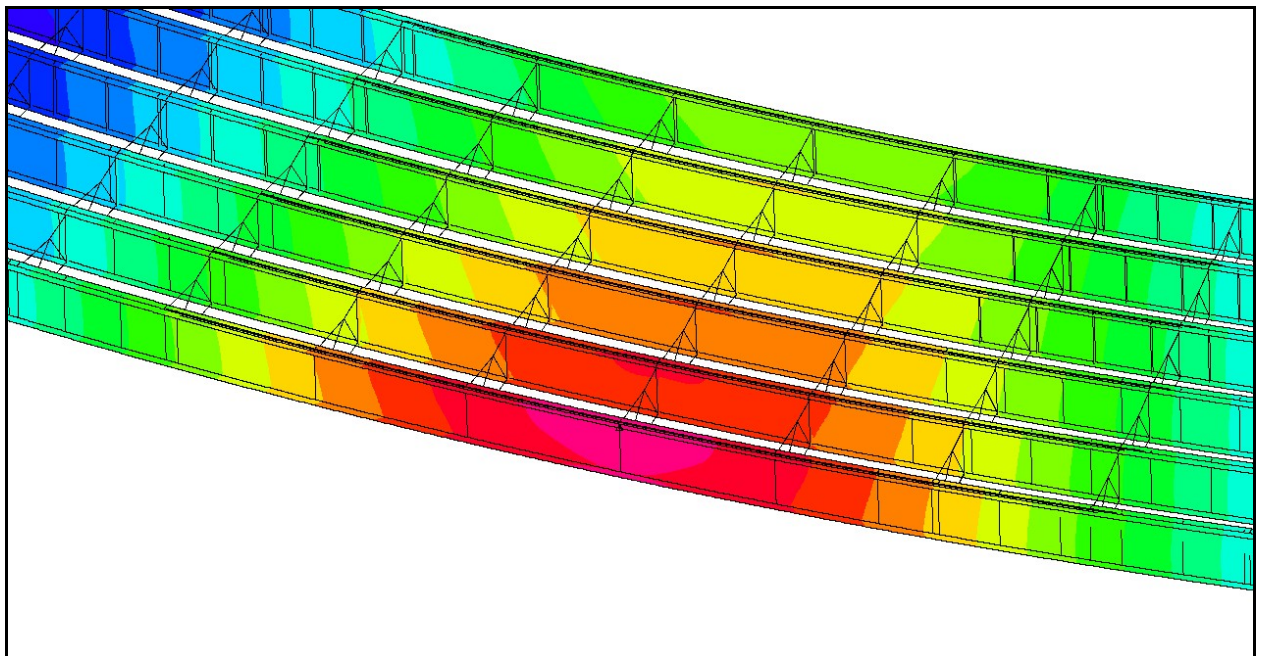


Figure 5.7 Displacement Magnitude Band Plot, 0.5L Center Span

5.3 CROSS FRAME FORCES

In regions of positive bending, there was little quantifiable change in the cross frame axial forces with respect to increasing degrees of web out-of-plumbness. In the top chords, application of up

to 3 degrees of out of plumbness produced some rise in cross frame demands, while further rotations mitigated these additional demands somewhat. Regardless of the radius of curvature, the maximum additional imposed cross frame force requirement was 0.2 kips under steel dead load in the outermost girder line at the center span's midpoint. For the bottom chord in the positive moment regions, varying trends surfaced. For the cross frame sets on the outside of the bridge centerline, increasing degrees of out-of-plumbness served to lessen the demands on the bottom chords while for the inside bays (as measured from the bridge centerline), the opposite trend exists. This is due to the influence of each girders' respective torsional rigidity. The more robust torsional stiffness of the inside girders (due to decreased span length) tends to provide more rigid supports for the bottom chords, thus permitting for the transfer of axial load between girder lines via the cross frames. The exterior girders provide for less stiff "supports" (in the flange bending sense) to the horizontal bracing members comprising the bottom cross frame chords, and thus resist the progressively higher degrees of out of plane deflections and rotation. This supports the results of the inside girders' top flange tip stresses decreasing with increasing degrees of web out-of-plumbness with superposition of the effects of decreasing eccentricity from the elastic neutral axis.

For the negative moment region over pier 3, the cross frame forces displayed considerable variation due to increasing degrees of out-of-plumbness. An important trend surfaced in the data indicating that the outermost cross frame sets were sensitive to the web out-of-plumb condition. For the outermost cross frame set, the 5 degree out-of-plumb condition amplified the top chord cross frame demands by 150%. Interior cross frame bays displayed relative immunity to the out-of-plumb condition, the effect generally decreasing with the innermost cross frames showing a 6% escalation for the 5 degree case.

6.0 CONCLUSIONS

In conducting detailed analysis of a typical horizontally-curved steel I-girder bridge, a non-linear finite element model is employed. By artificially inducing initial out-of-plumb conditions of up to 5 degrees (measured at the centerlines of each of the three spans) investigations to determine the effects of the out-of-plumb condition on maximum flange tip longitudinal stresses, vertical and lateral deflections, and cross frame demands, were carried out.

Examination of the model results indicated that outer edge bottom flange tip longitudinal stress within the positive moment regions increased due to the out-of-plumb condition because of the increasing distance of the flange tip from the elastic neutral axis. Results from the finite element model yielded an increase of 12% over the plumb case for a 2-degree rotation at the region of maximum positive bending for the outermost girder line and 23% for the innermost girder line. A reduction in top flange outer edge tip longitudinal stress was observed at the same location due to the decreasing distance from the neutral axis. These results remained consistent for the positive moment region at the $0.4L$ location, adjacent to span 3. In the negative moment region over pier 3, significant effects from lateral flange bending were observed. The torsional moment caused by increasing eccentricity of the girders' centers of gravity at the pier location produced lateral flange bending that served to counter the flexural normal compressive stresses at the outer bottom flange tip and amplify the flexural normal tensile stresses at the outer top flange tip.

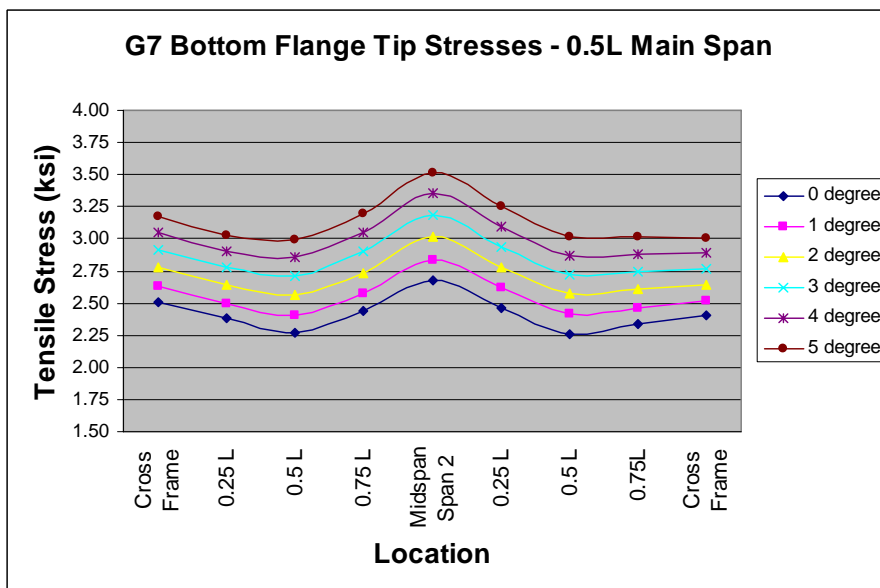
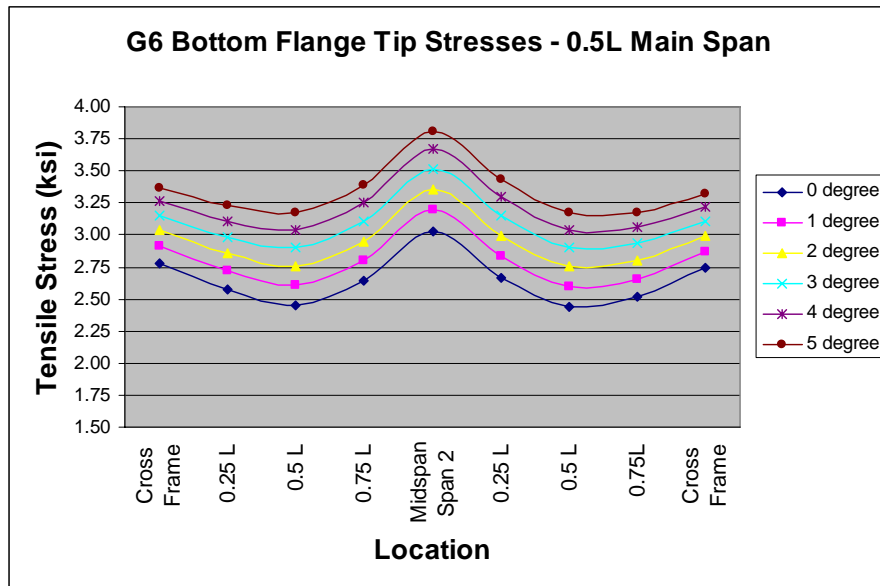
The results showed that increased degrees of web out-of-plumbness caused increased vertical and lateral deflections. The outermost girders, comprising the longest spans, showed the greatest amplification of deflections with the 2 degree case increasing the mid-span total (vertical and lateral) deflection by 100% under steel dead load. Vertical deflections showed relatively small effects from the out-of-plumb condition while lateral deflections showed far greater vulnerability, increasing by over 250% at the outermost girder mid-span.

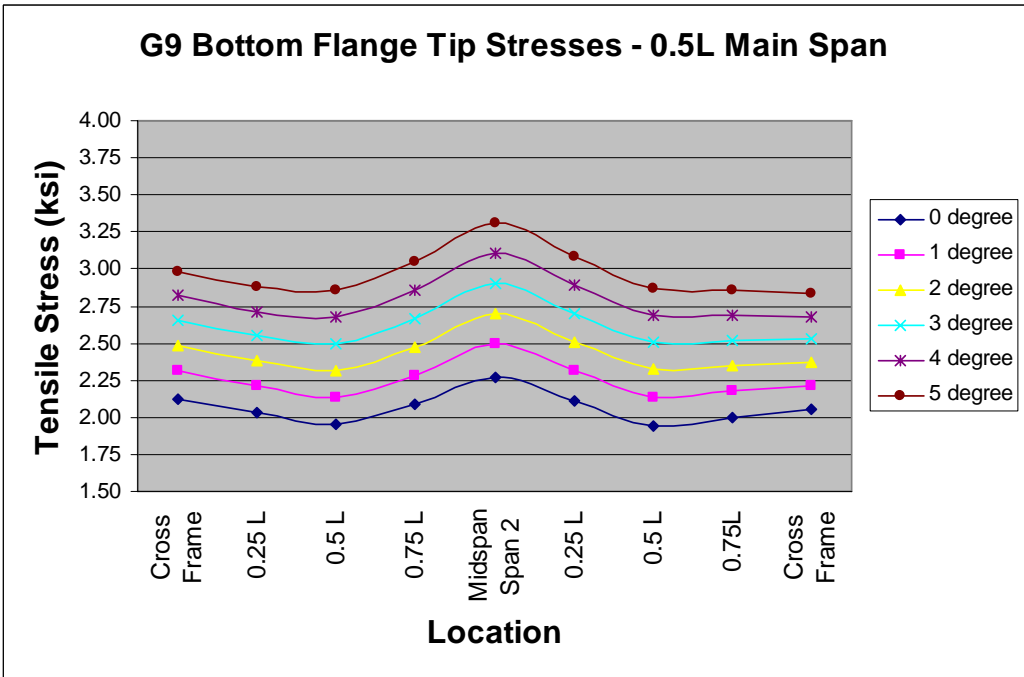
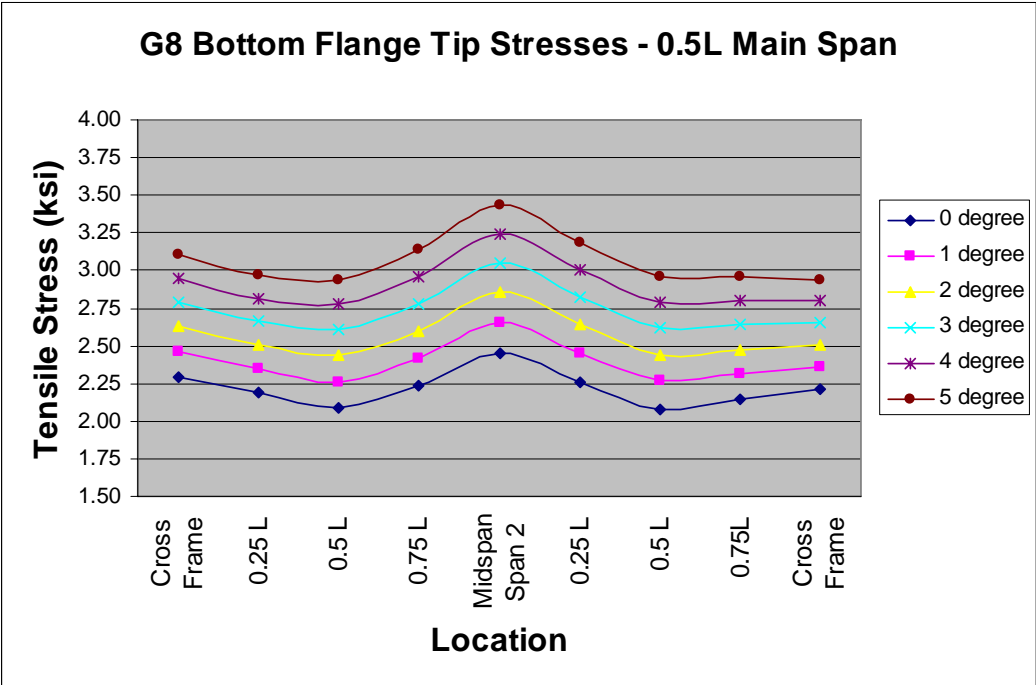
Finally, cross frame forces showed considerable sensitivity to increasing out-of-plumbness. Effects from girder torsional rigidity due to varying span lengths were shown to significantly affect cross frame demands as bay location, and thus girder span/radius, varied for constant cross frame geometry.

The results of this investigation confirm and quantify the detrimental effects on typically-proportioned curved bridge performance due to increasing degrees of web out-of-plumbness in terms of flange tip stresses, lateral deflections, and cross frame demands. Thus, it may be necessary in design to account for the occurrence of these field conditions under dead-load conditions in rectifying component misalignments and other constructability considerations.

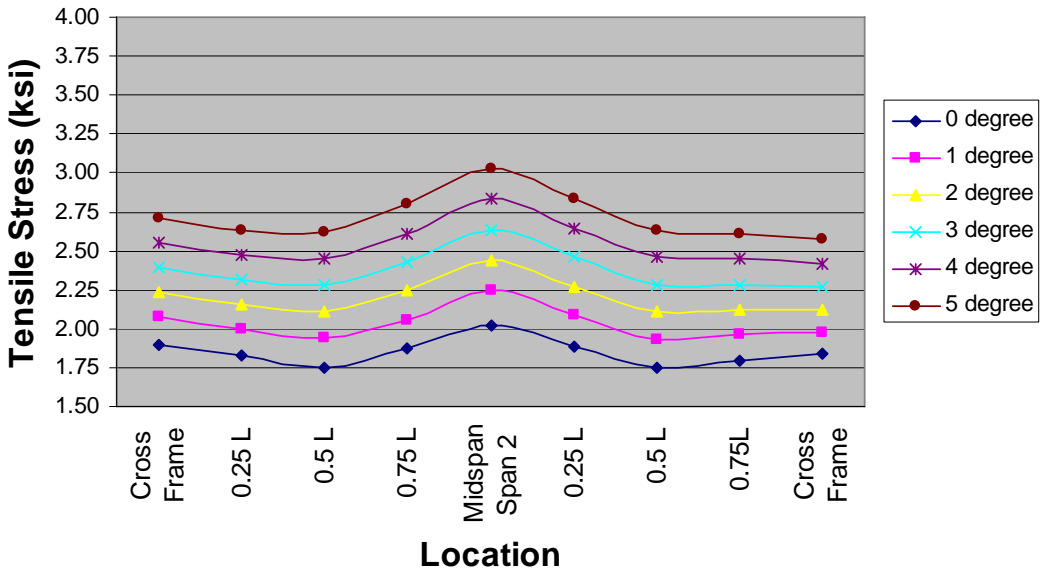
APPENDIX A

RESULTS TABLES AND GRAPHS

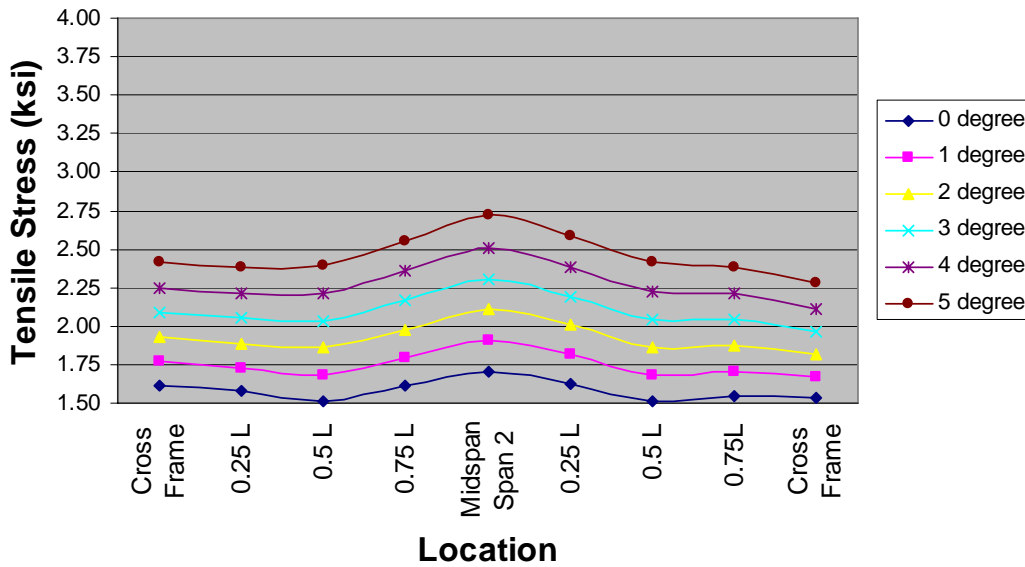


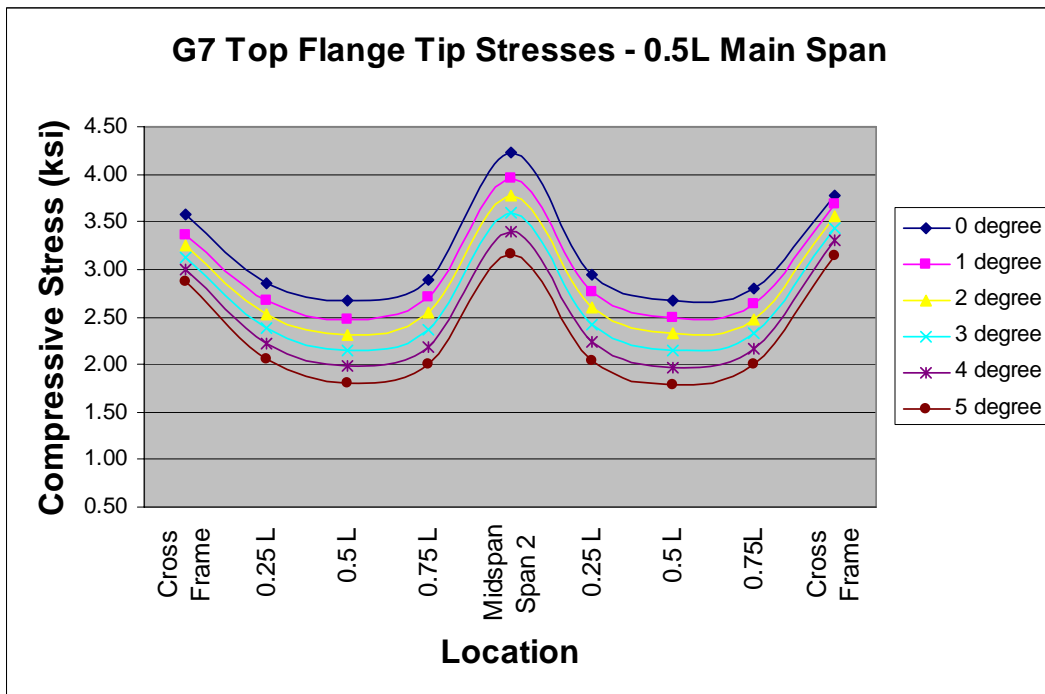
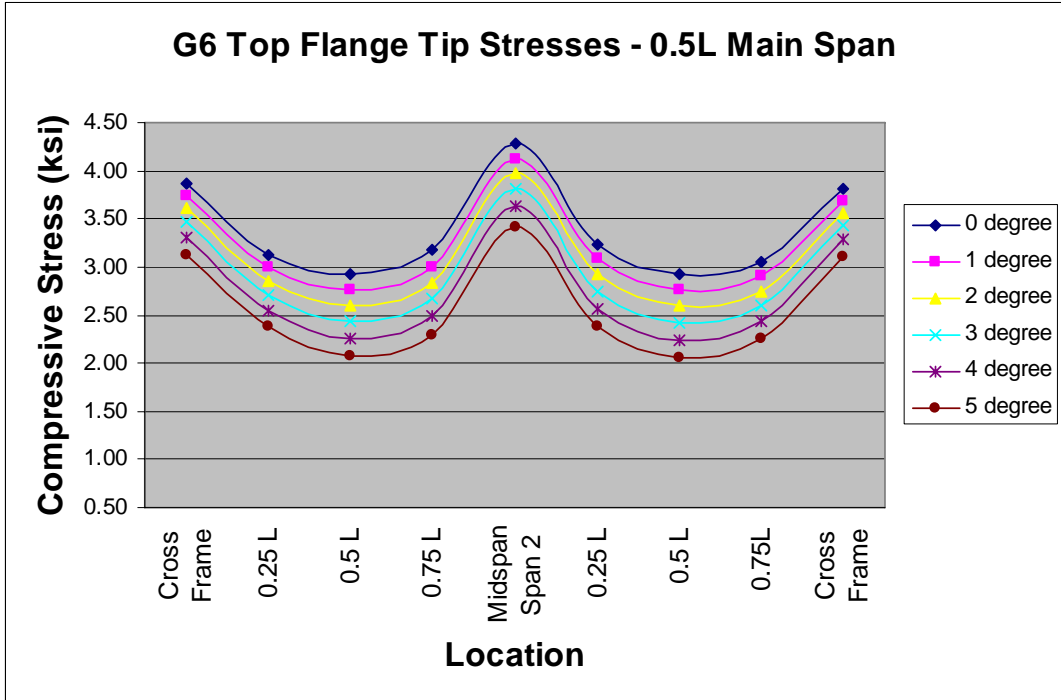


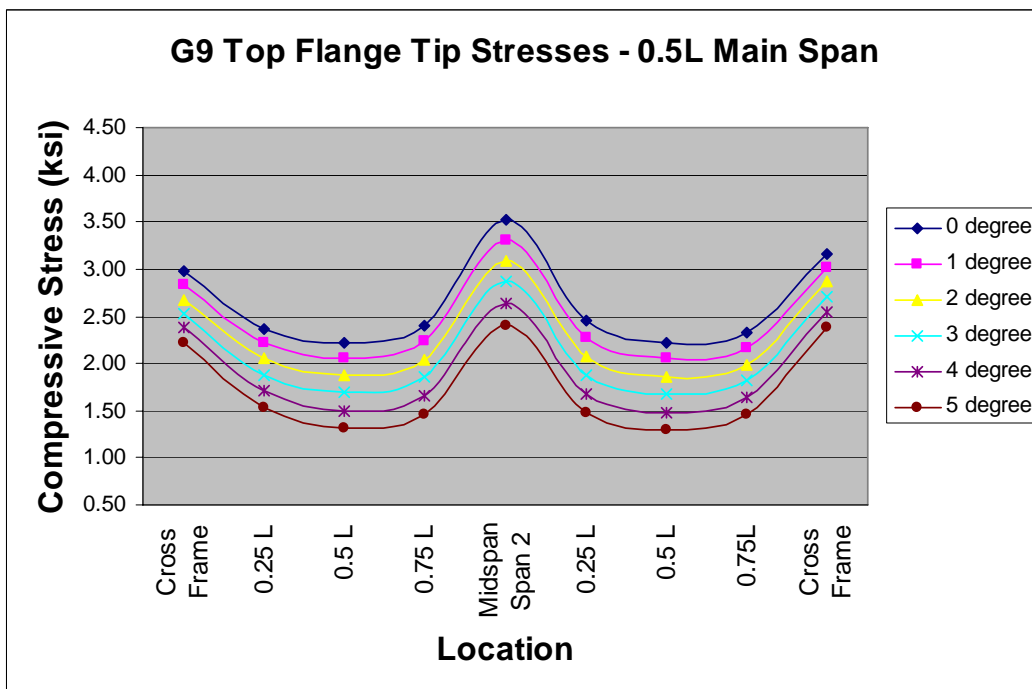
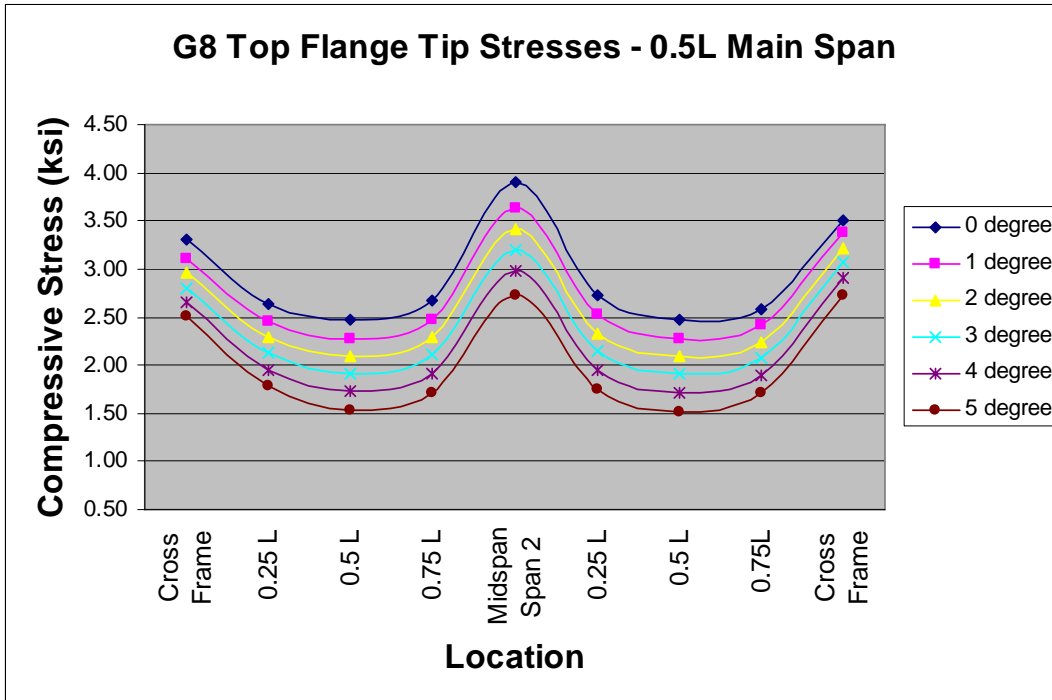
G10 Bottom Flange Tip Stresses - 0.5L Main Span

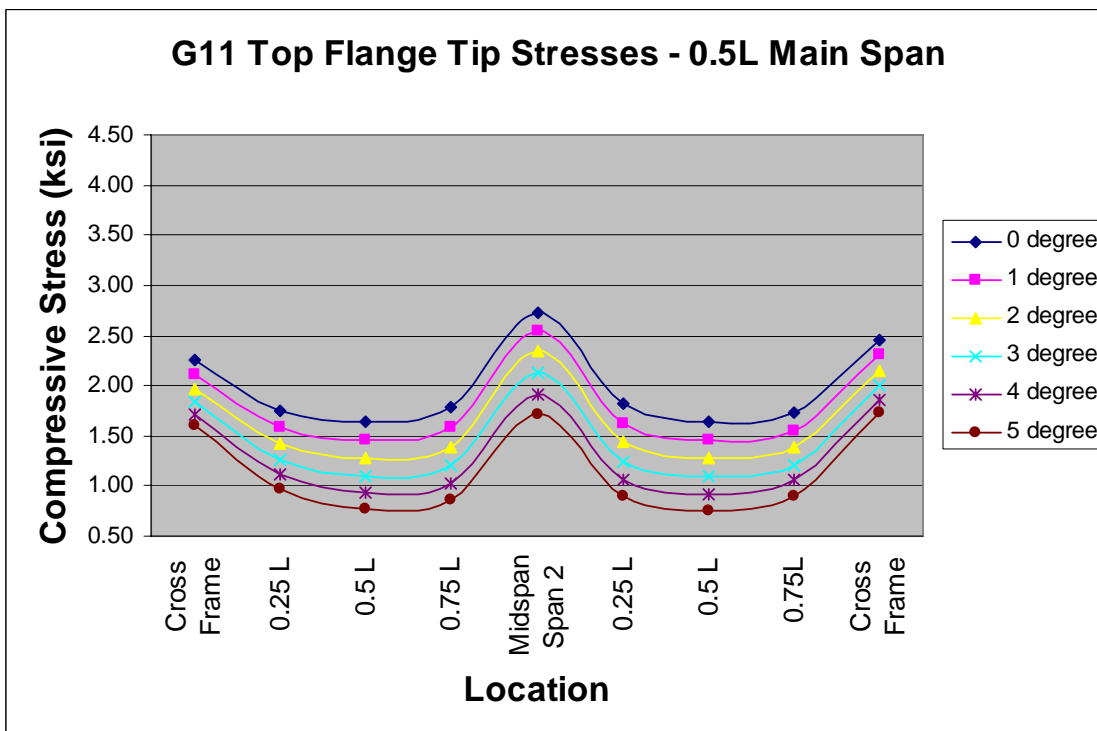
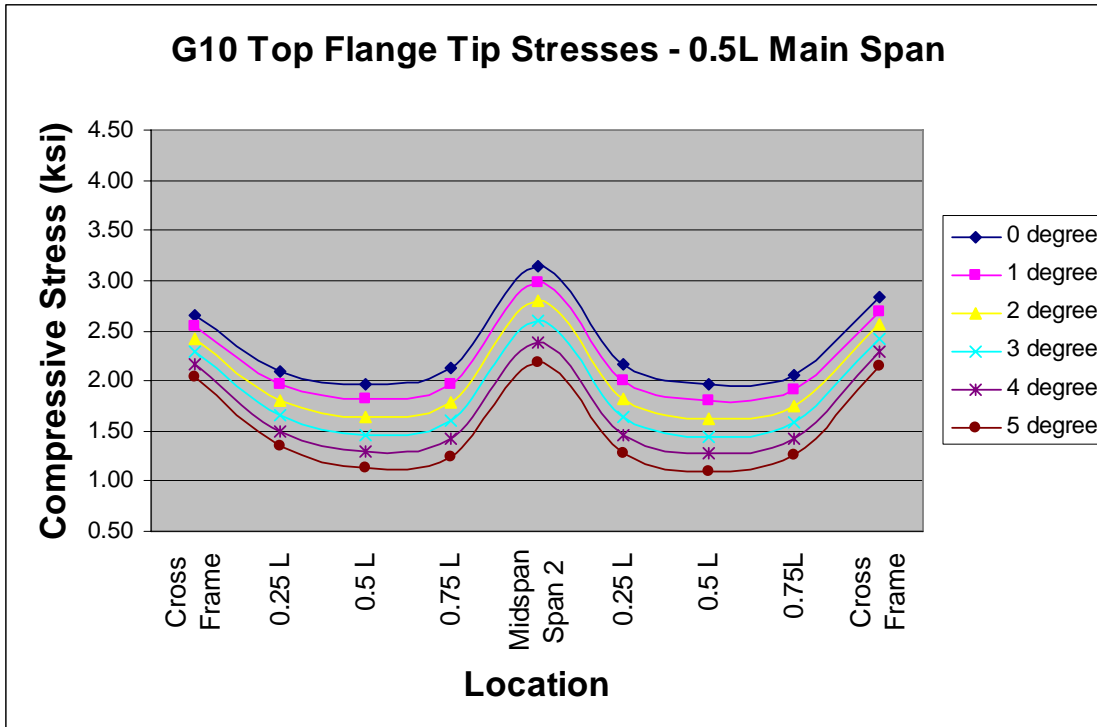


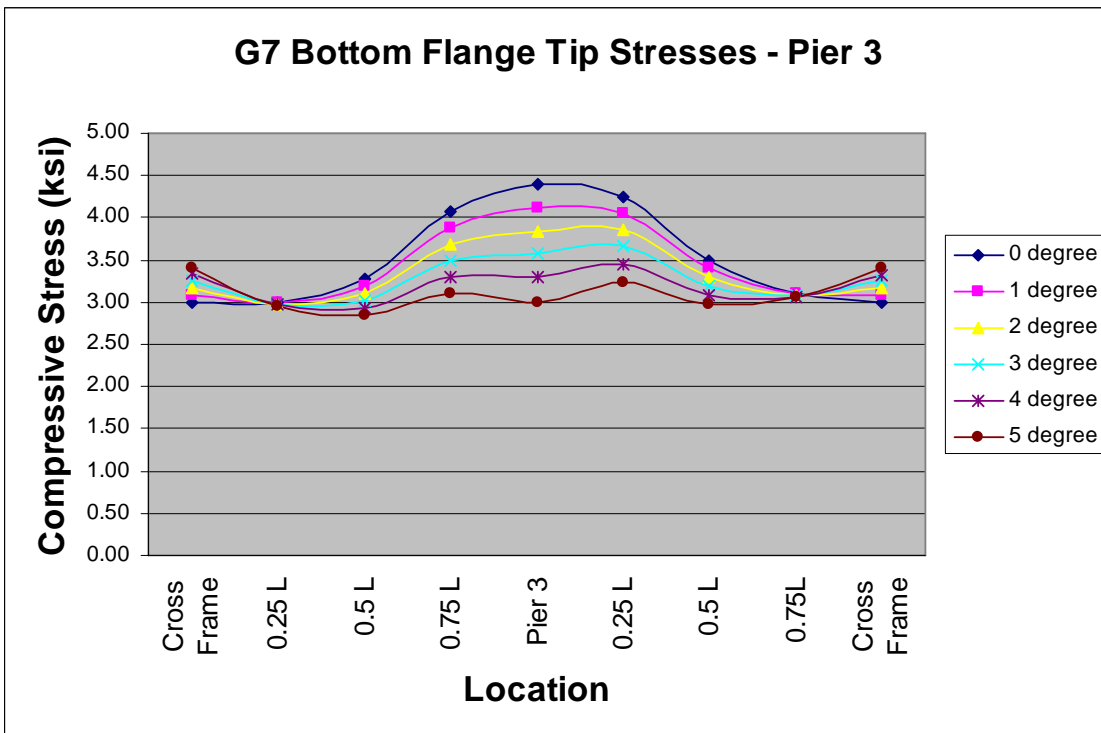
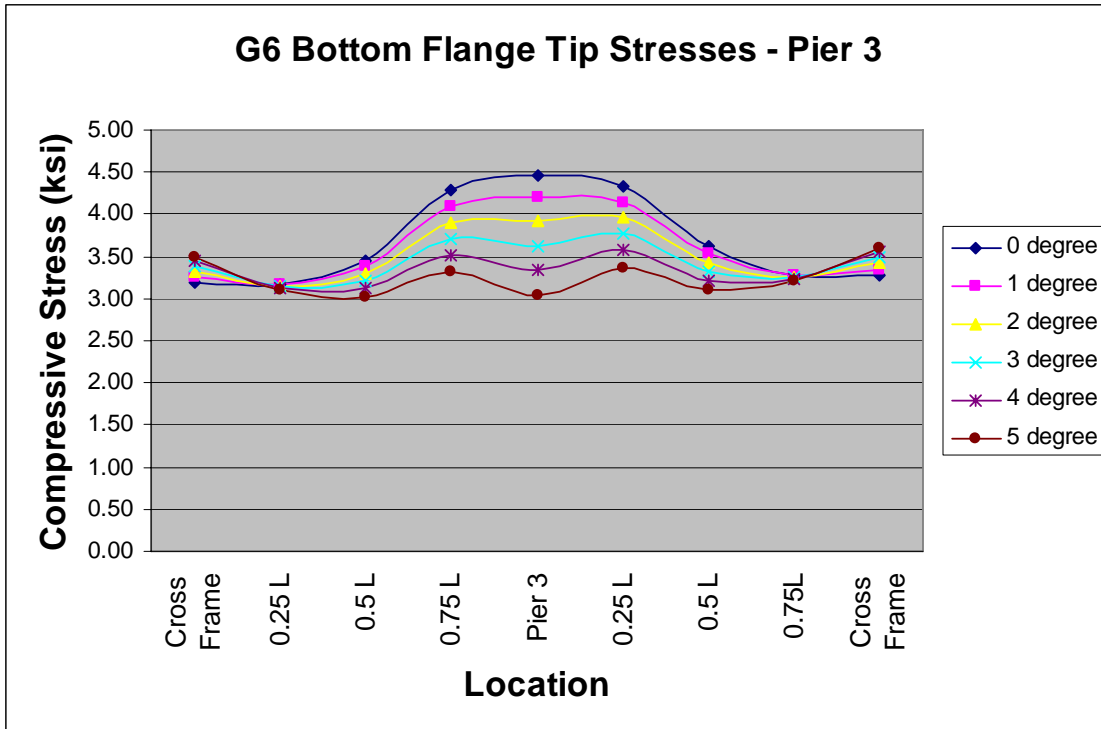
G11 Bottom Flange Tip Stresses - 0.5L Main Span

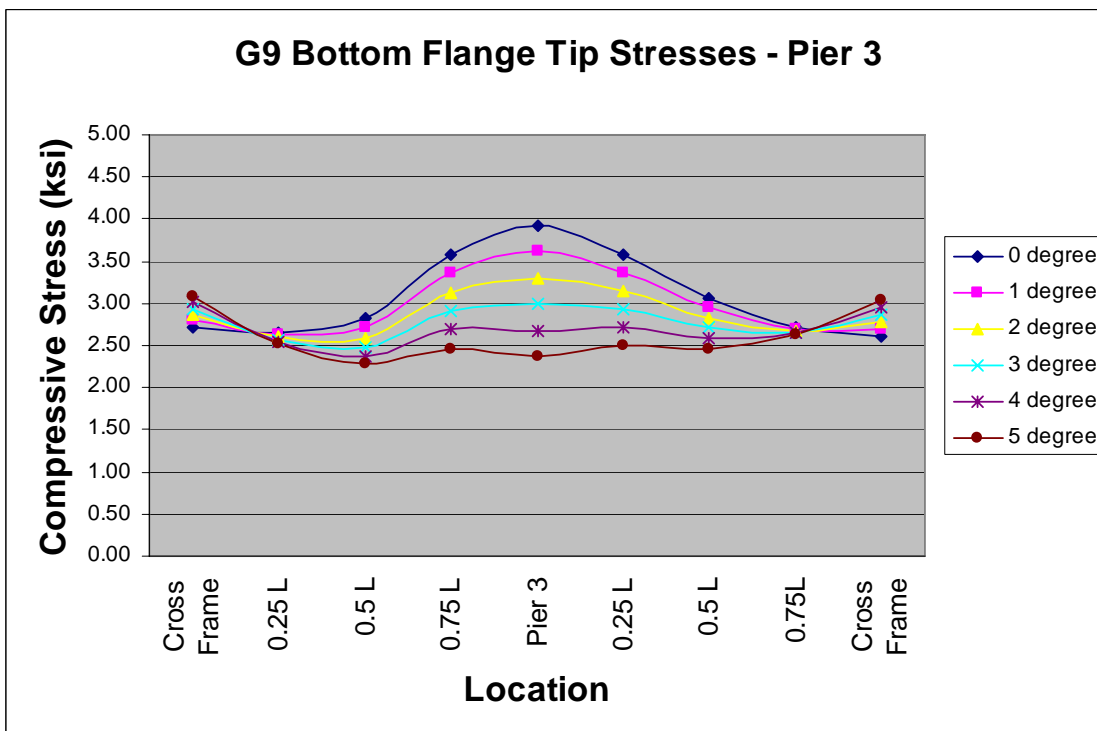
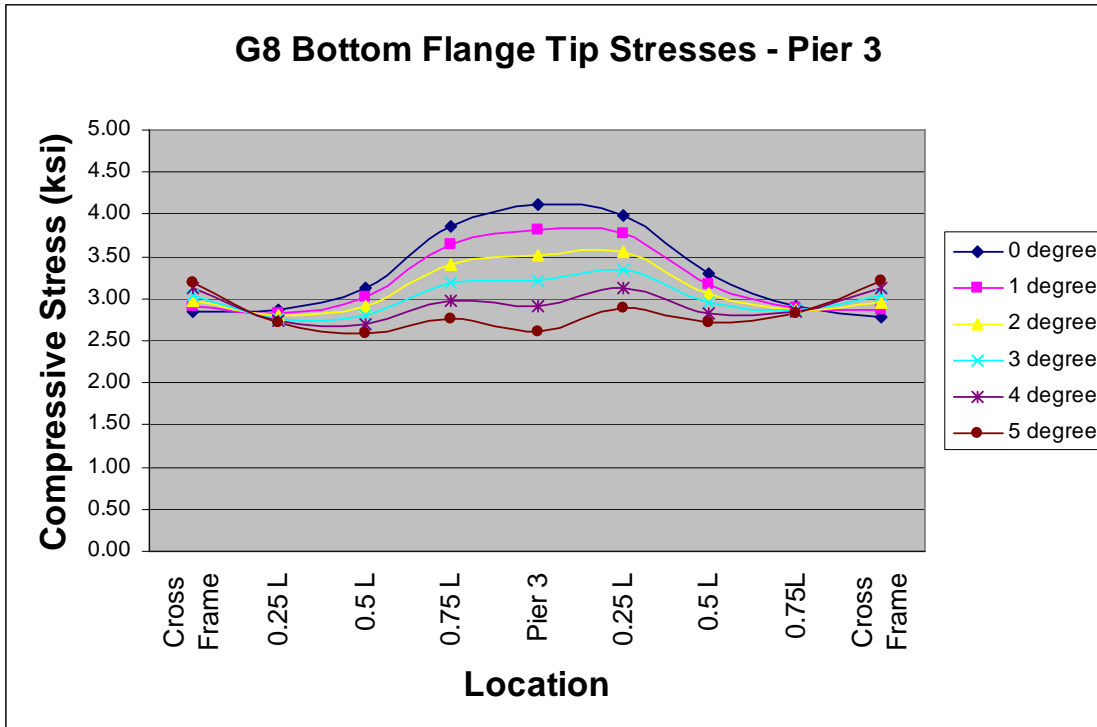


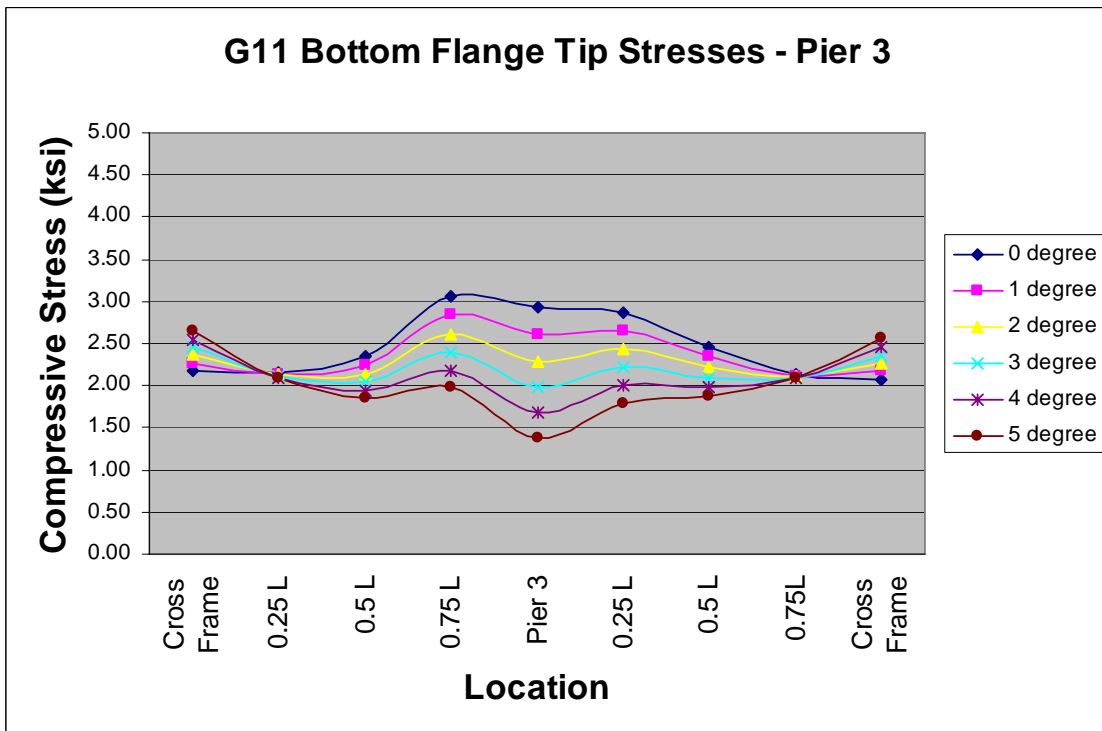
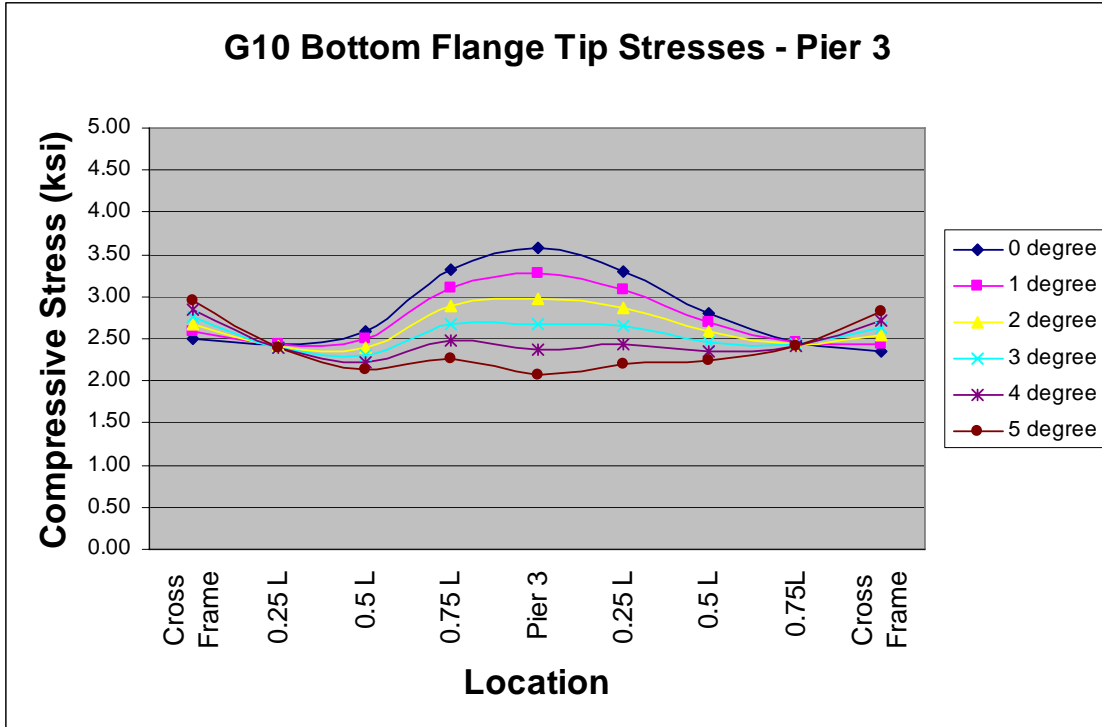


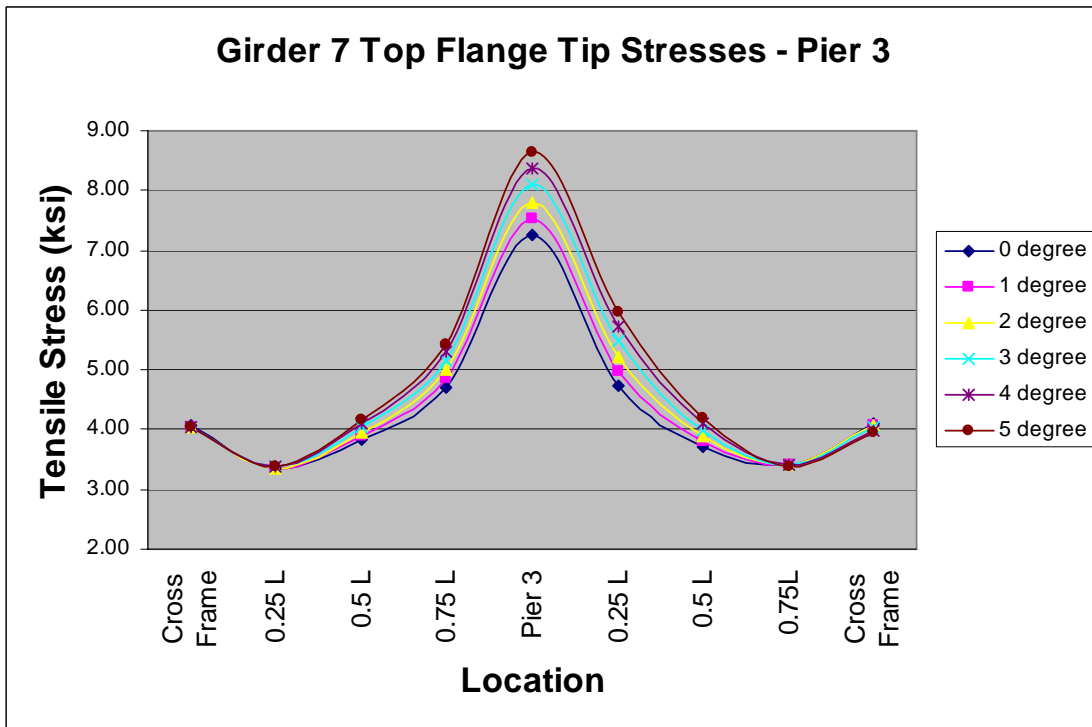
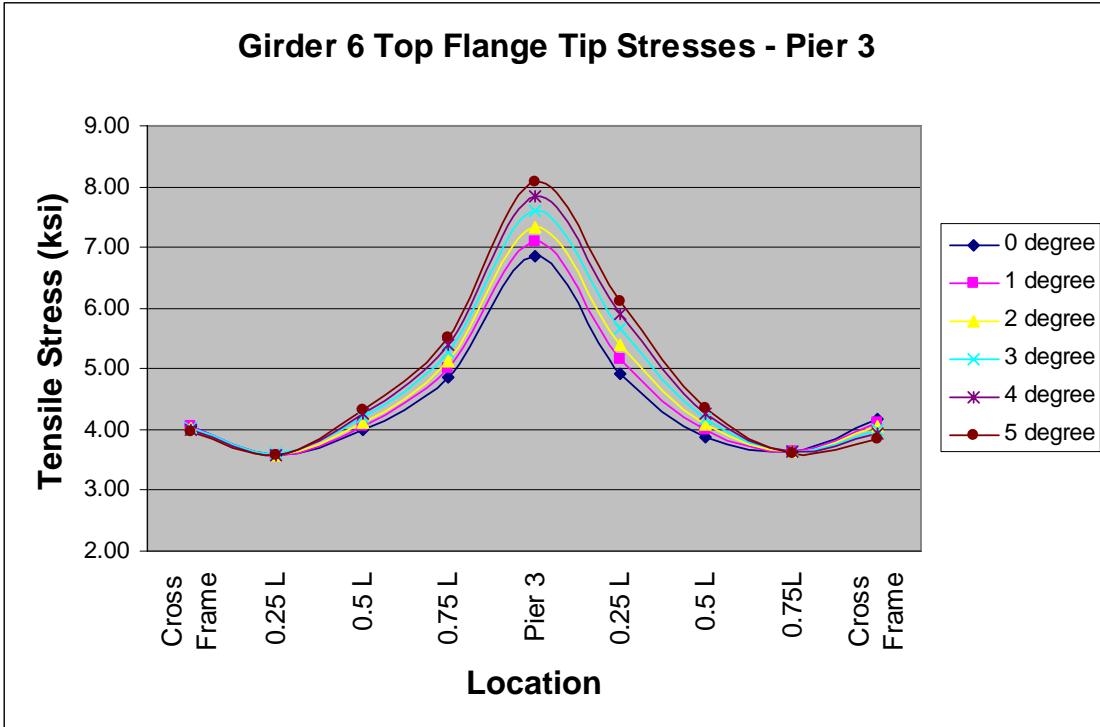


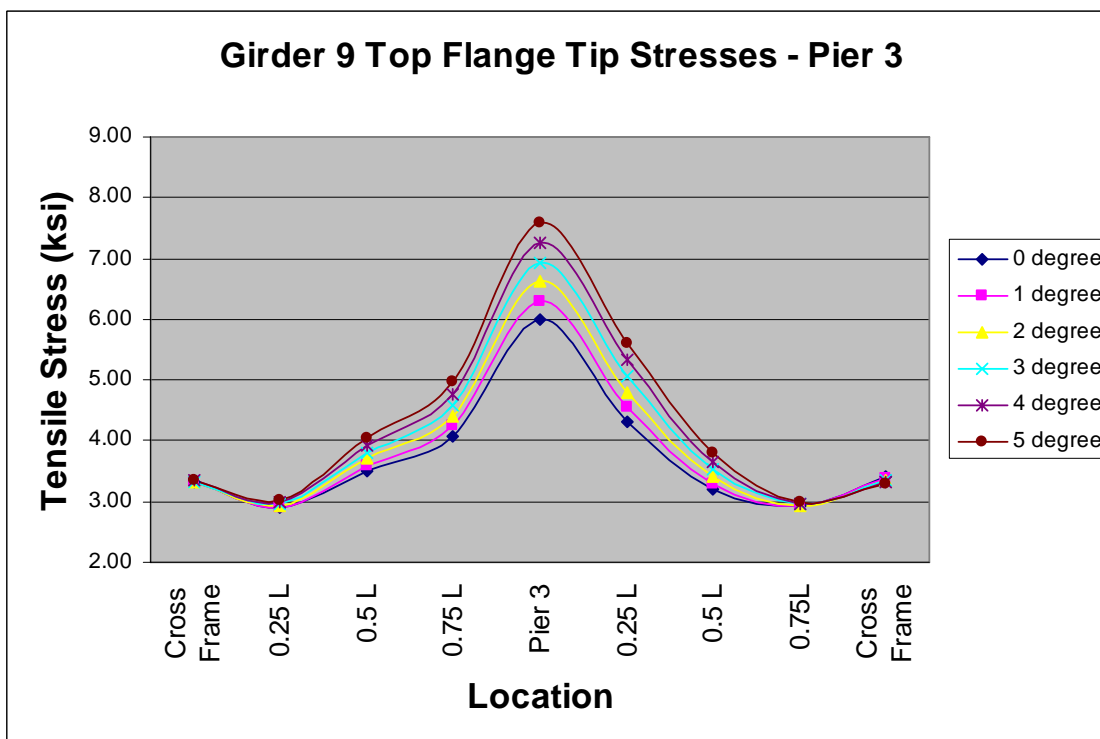
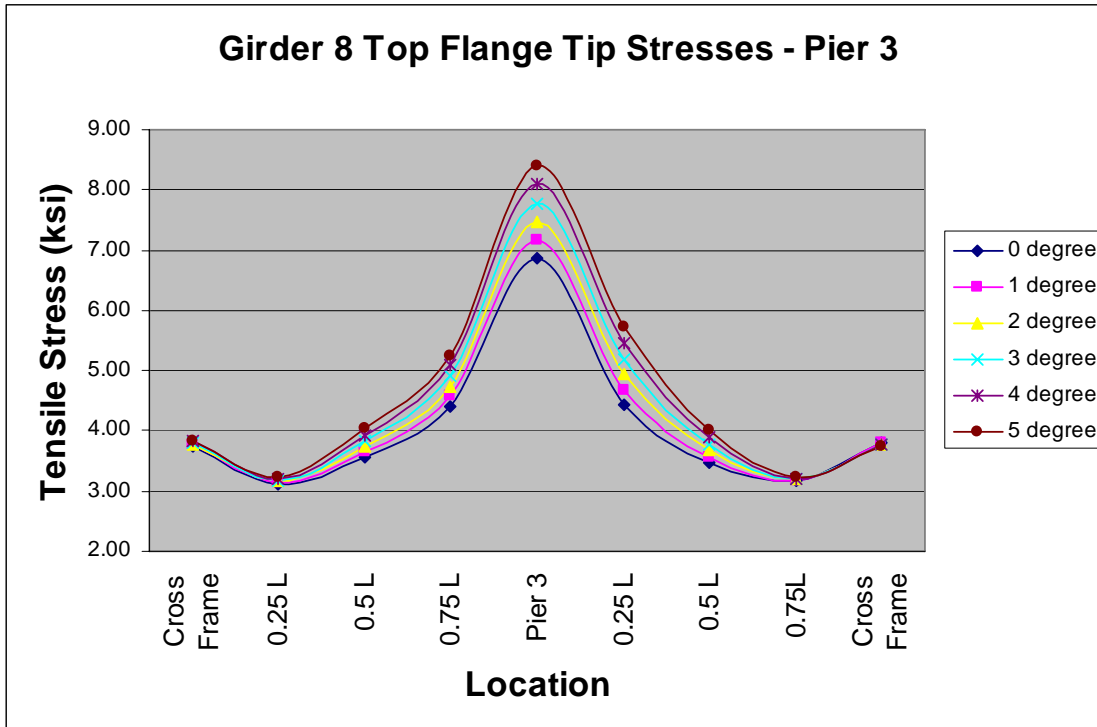


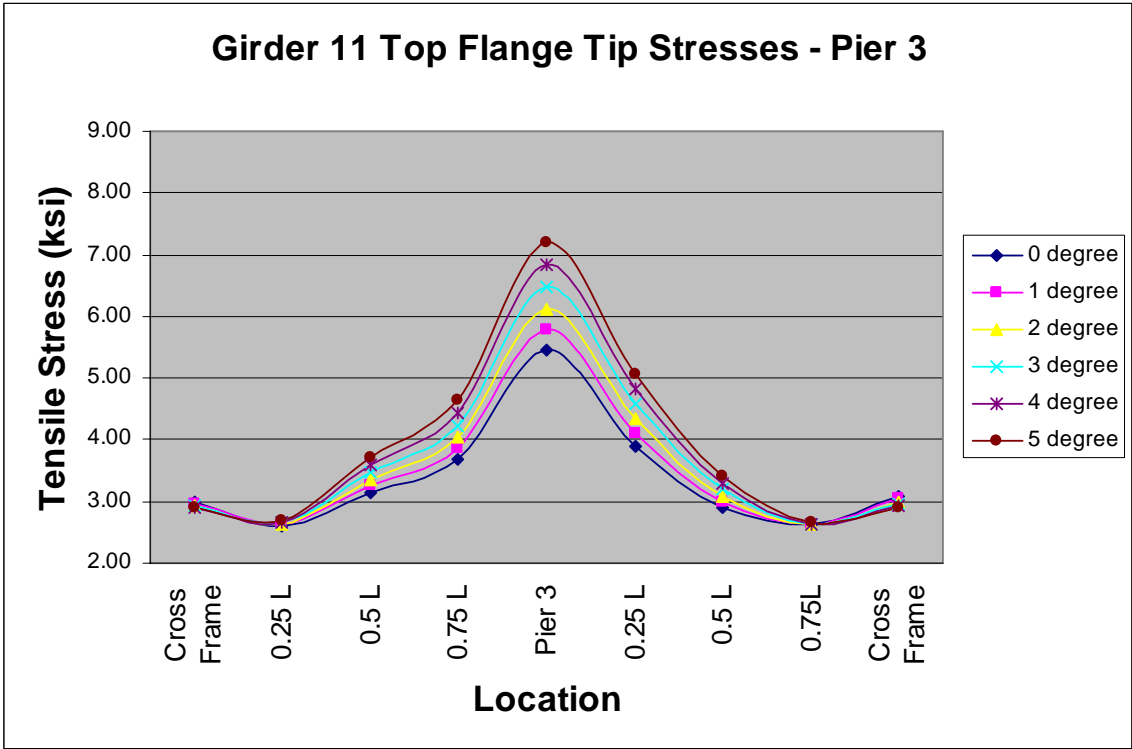
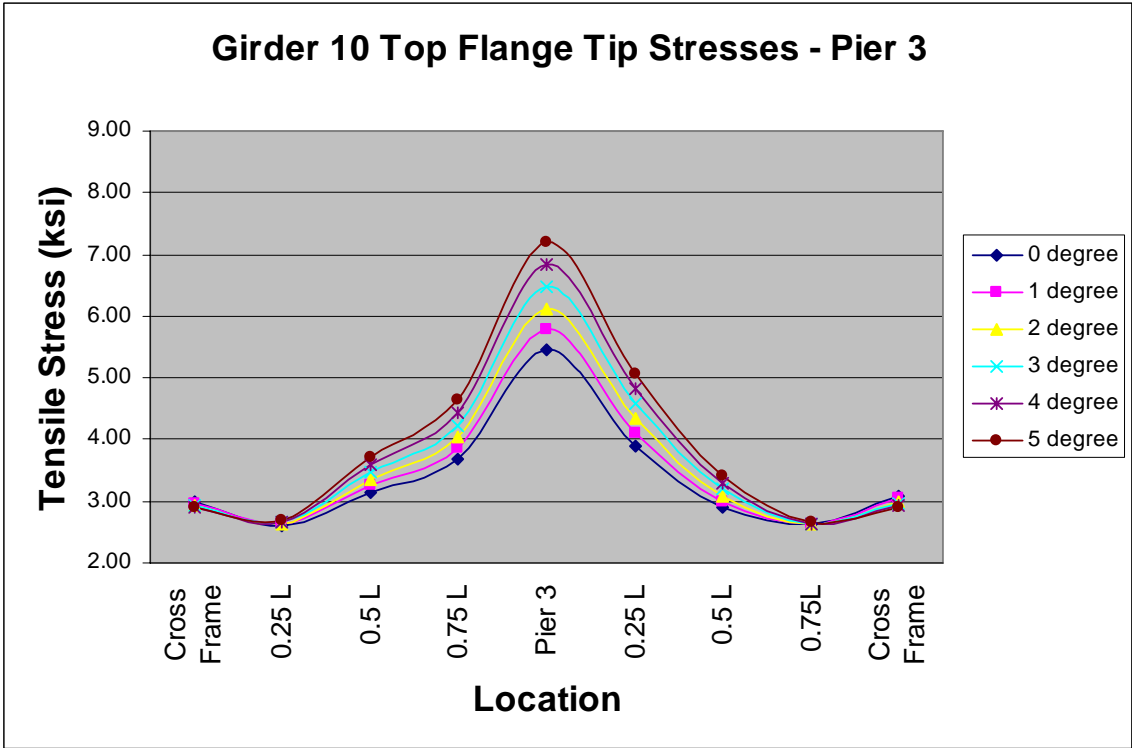


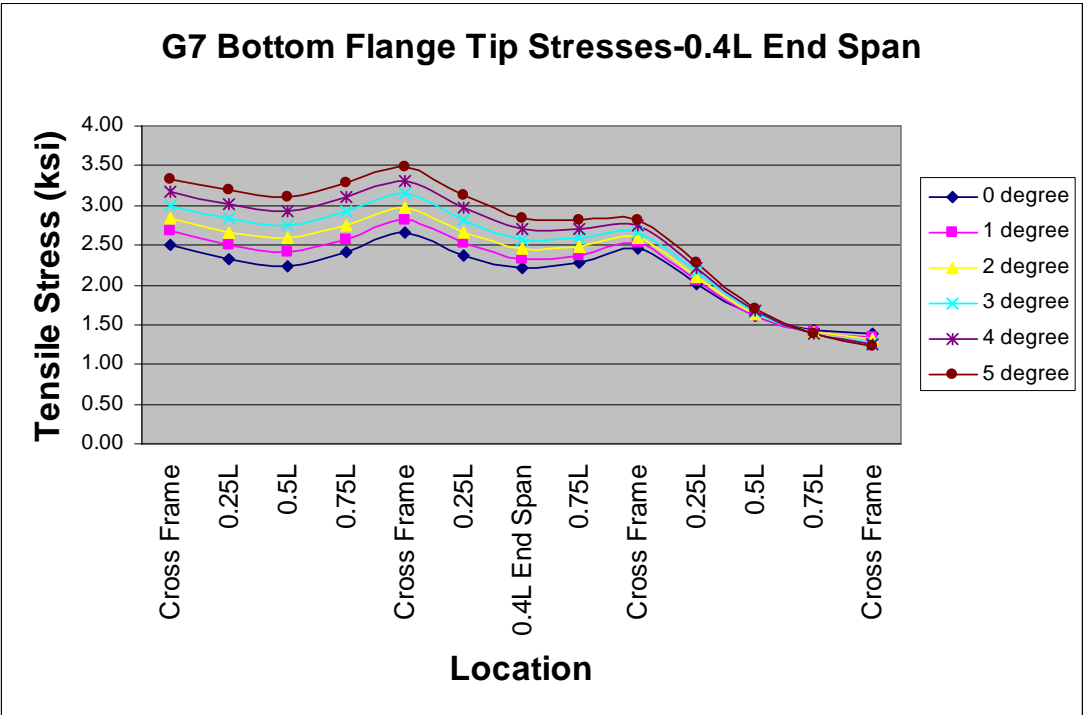
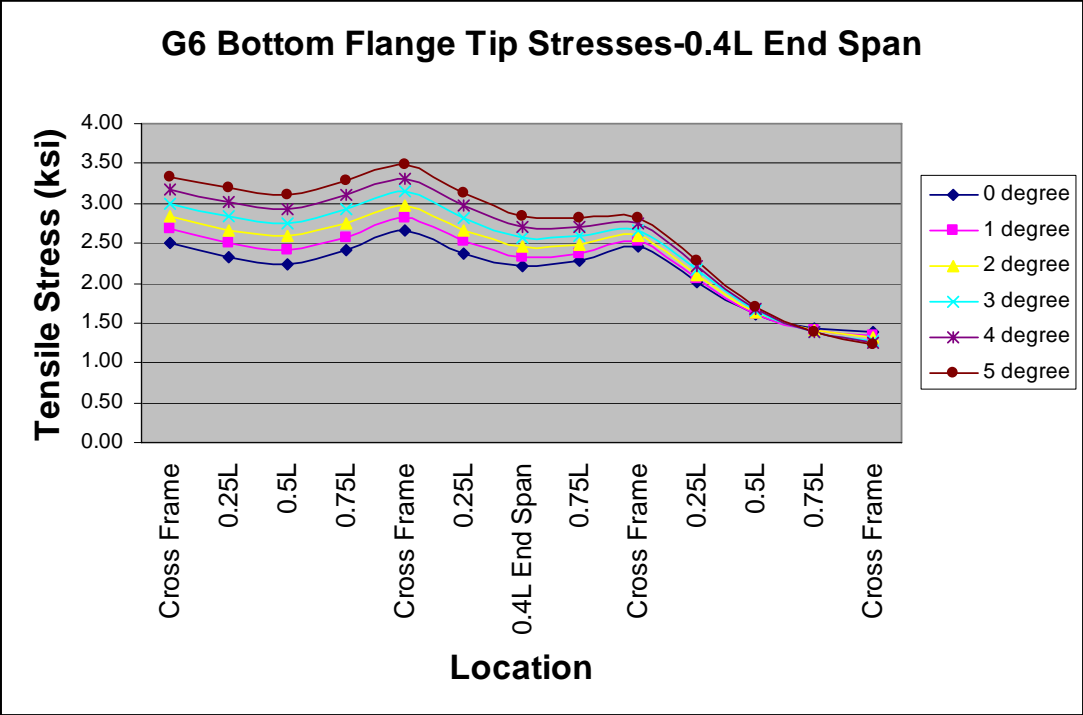


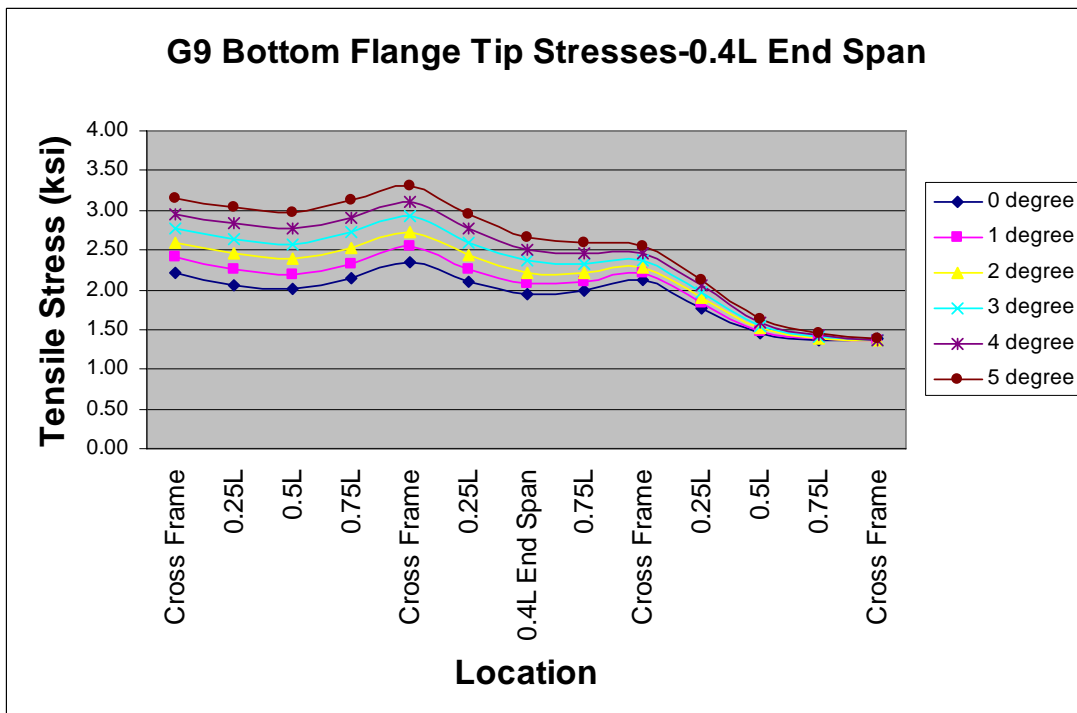
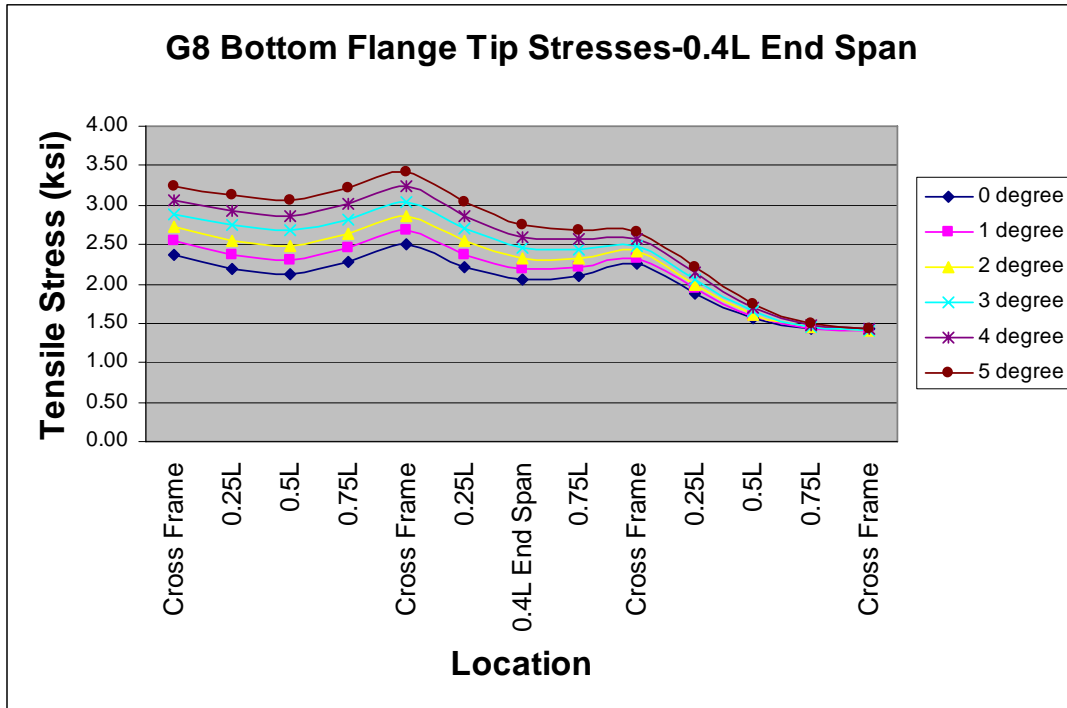


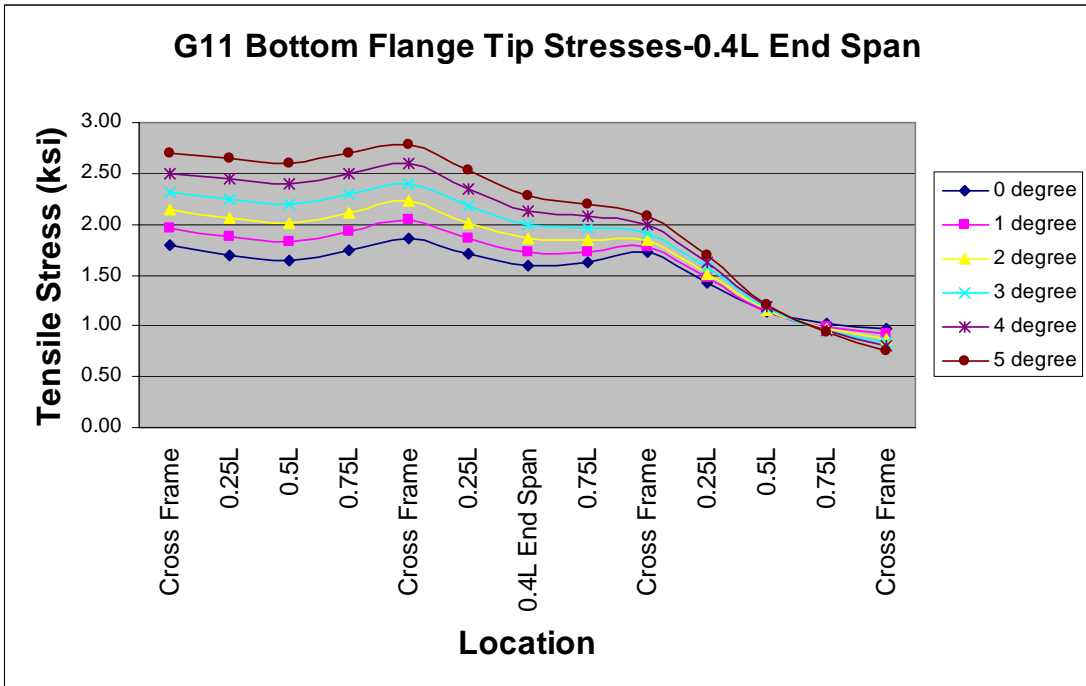
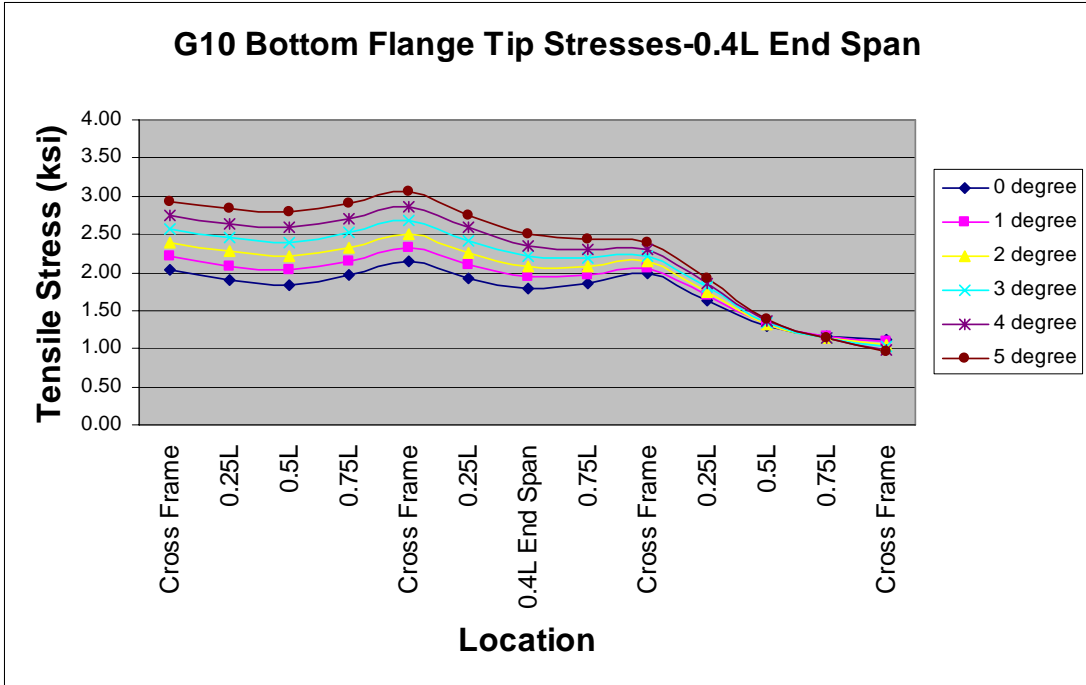


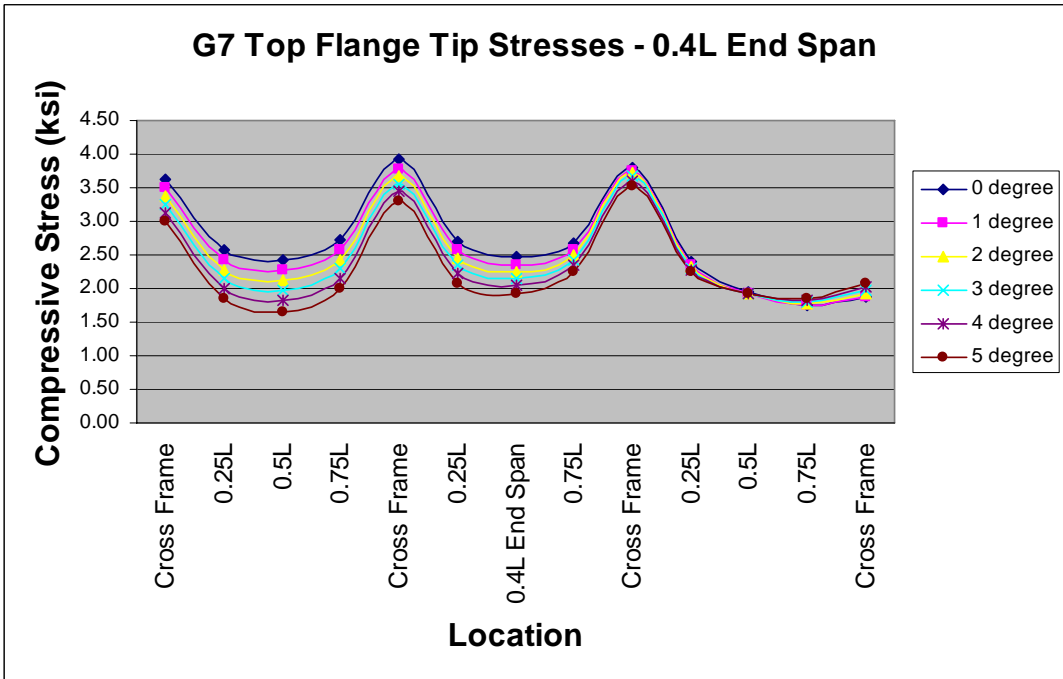
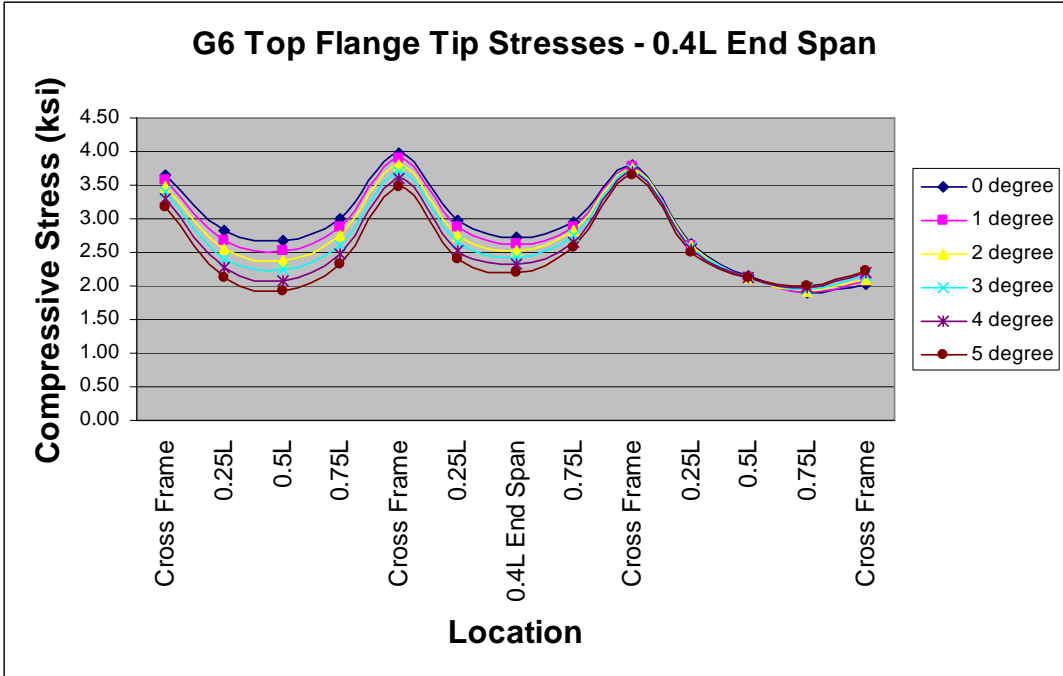


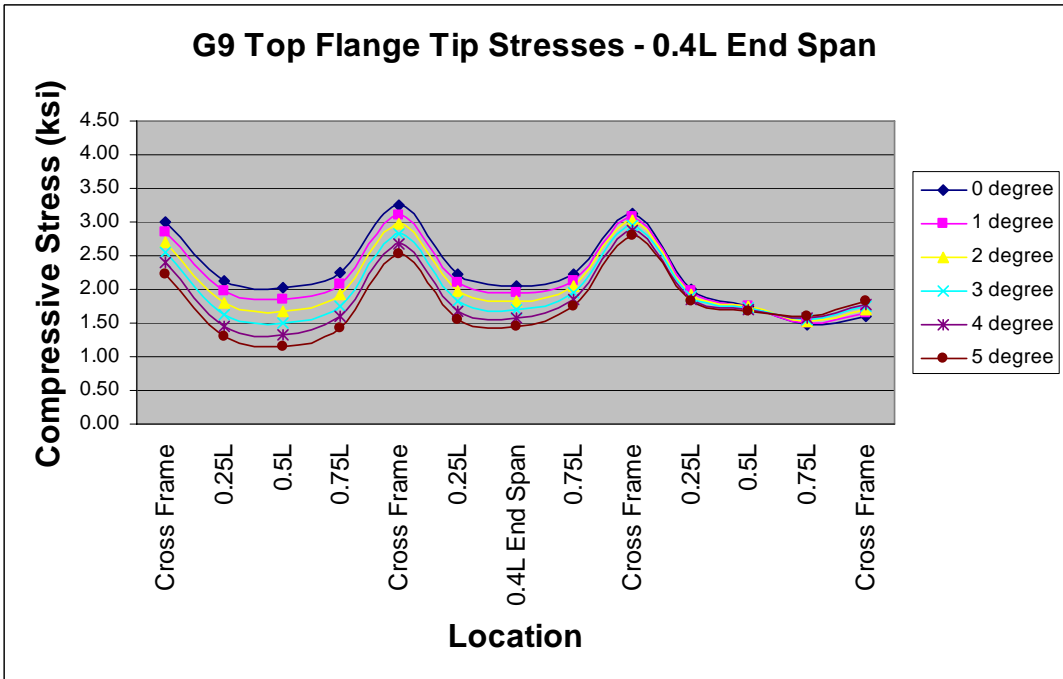
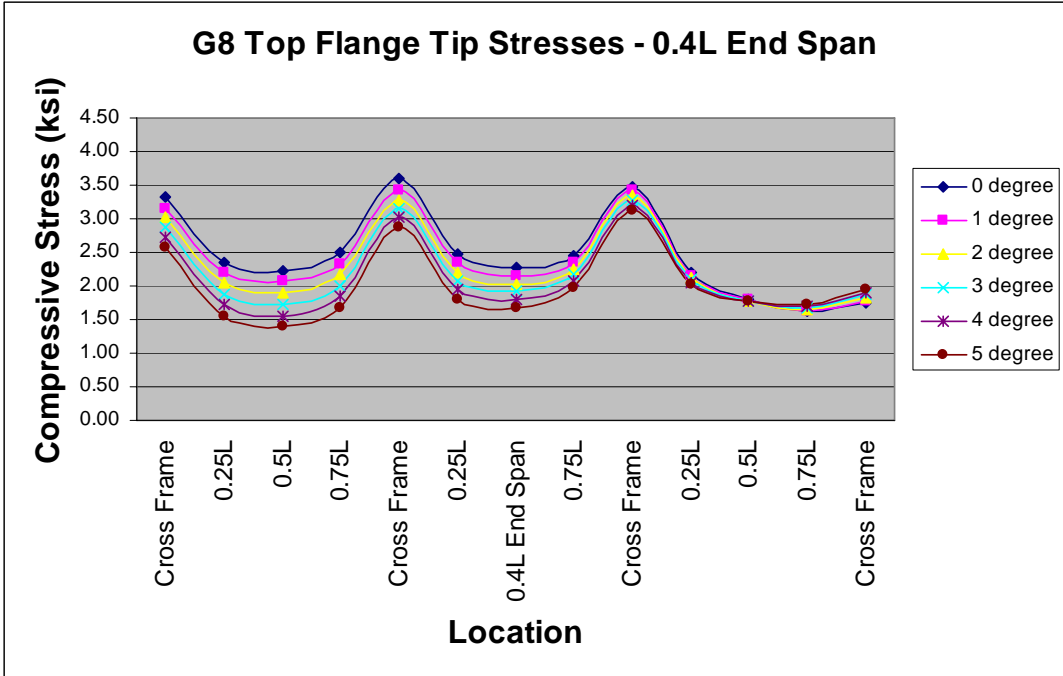


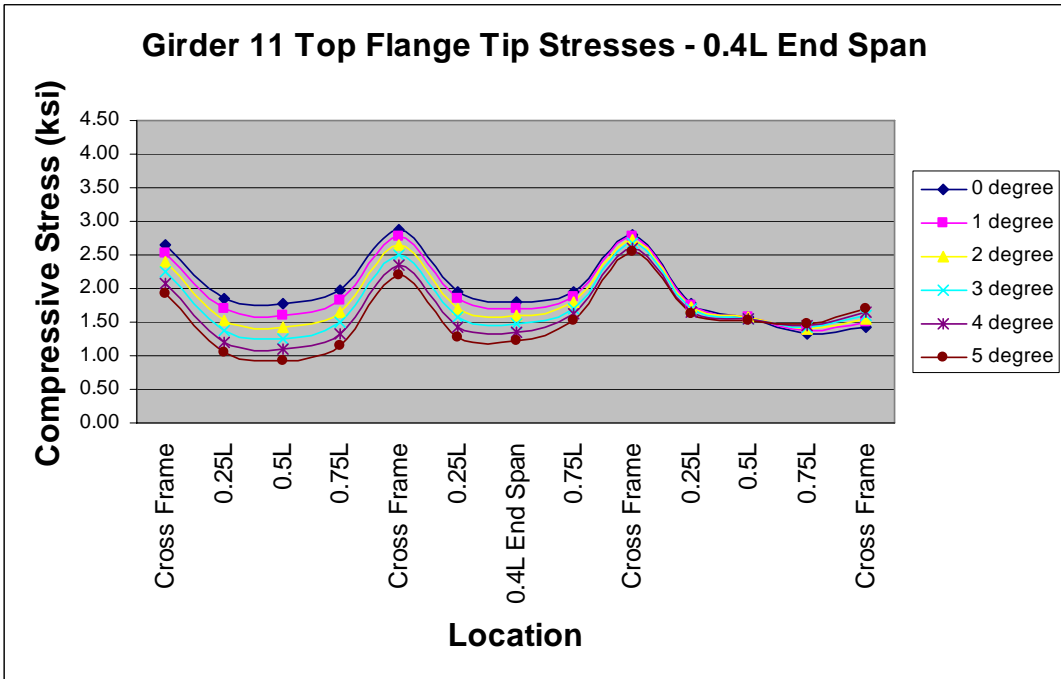
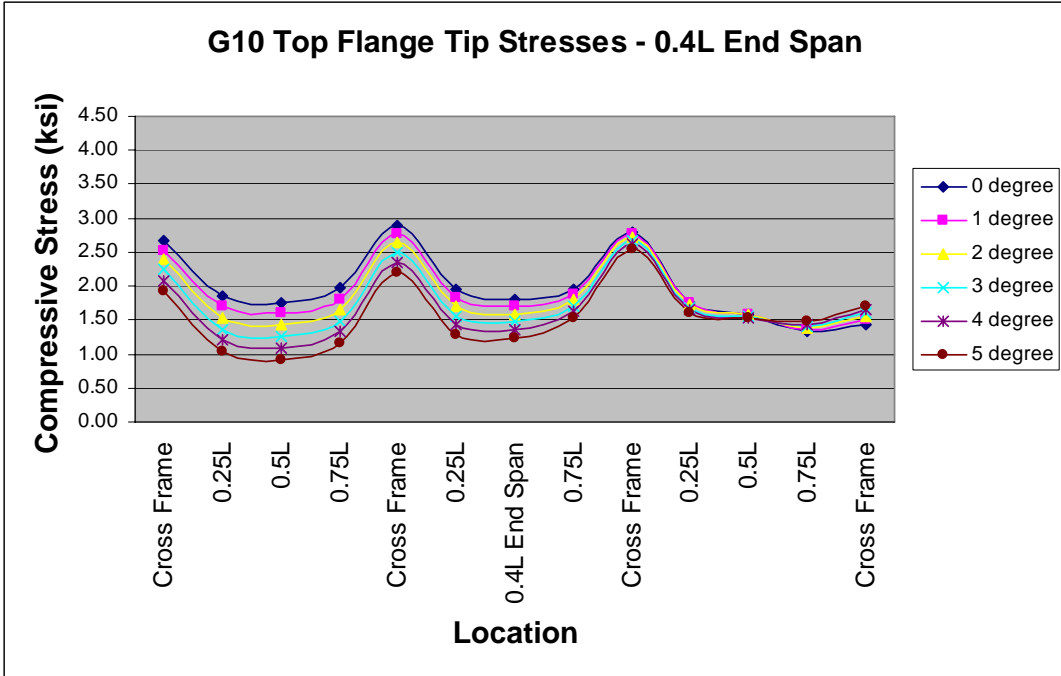


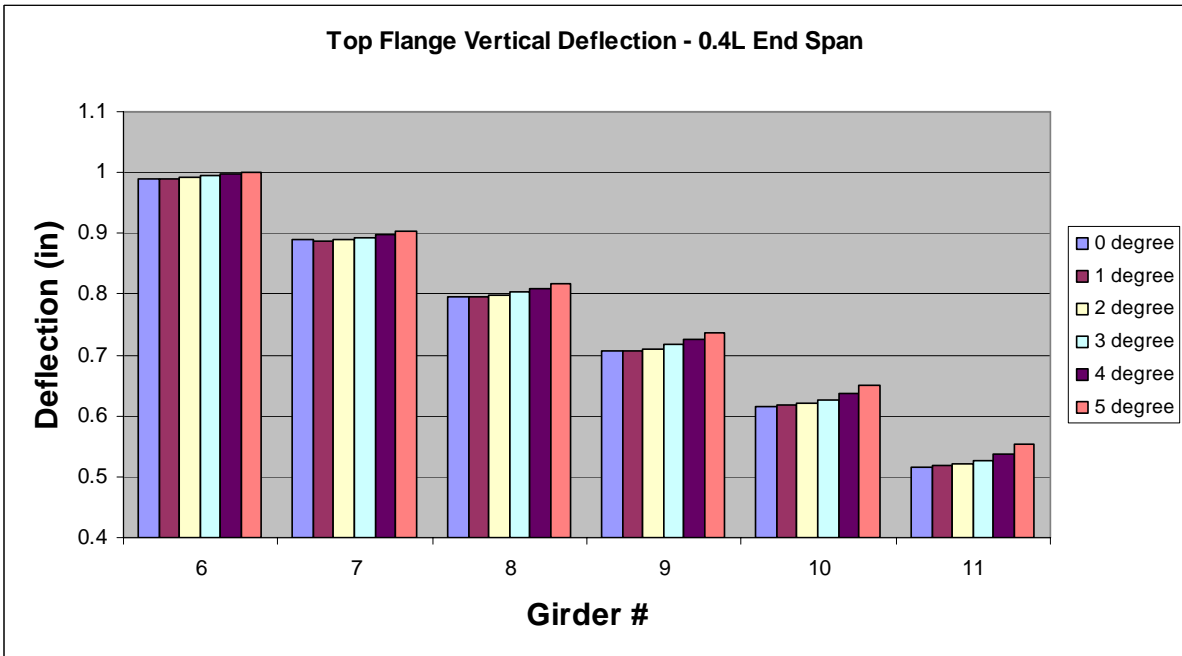
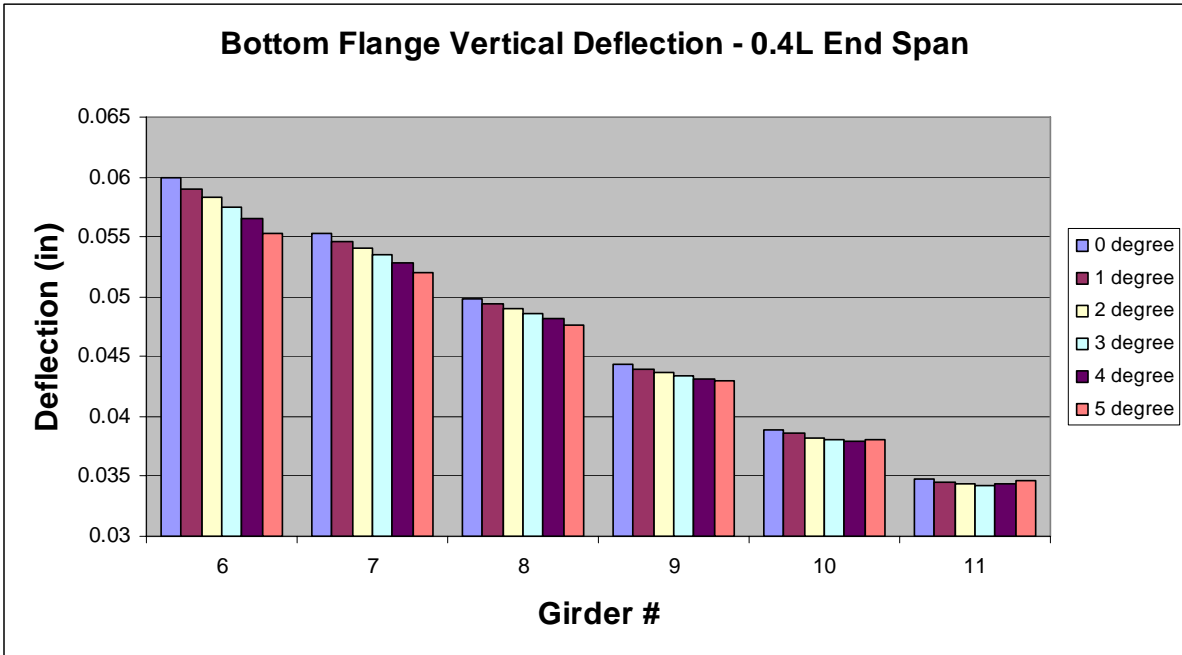


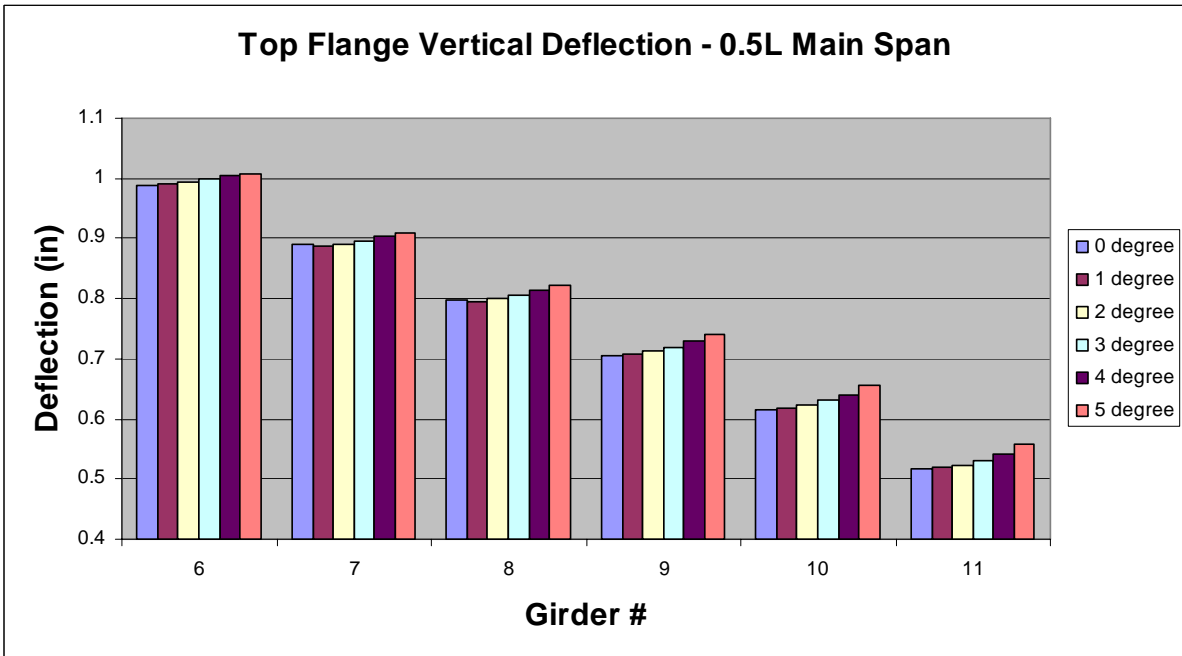
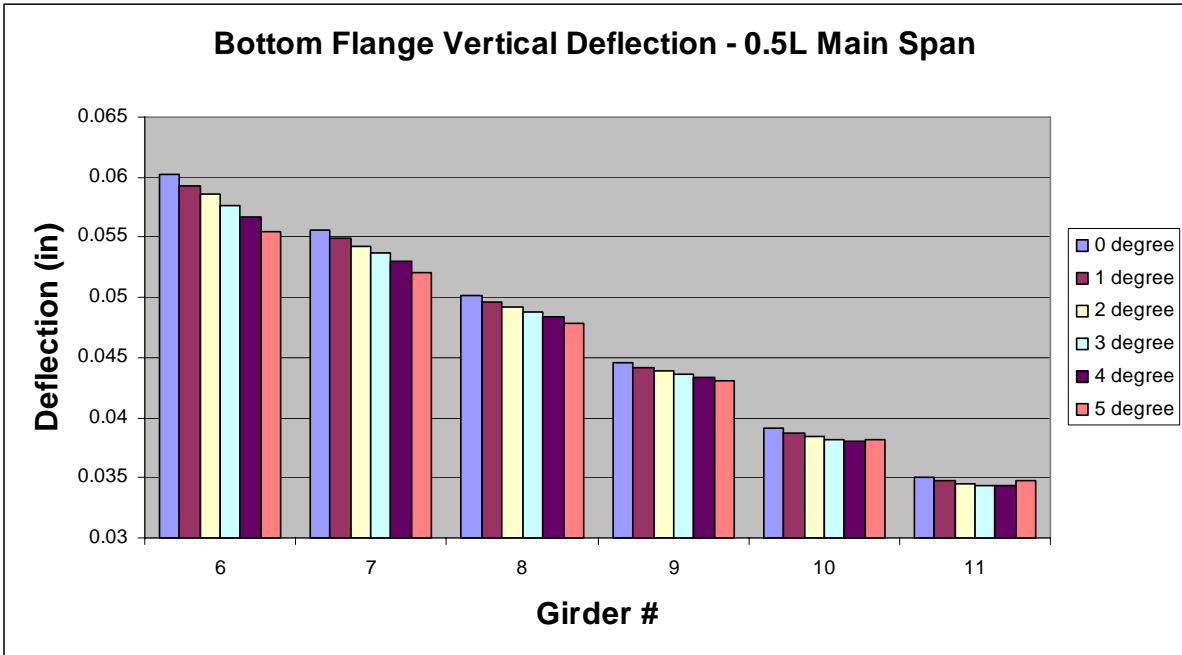


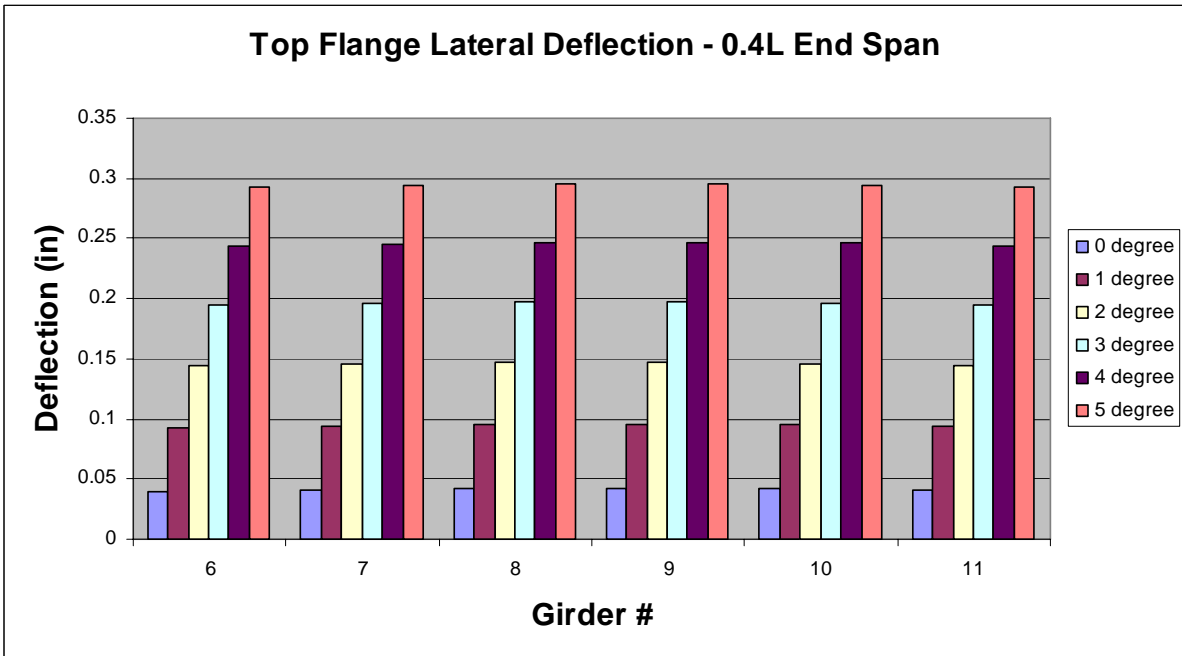
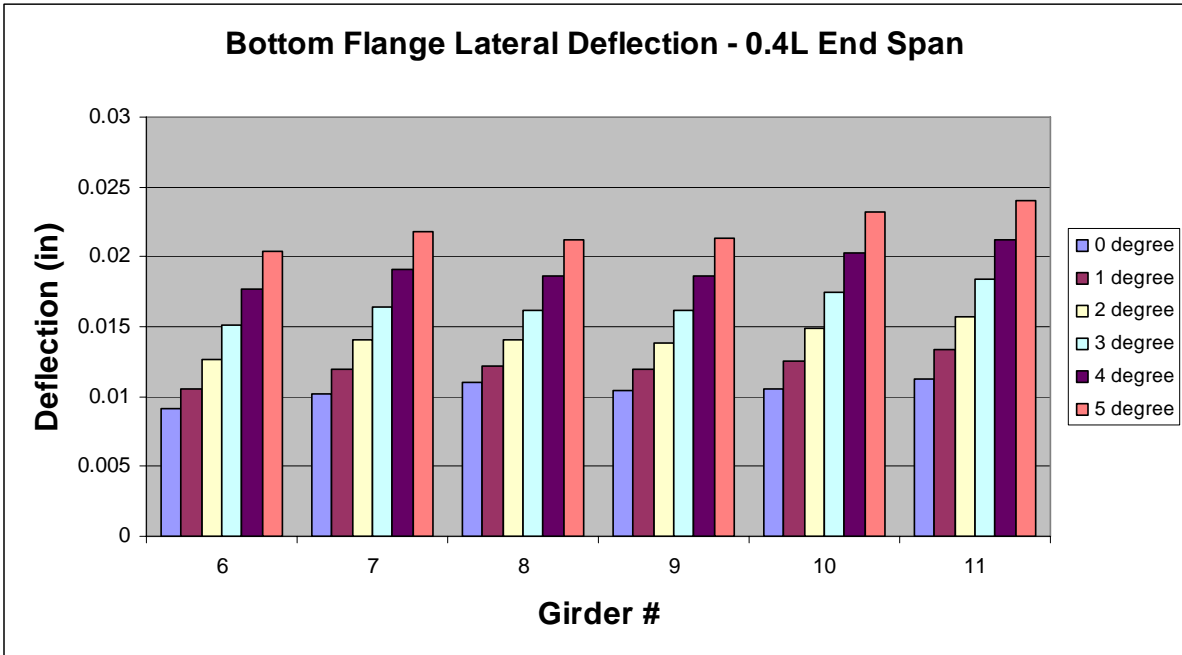


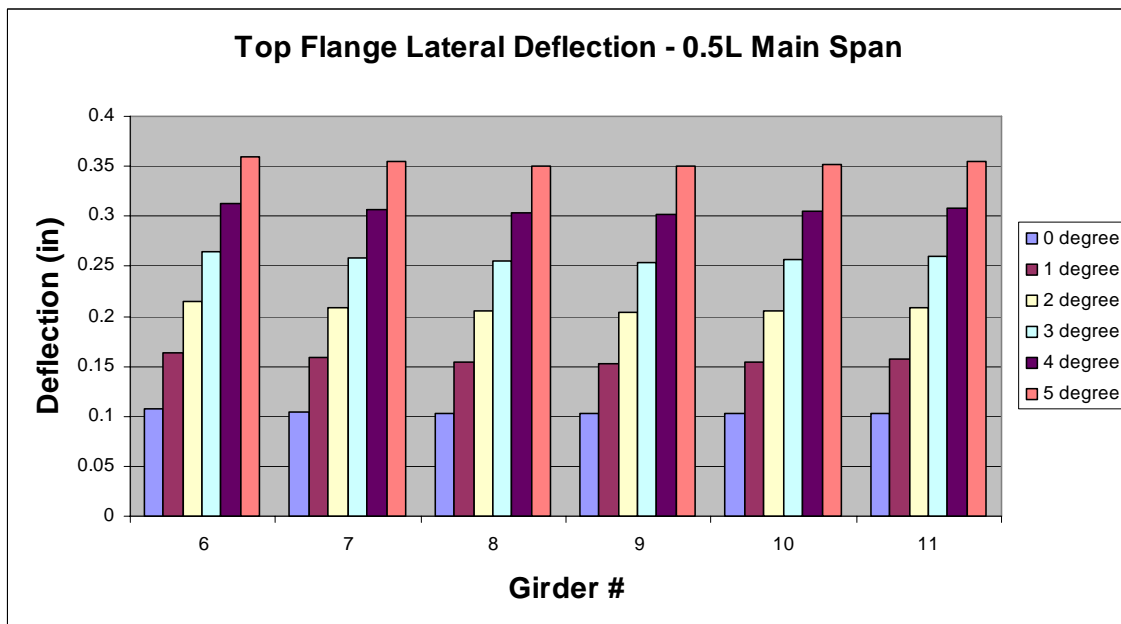
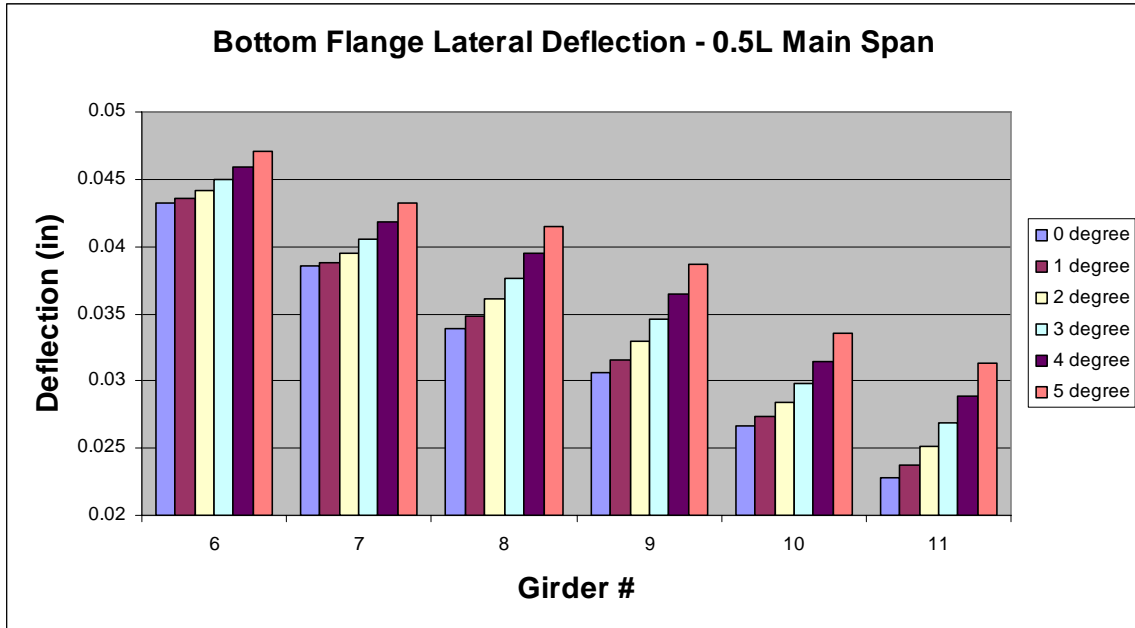


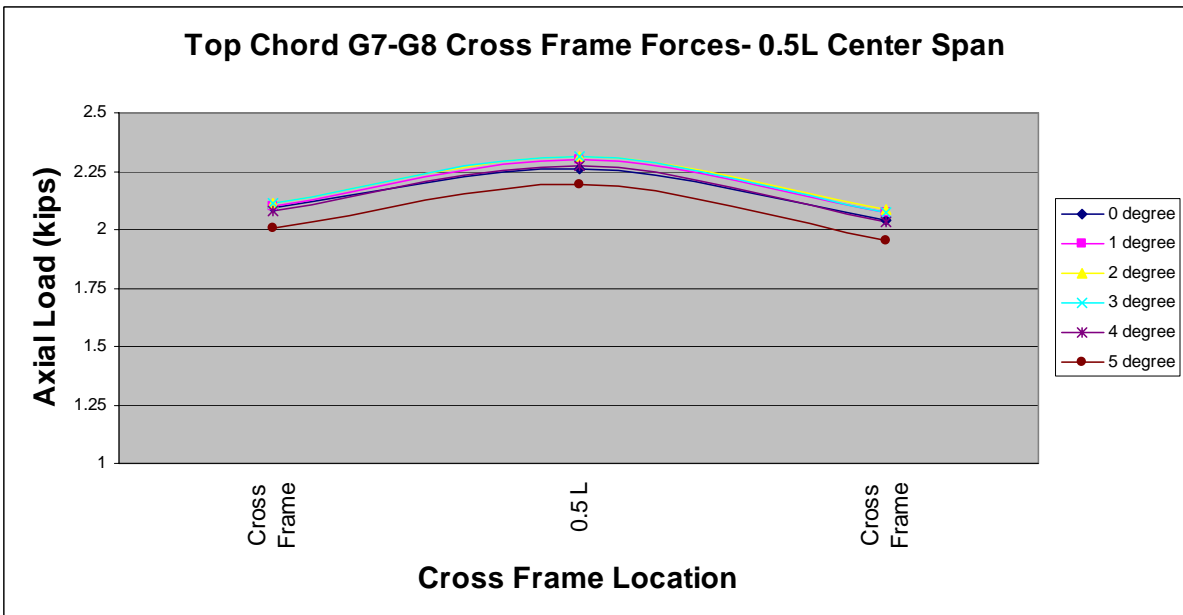
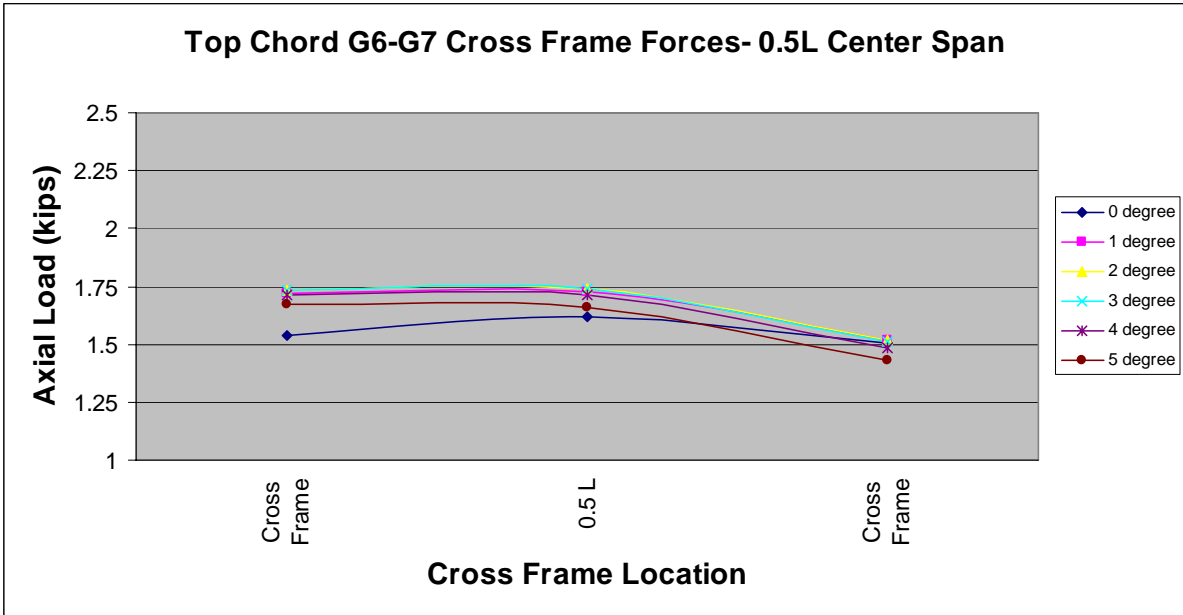


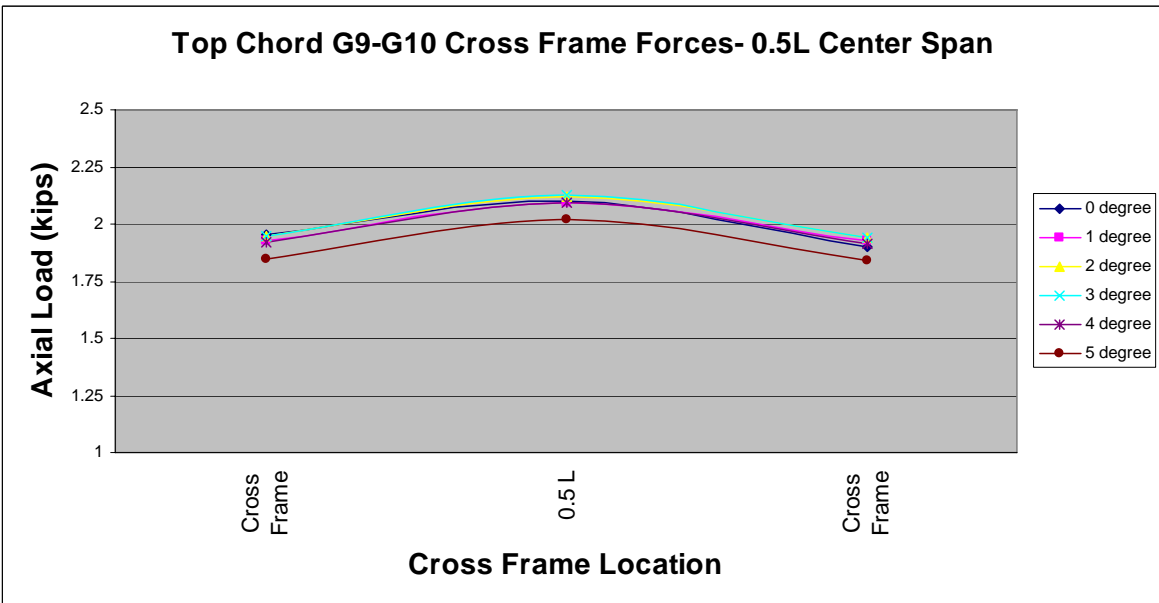
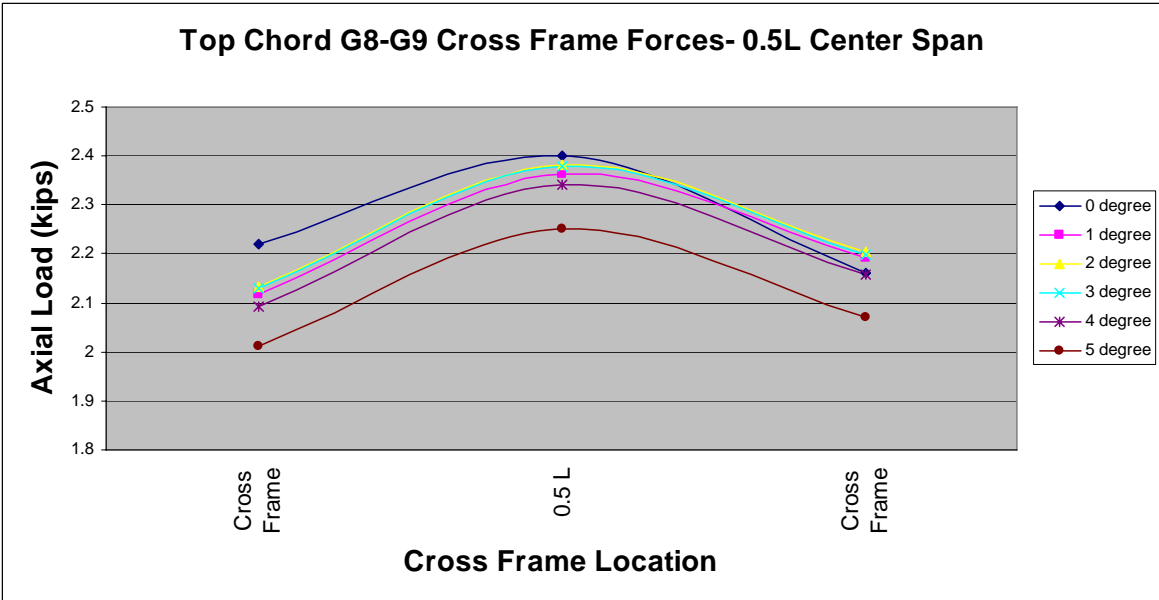


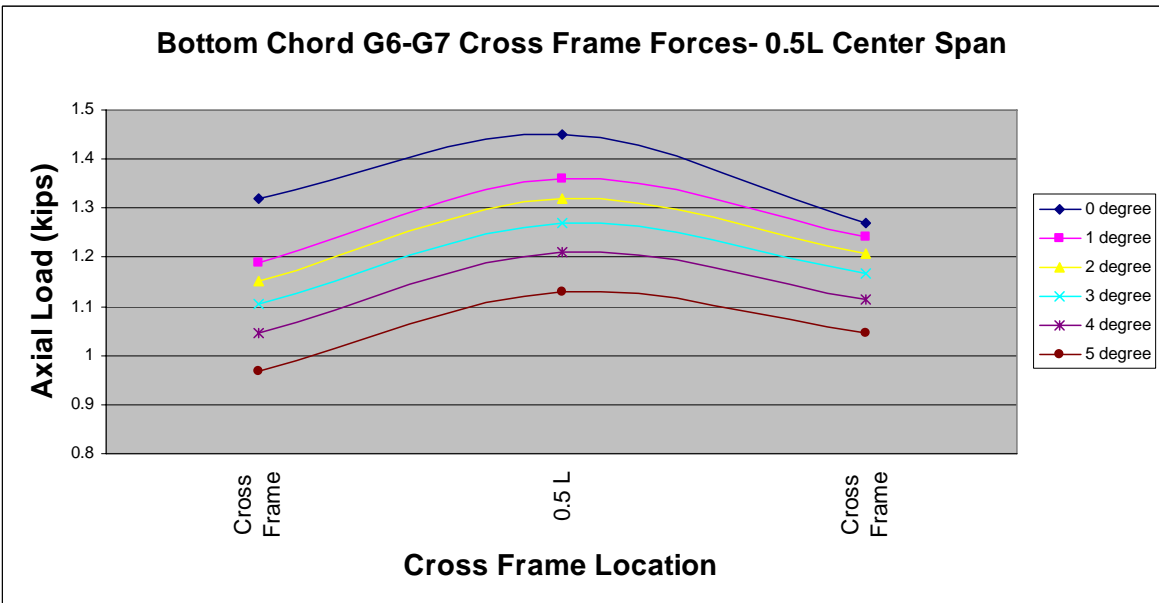


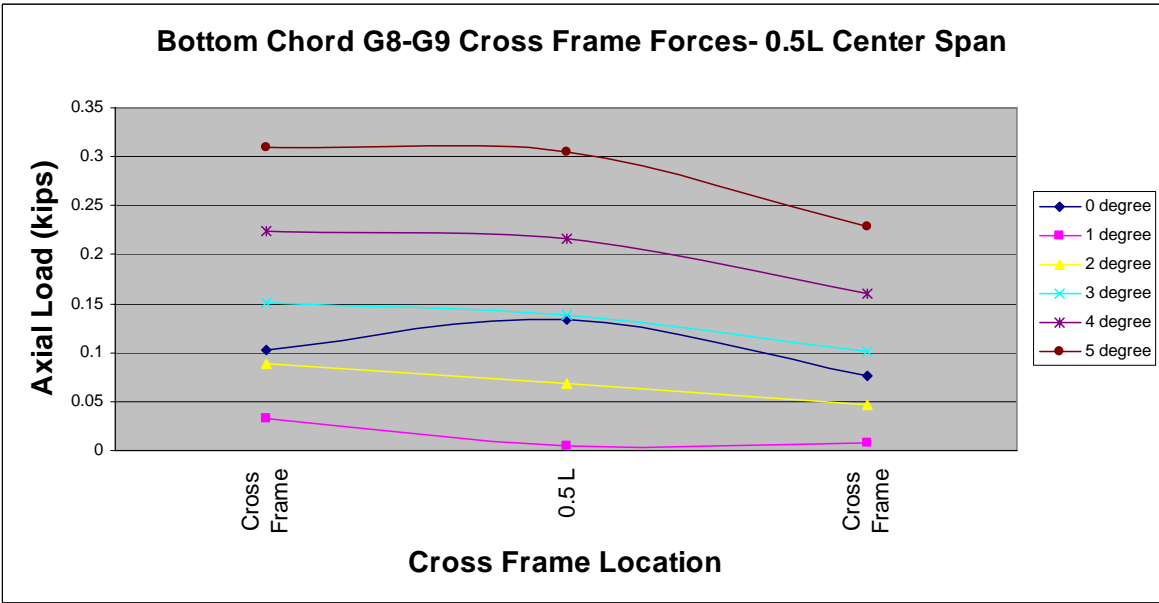
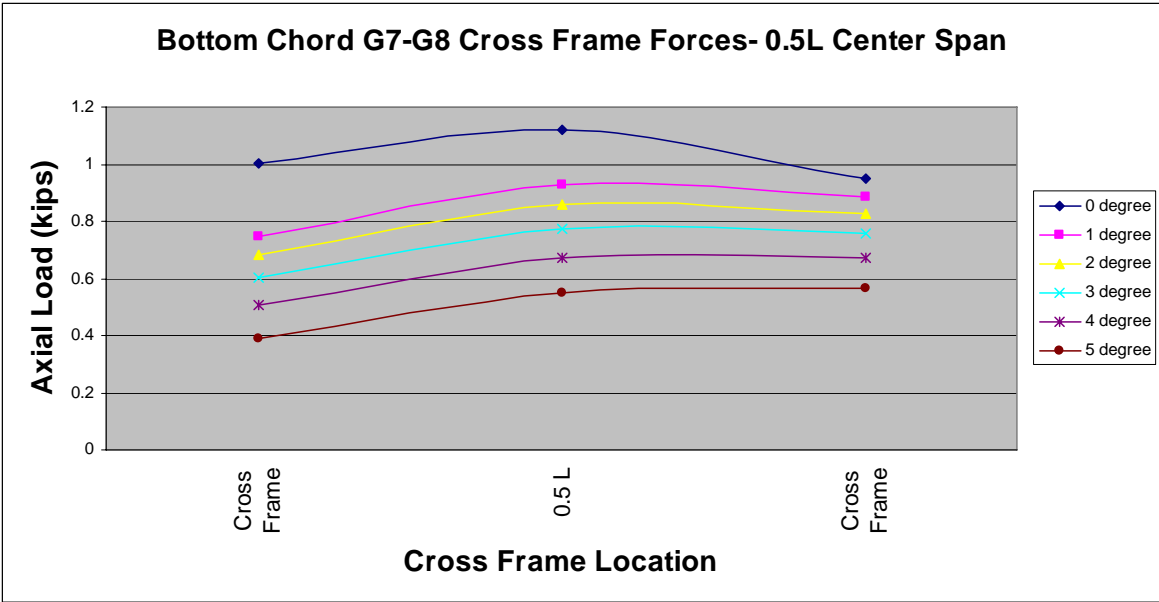


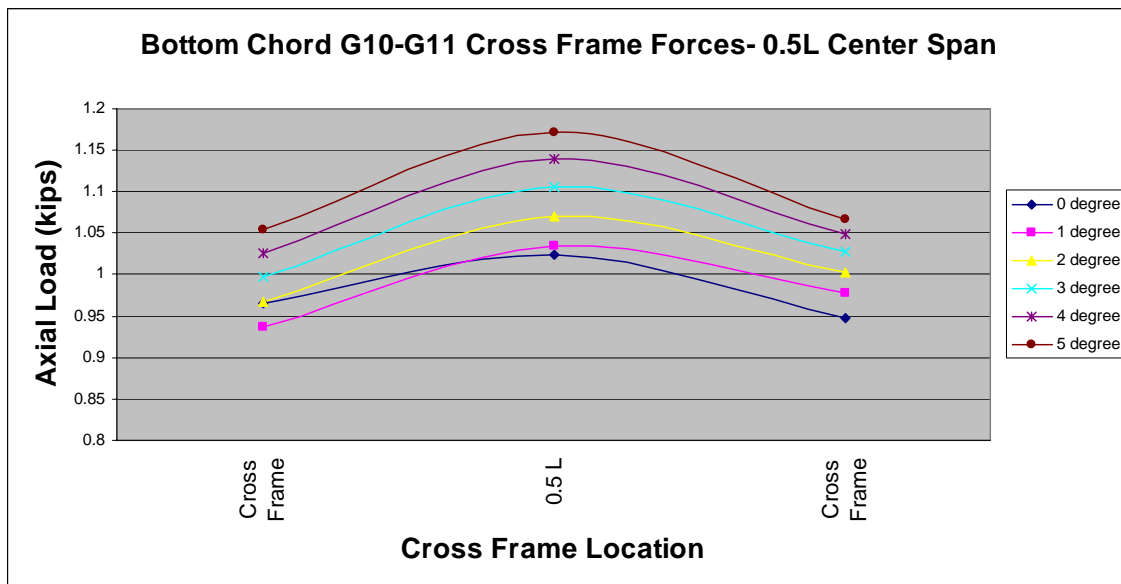
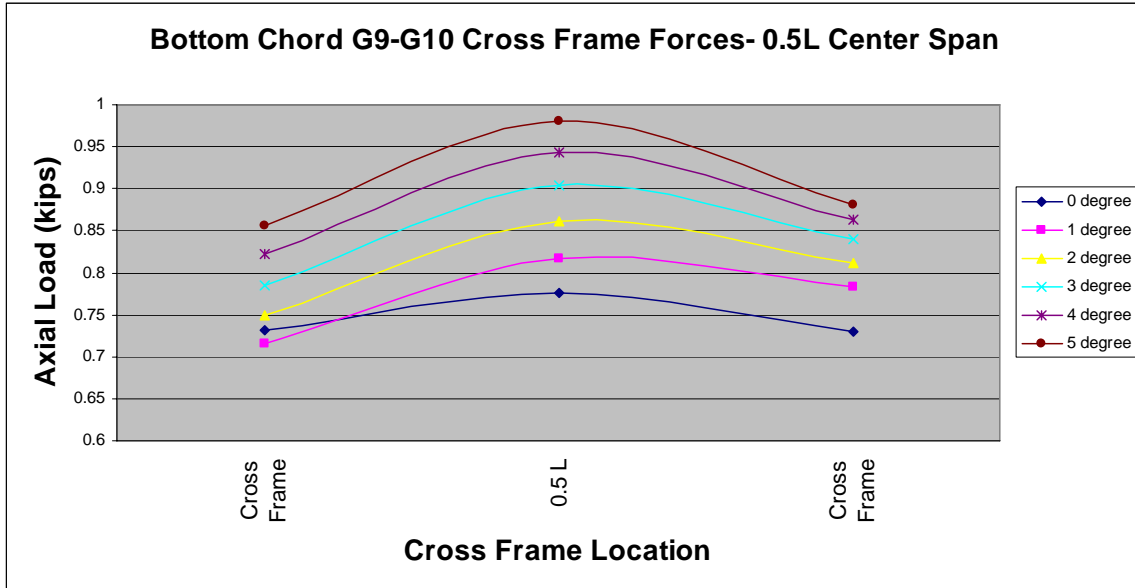


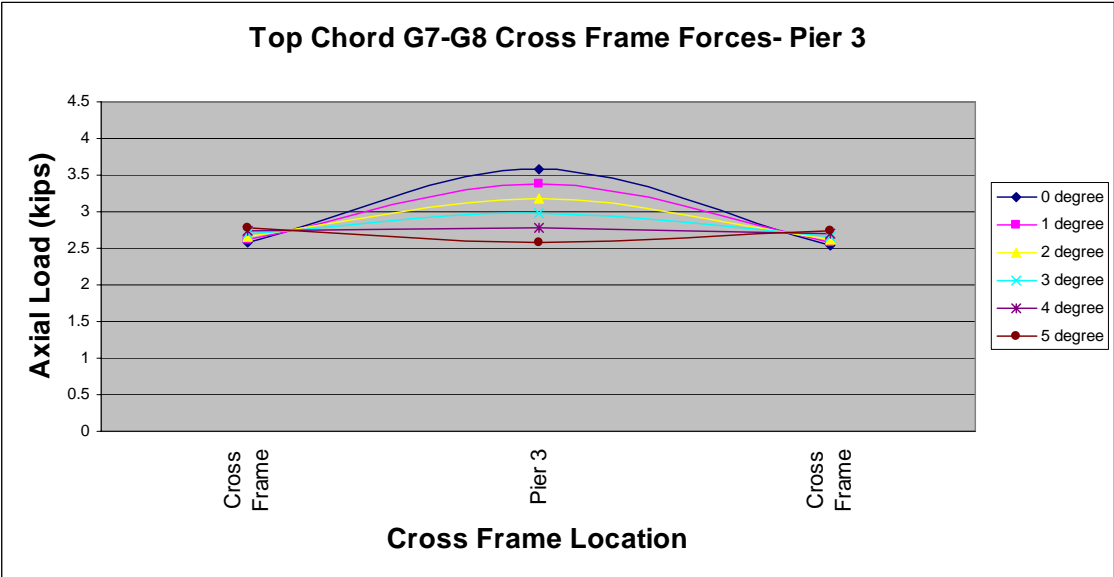
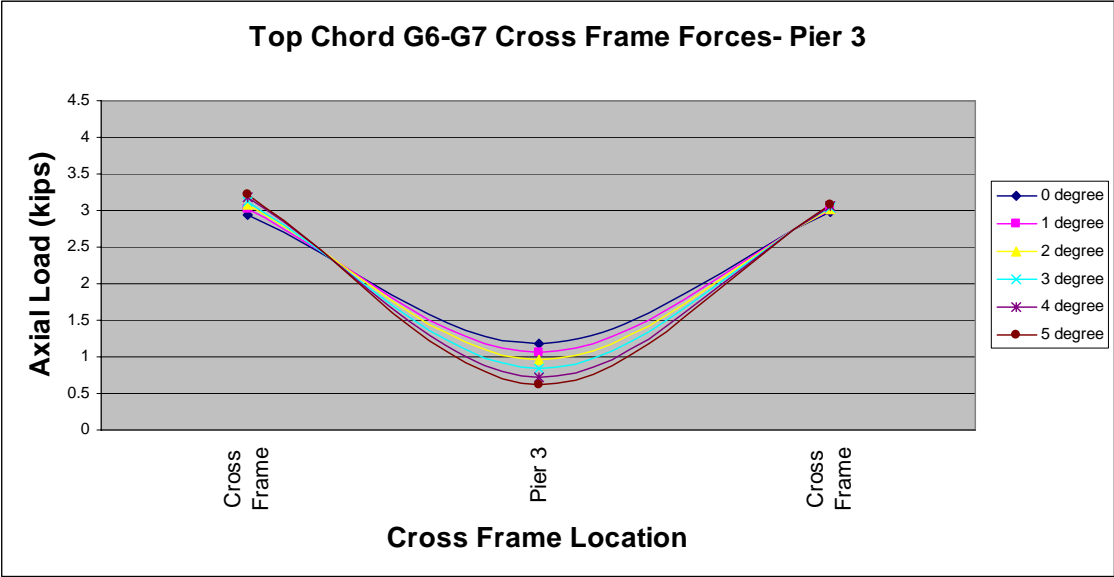


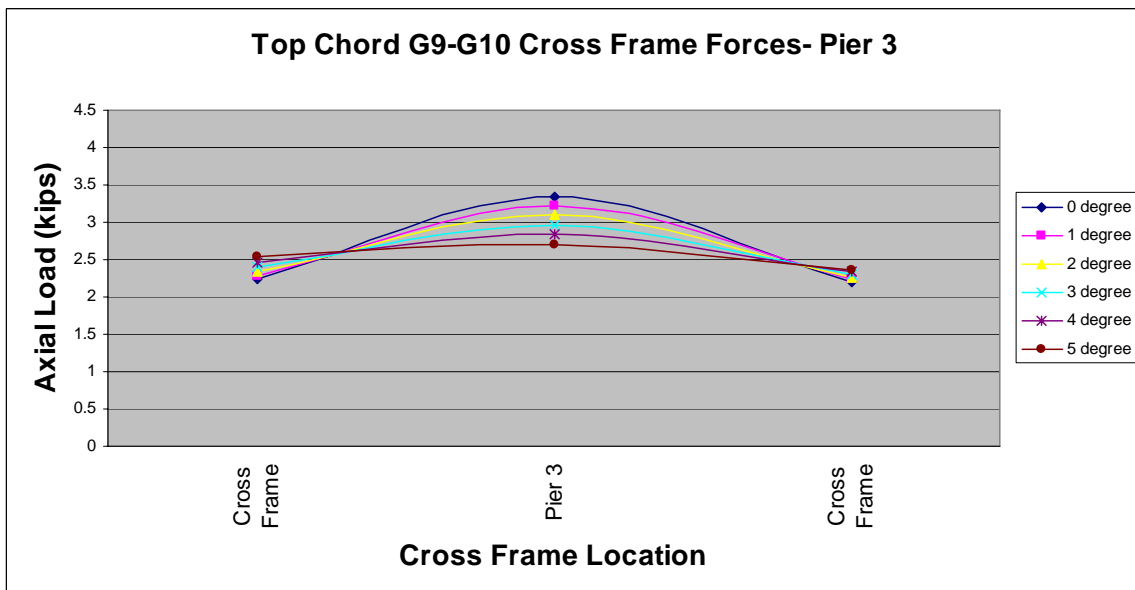
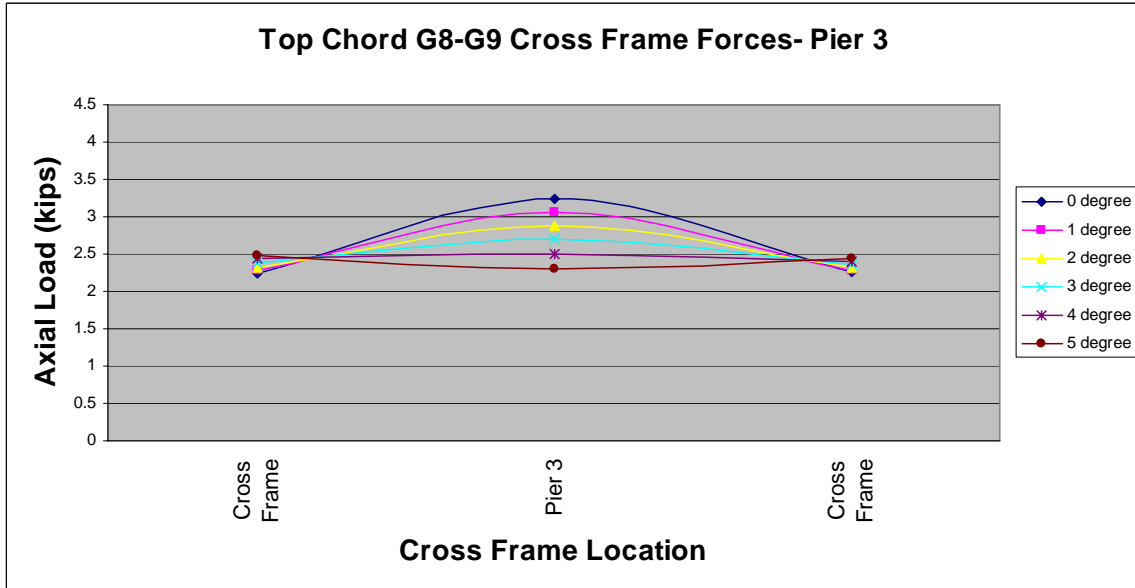


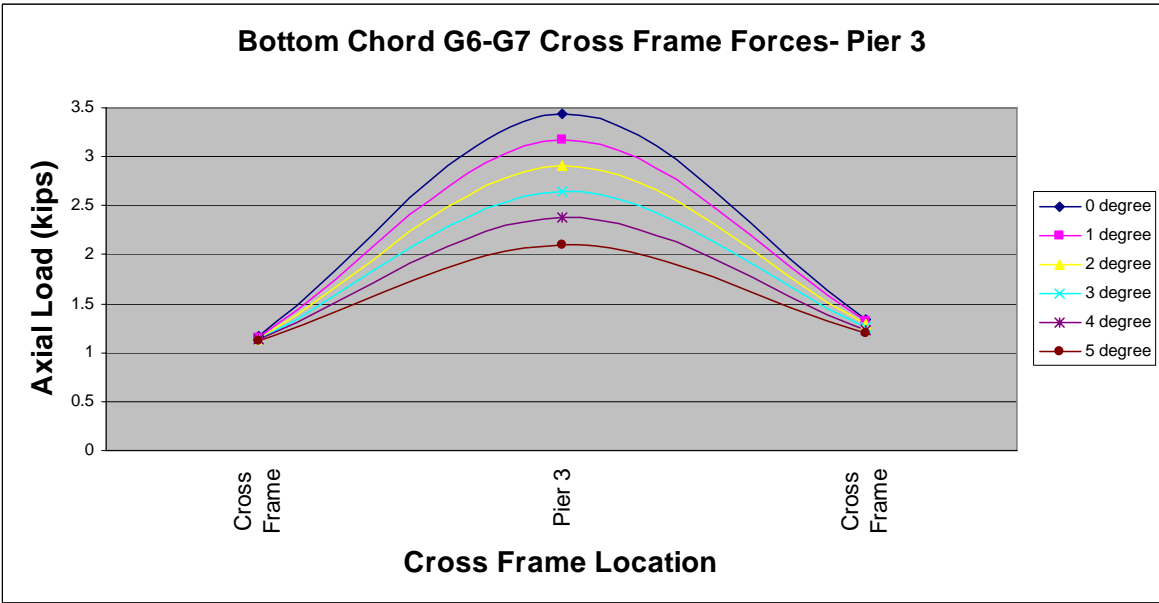
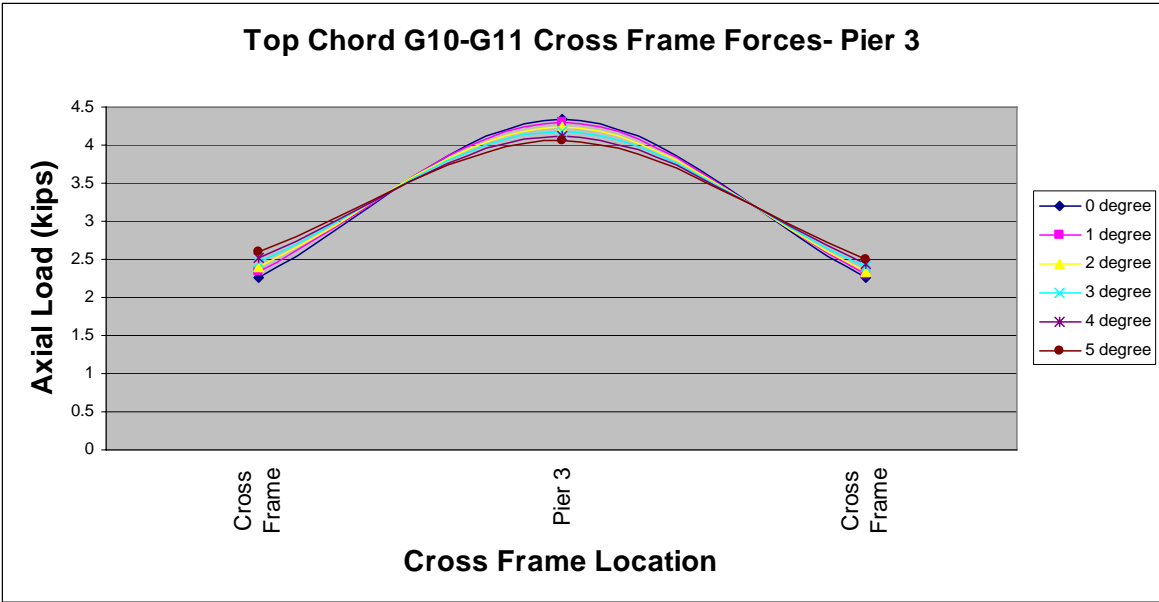


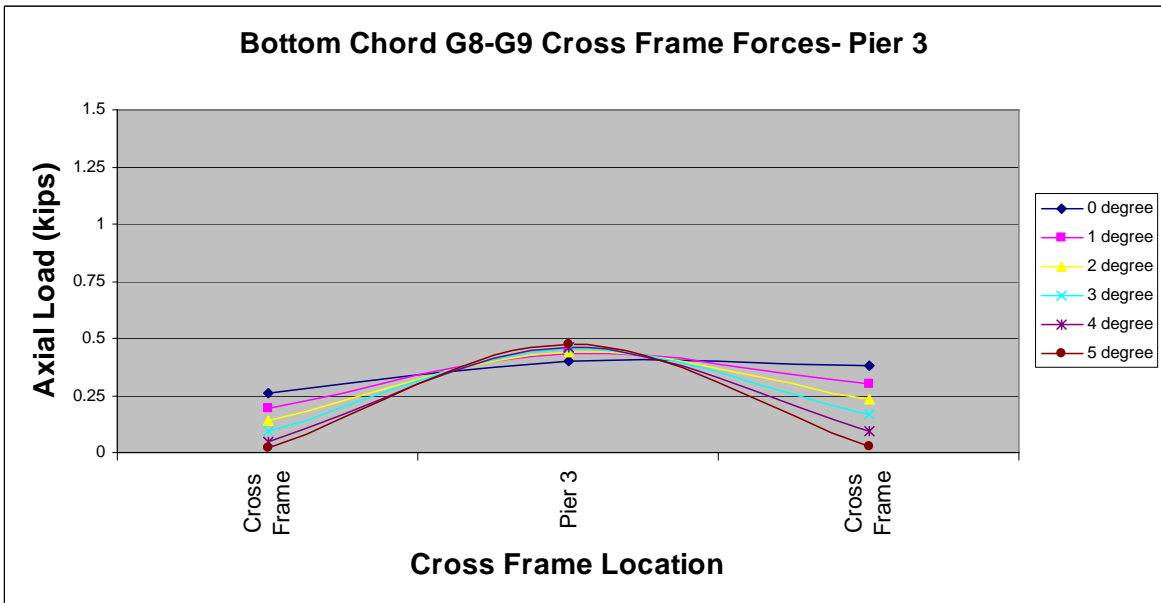
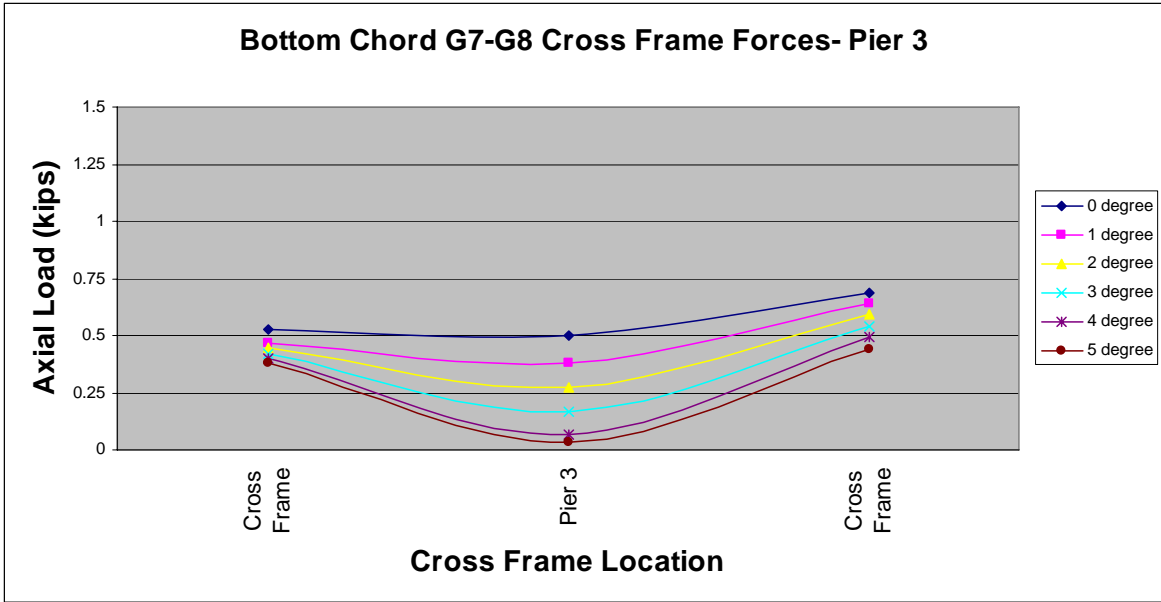


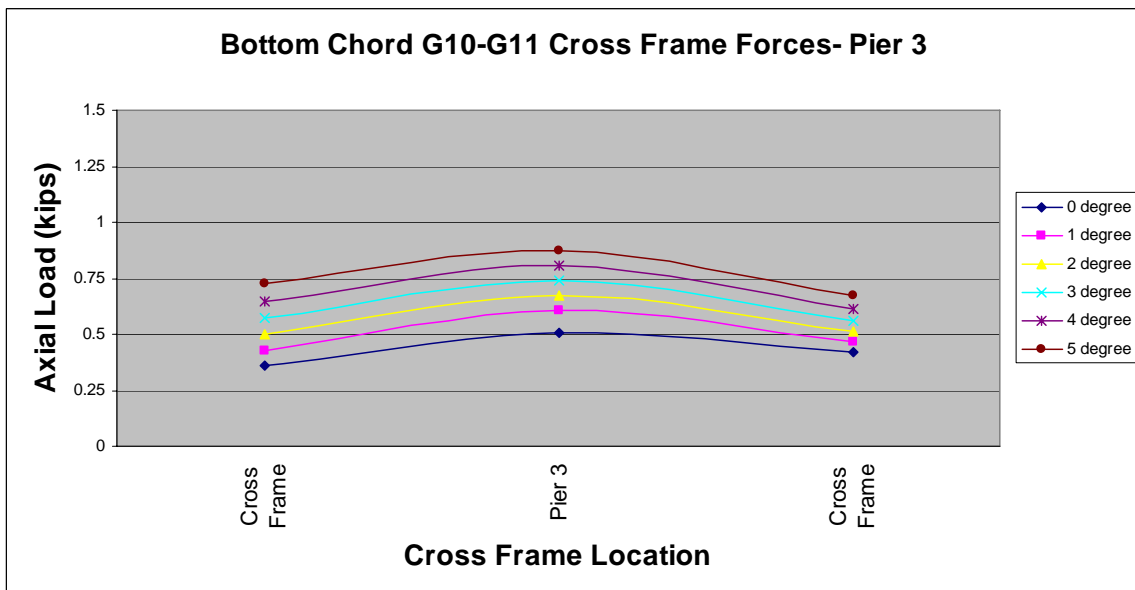
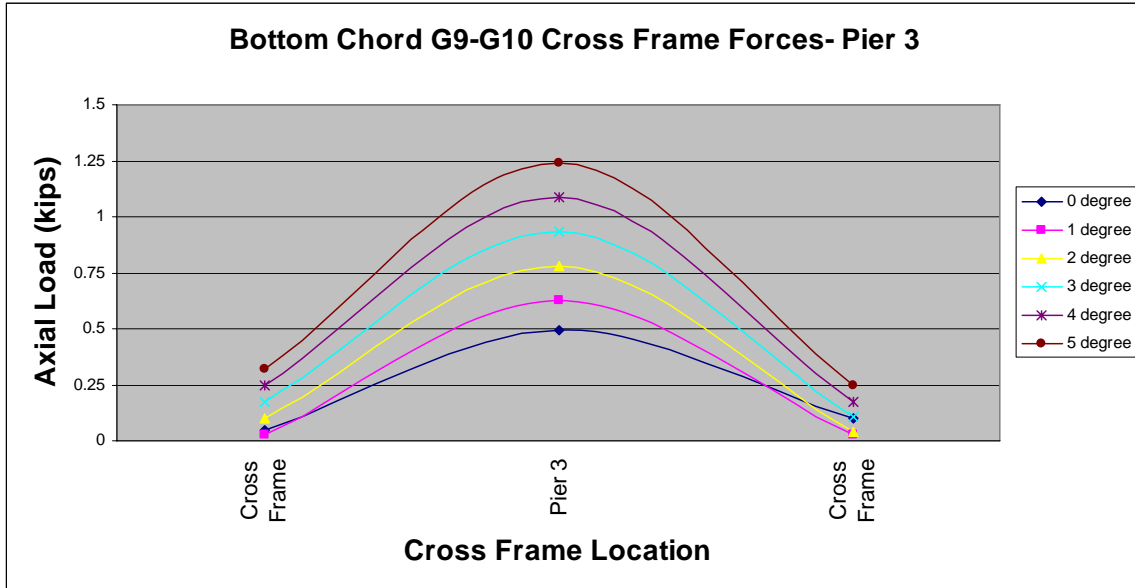












BIBLIOGRAPHY

- ADINA, (2003), Theory and Modeling Guide, Volume I: ADINA, *Report ARD 03-7*, ADINA Research and Development, Inc., Watertown, MA.
- American Association of State Highway and Transportation Officials (AASHTO), (1993 and 2003), *Guide Specifications for Horizontally Curved Steel Girder Highway Bridges*, Washington, D.C.
- American Association of State Highway and Transportation Officials (AASHTO), (2005), *AASHTO LRFD Bridge Design Specifications, 3rd Edition with 2005 Interim*, Washington, D.C.
- Boresi, A., Schmidt, R., (2003), *Advanced Mechanics of Materials, Sixth Edition*, John Wiley and Sons, New York.
- Chavel B.W., Earls, C.J., (2001), "Evaluation of Erection Procedures of the Curved Span of the Ford City Steel I-Girder Bridge," Report No. CE/ST 18, Department of Civil Engineering, University of Pittsburgh, Pittsburgh, Pennsylvania.
- Chavel, B.W., Earls, C.J., (2001), "Evaluation of Erection Procedures of the Horizontally Curved Steel I-Girder Ford City Bridge," Thesis in Civil Engineering, University of Pittsburgh, 2001.
- Chavel B.W., Earls, C.J., (2004), "Deflection of Horizontally Curved I-Girder Bridge Members Under Construction," Report No. CE/ST 28, Department of Civil Engineering, University of Pittsburgh, Pittsburgh, Pennsylvania.
- Davidson, J. S., Keller, M. A., Yoo, C. H., (1996), "Cross frame Spacing and Parametric Effects in Horizontally Curved I-Girder Bridges," *ASCE Journal of Structural Engineering*," Vol. 122, No. 9, pp. 1089-1096.
- Domalik, D., Shura, J., Linzell, D. (2005), "The Design and Field Monitoring of a Horizontally Curved Steel Plate Girder Bridge," *Proceedings of the International Bridge Conference*, Vol. 05-46.
- Galambos, T. V., Hajjar, J. F., Huang, W. H., Pulver, B. E., Leon, R. T., Rudie, B. J., (2000), "Comparison of Measured and Computer Stresses in a Steel Curved Girder Bridge," *ASCE Journal of Bridge Engineering*, Vol. 5, No. 3, pp. 191-199.

- Galambos, T.V., Hajjar, J.F., Leon, R.T., Huang, W.-H., Pulver, B.E., Rudie, B.J. (1996), "Stresses in a Steel Curved Girder Bridge," Report No. MN/RC-96/28, Minnesota Department of Transportation, St. Paul, Minnesota
- Gillespie, James W., (1968) "Analysis of Horizontally Curved Bridges," *AISC Engineering Journal*, October 1968, p. 141.
- Grubb, M.A., (1984), "Horizontally Curved I-Girder Bridge Analysis: V-Load Method," *Transportation Research Record*, 1984, p 26-36.
- Grubb, M.A., Yadlosky, J. M., Duwaldi, S. R., (1996), "Construction Issues in Steel Curved-Girder Bridges," *Transportation Research Record* 1544, National Research Council, pp. 64-70.
- Linzell, D., Leon, R.T., Zureick, A.H. (2004), "Experimental and Analytical Studies of a Horizontally Curved Steel I-Girder Bridge During Erection," *ASCE Journal of Bridge Engineering*, Vol. 9, No. 6, pp. 521-530.
- Linzell, D.G., (1999), "Studies of Full-Scale Horizontally Curved Steel I-Girder Bridge Systems Under Self Weight," Ph.D. Dissertation, School of Civil and Environmental Engineering, Georgia Institute of Technology.
- Lobo, J.A., (2002), "Effect of Geometric Imperfections on Horizontally Steel Curved Girder Bridges," Master's Thesis, *The Pennsylvania State University*.
- Nakai, H., Yoo, C.H., (1988), *Analysis and Design of Curved Steel Bridges*, McGraw-Hill, New York.
- Thatcher, W.M., (1967), "Horizontally Curved Steel Girders-Fabrication and Design," *AISC Engineering Journal*, July 1967, p.107.
- Yadlosky, J. M., Fuller, J., (2001), "Out of Plumb: Combating Erection and Construction Problems in Curved Girder Bridges," *HDR Bridgeline*, Vol. 11 No. 1.